

THE HISTONE DEMETHYLASE KDM4B CONTRIBUTES TO THE PERITONEAL
DISSEMINATION OF OVARIAN CANCER

By

LEI QIU

Submitted to the graduate degree program in Pathology and Laboratory Medicine and
the Graduate Faculty of the University of Kansas in partial fulfillment of the requirements
for the degree of Doctor of Philosophy.

Co-Chair (Mentor): Adam J. Krieg, Ph.D.

Co-Chair: Soumen Paul, Ph.D.

Fariba Behbod, Pharm.D, Ph.D.

Katherine F. Roby, Ph.D.

Chad Slawson, Ph.D.

Date Defended: 04/29/2015

The Dissertation Committee for Lei Qiu
certifies that this is the approved version of the following dissertation:

THE HISTONE DEMETHYLASE KDM4B CONTRIBUTES TO THE PERITONEAL
DISSEMINATION OF OVARIAN CANCER

Co-Chair (Mentor): Adam J. Krieg, Ph.D.

Co-Chair: Soumen Paul, Ph.D.

Date approved: 04-29-2015

ABSTRACT

Solid tumors contain hypoxic regions due to their unchecked proliferation. This hypoxic microenvironment induces cancer cell metastasis and angiogenesis to promote tumor survival. The hypoxia-inducible factors (HIFs) are the primary regulators of the hypoxic response, inducing genes involved in important tumor progression pathways. The lysine (K)-specific demethylase KDM4B is a direct target of HIF, creating an intriguing link between the hypoxic tumor microenvironment and downstream gene expression beyond the direct actions of HIF stabilization. The findings that hypoxia-inducible KDM4B overexpression occurs in multiple cancer types suggest a general KDM4B function in these cancers. However, our current knowledge on KDM4B function in each cancer type seems to rely on tissue-specific pathways. In a microarray analysis using transient knockdown of KDM4B, we identified a set of potential KDM4B targets with clear associations to tumor cell growth, migration, and metastasis. Microarray data from HCT116 colon carcinoma, SKOV3ip.1 ovarian cancer and RCC4 renal cell carcinoma cells identified numerous genes specifically regulated in each cell type, as well as 16 common targets shared by all three cell lines. Through Ingenuity Pathway Analysis, we found that KDM4B also regulated different pathways under different oxygen conditions. In general, KDM4B regulated proliferative genes in normoxia, and metastatic genes in hypoxia. We have also demonstrated that KDM4B regulated these target genes by binding and demethylating near the promoter regions of these genes. Our findings suggest that KDM4B regulates pathways specific to each cancer type and tumor microenvironment to support cancer cell survival. Hypoxia has been linked to poor prognosis of epithelial ovarian cancer (EOC), likely through regulating genes that

contribute to the widespread dissemination of peritoneal metastases observed in late-stage diagnosis. In this study, we have shown that KDM4B is expressed in high grade serous adenocarcinoma and EOC cell lines, especially in hypoxia. Suppressing KDM4B inhibits ovarian cancer cell invasion, migration and spheroid formation *in vitro*. KDM4B is also crucial for seeding and growth of peritoneal tumors *in vivo*, where its expression corresponds to hypoxic regions. Thus, KDM4B is a potent contributor to the seeding and growth of peritoneal tumors, one of the predominant factors affecting prognosis of EOC.

ACKNOWLEDGEMENTS

I would like to thank my family for their unrestrained support, guidance, and encouragement to me over all these years. My father Mr. Wenjie Qiu did not have the opportunity for much schooling, which he has always dreamed. Therefore, he has worked very hard to support me for as much school as I wanted and felt confident for. My mother, Ms. Zhongjie Diao has provided me much love, care and encouragement, which has been priceless for this journey. I shall be forever grateful to both of them, especially for their support for me to come to the United States to pursue a better education. Another family member I owe many thanks to is my aunt, Wenzhi Qiu. Being my high school Biology teacher, she was the first person who roused my interest in pursuing this subject as my career. She has also supported me both intellectually and financially on this journey to fulfill my dream in becoming a Biologist. I would also love to give my special gratitude to my American parents, Mr. Garen D. Forsythe and Mrs. Patricia A. Forsythe, who have shown me how to live my life to the fullest and to put my best effort to my study and my work. My friends, Ying Mu, Qiang Zhang, Minghui Tai and Jacob New, have provided me with tremendous support during this journey.

I would like to give special thanks to my mentor Dr. Adam J. Krieg, who has patiently guided me to become a true scientist. I owe him a life time of gratitude for his training and support, without which this work would not have been possible. His passion for science has been very infectious, and I hope to carry on my future research activities based on this foundation of strong scientific ethic and commitment I learned from him. I would like to give my heartfelt thanks to our research associate, Yan Hong, for her

tremendous help and advice on histology. Cailin B. Wilson has also been a great co-worker and has contributed to many aspects of this project.

I would like to thank my committee members for their great advice for my project. Their challenges have also been very beneficial in helping me establish a stronger scientific foundation for my future career.

I would also like to give special gratitude to Dr. Yafeng Dong for providing the equipment used in this study. Dr. Dong also gave me important advice on setting future career goals. Special thanks to Ms. Norma Turner for helping me acquire the tools and reagents for my experiments, without which much of the research work would not have been possible.

I would like to thank Dr. Sumedha Gunewardena and Clark Bloomer in the Bioinformatics core (University of Kansas Medical Center) for helping me with generation and analysis of microarray data. I would like also to express my gratitude to the staff of the University of Kansas Cancer Center's Biospecimen Repository Core Facility staff for providing consented human specimens (Colleen Reilly and Zaid Naima) and for excellent histological and immunohistochemical expertise in the creation of the TMAs used in this study (Dr. Rashna Madan and Tara Meyer).

I would like to give special appreciations to our collaborator Dr. Denise A. Chan, formerly of UCSF, who provided crucial assistance in the extraction of TMA spot images. I would also like to thank our collaborators on campus, Dr. Michael Soares, Dr. Katherine Swenson-Fields, Dr. Jeremy Chien, Dr. Luciano DiTacchio, Dr. Andrew Godwin, and their lab members for kindly providing me with equipment and reagents

that were valuable for my research. Last but not least, I would like to acknowledge the American Cancer Society and the University of Kansas Medical Center for providing grants to support this study.

TABLE OF CONTENTS

ABSTRACT	iii
ACKNOWLEDGEMENTS.....	v
TABLE OF CONTENTS.....	viii
List of Figures	xi
List of Tables	xv
CHAPTER 1:.....	1
GENERAL INTRODUCTION	1
Hypoxia in Tissue	2
The Hypoxic Tumor Microenvironment	2
The Hypoxia Inducible Factors	5
Hypoxia and Epigenetic Regulation	9
The Nucleosome.....	10
Histone Methylation	10
Histone Demethylases	13
Histone Demethylases in Cancer.....	13
KDM4B Function in Cancer	17
Heterogeneity of Cancer.....	19
Colorectal Cancer	19
Renal Cell Carcinoma.....	22
HIF and Ovarian Cancer	23
Epithelial Ovarian Cancer	24

Current Therapies for HGSA.....	26
Research Objectives: KDM4B Function and Regulatory Mechanism in Cancer	27
CHAPTER 2:.....	30
KDM4B REGULATES DISTINCT PATHWAYS IN THREE DIFFERENT CANCERS AND IN DIFFERENT OXYGEN CONDITIONS	30
ABSTRACT	31
INTRODUCTION	32
MATERIALS AND METHODS	35
RESULTS	45
KDM4B Regulates Common and Tissue-Specific Targets in Three Cancer Types	45
KDM4B Regulates Distinct Pathways in Different Oxygen Conditions in HCT116 and SKOV3ip.1	51
KDM4B Differentially Regulates Gene Expression in Atmospheric and Hypoxic Growth Conditions in Ovarian Cancer Cell Lines.....	67
KDM4B Binds and Demethylates Regulatory Regions of Target Genes to Promote Expression.....	81
DISCUSSION.....	85
CHAPTER 3:.....	93
THE HISTONE DEMETHYLASE KDM4B CONTRIBUTES TO PERITONEAL DISSEMINATION OF OVARIAN CANCER	93
ABSTRACT	94
INTRODUCTION	95

MATERIALS AND METHODS	98
RESULTS	107
KDM4B is Abundantly Expressed in High Grade Ovarian Serous Adenocarcinoma Tumors and OVCAR Cell Lines	107
KDM4B Regulates <i>In Vitro</i> Cell Invasion, Migration, and Anchorage-Independent Growth in Normoxia and Hypoxia	111
KDM4B is Required for Peritoneal Tumor Growth	121
KDM4B is Expressed in Hypoxic Regions of Tumors	124
DISCUSSION.....	145
CHAPTER 4:.....	150
GENERAL DISCUSSION	150
I. The Overall Importance of Our Study	151
II. Regulation of Cancer Progression by KDM4B is Dependent on Cancer Type and Oxygen Tension.....	151
III. Mechanism of KDM4B Function in Epithelial Ovarian Cancer	159
IV. KDM4B Function in Ovarian Cancer	162
V. Relevance of our study: KDM4B as a possible therapeutic target in ovarian cancer.....	164
VI. Future directions.....	167
VII. Significance	170
REFERENCES.....	171

LIST OF FIGURES AND TABLES

List of Figures

CHAPTER 1: GENERAL INTRODUCTION

Figure 1.1. Schematic Diagram Showing Hypoxic and Necrotic Regions In Multicellular Tissues.....	3
Figure 1.2. Schematic Diagram Showing HIF-1 α Stabilization in Hypoxia.	7
Figure 1.3. Schematic Diagram Showing The Basic Structure Of The Histone Core, With Depiction of Lysine Methylation.....	11
Figure 1.4. Schematic Diagram Showing The Enzymatic Functions Of Selected Hypoxia-Inducible Histone Demethylases.	14

CHAPTER 2: KDM4B REGULATES GENERAL AND SPECIFIC PATHWAYS IN EACH CANCER AND OXYGEN CONDITION

Figure 2.1. Identification of common KDM4B target genes in HCT116 colon carcinoma, SKOV3ip.1 ovarian cancer and RCC4 renal cell carcinoma cell lines.	46
Figure 2.2. KDM4B expression in HCT116 cells.	52
Figure 2.3. Common KDM4B targets in the SKOV3ip.1, HCT116 and RCC4 that are involved in tumorigenesis and proliferation pathways.	54
Figure 2.4. Common KDM4B Targets in the SKOV3ip.1, HCT116 and RCC4 that are involved in migration and metastasis pathways.	56

Figure 2.5. Common KDM4B Targets in the SKOV3ip.1, HCT116 and RCC4 that are involved in protein folding and processing and RNA processing.....	58
Figure 2.6. Common KDM4B Targets in the SKOV3ip.1, HCT116 and RCC4 that are involved in amyloid protein precursor cleavage, ion metabolism, and apoptosis.	60
Figure 2.7. Identification of KDM4B target genes in HCT116 colon carcinoma cells and in SKOV3ip.1 ovarian cancer cells.	62
Figure 2.8. H3K9 tri-methylation in SKOV3ip.1 transfected with siK4B.....	68
Figure 2.9. KDM4B regulates proliferative, inflammatory, and metastatic genes in SKOV3ip.1 cells.	70
Figure 2.10. Expression of KDM4 subfamily members in SKOV3ip.1 and OVCAR8 cells expressing shRNA to KDM4B.	73
Figure 2.11. H3K9me3 Level in SKOV3ip.1 and OVCAR8 ovarian cancer cell lines. ...	75
Figure 2.12. Modified Histone Peptide Array.....	77
Figure 2.13. Expression of KDM4 target genes in SKOV3ip.1 and OVCAR8 cells expressing shRNA to KDM4B.	79
Figure 2.14. Chromatin IP demonstrating that KDM4B binds and demethylates its target gene promoters.	82
Figure 2.15. Expression of LCN2 and LOX protein in SKOV3ip.1 cells with KDM4B knockdown.	86

CHAPTER 3: THE HISTONE DEMETHYLASE KDM4B CONTRIBUTES TO PERITONEAL DISSEMINATION OF OVARIAN CANCER

Figure 3.1. KDM4B is robustly expressed in ovarian cancer tissue and ovarian cancer cell lines compared to normal ovarian surface epithelial cells.	109
Figure 3.2. KDM4B protein expression in ovarian cancer cell lines.	112
Figure 3.3. Regulation of SKOV3ip.1 cell proliferation by KDM4B.	114
Figure 3.4. KDM4B supports SKOV3ip.1 cell invasion and migration.	117
Figure 3.5. KDM4B supports OVCAR8 cell invasion and migration.	119
Figure 3.6. KDM4B supports ovarian cancer cell attachment-free growth.	122
Figure 3.7. KDM4B regulates <i>in vivo</i> peritoneal growth of SKOV3ip.1 cells.	125
Figure 3.8. KDM4B regulates <i>in vivo</i> peritoneal growth of OVCAR8 cells.	127
Figure 3.9. KDM4B regulates <i>in vivo</i> peritoneal growth of ovarian cancer cells.	129
Figure 3.10. KDM4B regulates <i>in vivo</i> peritoneal growth and ascites formation of ovarian cancer cells.	131
Figure 3.11. KDM4B regulates <i>in vivo</i> peritoneal growth and dissemination of ovarian cancer cells.	133
Figure 3.12. KDM4B is expressed in hypoxic regions of tumor xenografts.	134
Figure 3.13. Post-mortem KDM4 Family Member Expression.	136
Figure 3.14. KDM4B is preferentially expressed in hypoxic ovarian cancer tumors to promote progression.	139

CHAPTER 4: GENERAL DISCUSSION

Figure 4.1. Mechanisms used by KDM4B to promote cancer progression.....	153
Figure 4.2 General model of KDM4B function in cancer cell progression.	156
Figure 4.3. Mechanism of the contribution of KDM4B signaling to ovarian cancer progression.	163

List of Tables

CHAPTER 2: KDM4B REGULATES GENERAL AND SPECIFIC PATHWAYS IN EACH CANCER AND OXYGEN CONDITION

Table 2.1. Primers Used For Qrt-PCR.....	37
Table 2.2. Dilution information of antibodies Used in Immunoblotting.....	41
Table 2.3. Antibody Dilution Used in Chromatin IP.	43
Table 2.4. Primers Used in Chromatin IP.....	44
Table 2.5. List of the 16 Genes Commonly Regulated by KDM4B in Three Cancer Cell Lines.....	49
Table 2.6. Molecular and Cellular Functions Regulated by KDM4B in Normoxia or Hypoxia in SKOV3ip.1, HCT116, and RCC4 Cells.....	65
Table 2.7. Disease and Disorders Regulated by KDM4B in Different Oxygen Conditions in SKOV3ip.1, HCT116, and RCC4 Cells.....	66

CHAPTER 3: THE HISTONE DEMETHYLASE KDM4B CONTRIBUTES TO PERITONEAL DISSEMINATION OF OVARIAN CANCER

Table 3.1. Antibody Dilutions.....	100
Table 3.2. QPCR Primers Used in This Chapter.	103
Table 3.3. Analysis of KDM4B expression in normal ovary, and primary EOC tumors with matched metastatic and recurrent tumors.....	108
Table 3.4. Immunohistochemical Scoring Data for KUCC OVCAR TMAs.....	141

CHAPTER 1:

GENERAL INTRODUCTION

Hypoxia in Tissue

In multicellular tissue, oxygen can only freely diffuse to cells within a distance of approximately 100 μm (Thomlinson and Gray 1955). Past this distance, cellular metabolism depletes the microenvironment of the remaining oxygen, creating a gradient of decreasing oxygen (hypoxia). Some organs and tissues experience hypoxic microenvironment due to their distance from the functional blood supply (Brigati et al. 2010). For example, the inner part of the retina experiences a PO_2 of 15-20 mm Hg (~2-4% O_2). Similarly, the kidney can sustain an oxygen level that is 7.2 mm Hg (~1% O_2) (Birol et al. 2007; Simon and Keith 2008). This interplay between tissue vasculature and cellular metabolism, as illustrated in Figure 1.1, is particularly important when considering the role of oxygen in the tumor microenvironment. Over the past decade, tumors have increasingly been recognized as complex organs rather than homogenous tumor masses (Hanahan and Weinberg 2000). Growing evidence suggests that host and stromal factors in the tumor microenvironment are equally important as genetic events in the tumor cells. A solid tumor includes not only cancer cells but also matrix components, stromal cells and inflammatory cells. Moreover, due to the fast growth of the cancer cells, tumor vasculature usually has leaky walls. Even so, tumor angiogenesis is still slower than cancer cell proliferation. Therefore, solid tumors typically contain hypoxic regions.

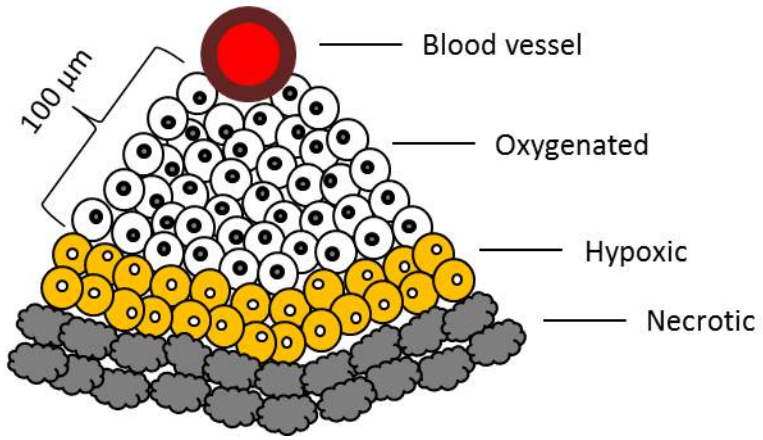
The Hypoxic Tumor Microenvironment

Tumor hypoxia often leads to cancer malignancy and predicts a poor response to chemotherapy and radiation treatment (Teicher 1994; Vaupel 2004). Since these

Figure 1.1. Schematic Diagram Showing Hypoxic and Necrotic Regions In

Multicellular Tissues. Only cells in 100 μm distance from the blood vessel may acquire enough oxygen for their own growth. Beyond this distance, cells experience hypoxia.

Further away, cells may go through necrosis.



regions are farther from the blood vessels, cells in this area do not obtain enough nutrients or oxygen. In response to this nutrient deprivation, the cells proliferate more slowly, decreasing efficiency of most current cancer therapies that target the actively proliferating cells. It is also more difficult for chemotherapeutic drugs to reach cells in these regions. In addition, hypoxic stress stimulates mechanisms in cells to manipulate their metabolism to adapt to the environment (Semenza et al. 1994), to send out signals for angiogenesis (Blancher et al. 2000), or to migrate to a distant location where oxygen is more abundant (Erler and Giaccia 2006). These cellular adaptations combined with the physical barriers to conventional therapies select for a more resistant tumor phenotype.

The Hypoxia Inducible Factors

In response to hypoxia, cells initiate a series of cellular responses through a family of transcription factors called hypoxia inducible factors (HIFs) (Semenza and Wang 1992; Wang and Semenza 1993a; Wang and Semenza 1993b; Semenza 1998). Functional HIFs are heterodimers containing an α subunit that is tightly regulated by oxygen concentrations and a β subunit (also called aryl hydrocarbon receptor nuclear translocator, ARNT) that does not respond to oxygen (Semenza et al. 1997; Majmundar et al. 2010). There are three identified mammalian HIF- α isoforms (HIF-1 α , HIF-2 α and HIF-3 α), among which HIF-1 α is the best studied (Majmundar et al. 2010). HIF-1 α and HIF-2 α share much similarity, except that HIF-1 α is expressed in most tissue whereas HIF-2 α is restricted to certain organs such as vascular endothelium and hepatocytes (Wiesener et al. 2003). Moreover, HIF-1 α and HIF-2 α share common targets but also regulate the expression of distinct sets of genes (Ratcliffe 2007; Loboda et al. 2010).

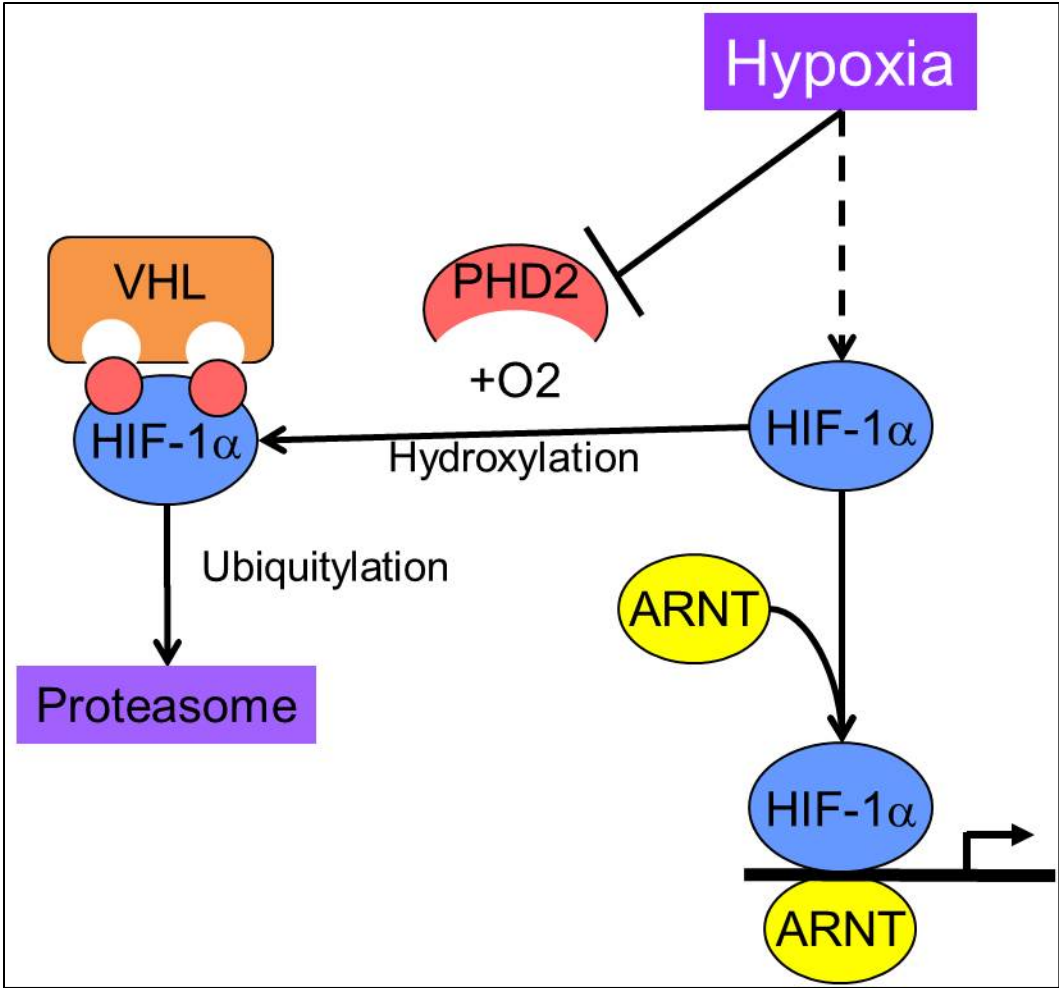
HIF-3 α is less related to the other two variants and not very well studied. Interestingly, an alternatively spliced variant of HIF-3 α acts as a dominant negative regulator of HIF-1 α (Makino et al. 2001). HIF- α (HIF-1 α or HIF-2 α) and HIF- β together form a complex that binds to the hypoxia response elements (HREs) in the promoter region of target genes (Semenza et al. 1996; Koi and Boland 2011).

When oxygen is sufficient, HIF-1 α is constantly degraded through binding and ubiquitylation of the tumor suppressor protein von Hippel-Lindal (VHL), which is a part of the E3 ubiquitin ligase complex (Maxwell et al. 1999; Ohh et al. 2000). HIF-alpha prolyl hydroxylases (PHDs) regulate this binding between HIF-1 α and VHL by hydroxylating proline residue 402 and 564 in the HIF-1 α subunit (Ivan et al. 2001; Jaakkola et al. 2001; Chan et al. 2002; Chan et al. 2005). Since proline hydroxylation requires oxygen, PHDs are inhibited under hypoxia, HIF-1 α is then stabilized and is able to interact with the β -subunit (ARNT) and additional co-activators (Rohwer and Cramer 2011) (Figure 1.2).

Factor inhibiting HIF1 (FIH1) is another oxygen-sensitive enzyme that hydroxylates HIF-1 α asparagine 803 (Mahon et al. 2001; Lando et al. 2002; McNeill et al. 2002). This hydroxylation blocks the interaction between HIF-1 α and the co-activators p300 and CREB binding protein (CBP) (Mahon et al. 2001). Hypoxia disrupts FIH1 enzymatic activity, enabling interaction of the HIF1/CBP/p300 complex, and enhancing transcription of HIF target genes (Yang et al. 2009).

HIF is a master regulator of a number of downstream target genes involved in various pathways. Vascular endothelial growth factor (VEGF) is associated with poor prognosis in various cancer types (Blancher et al. 2000; Jones et al. 2001). Its

Figure 1.2. Schematic Diagram Showing HIF-1 α Stabilization in Hypoxia. In normoxia, HIF-1 α is hydroxylated by PHD2 and ubiquitinated by VHL for proteasome degradation. In hypoxia, PHD activity is inhibited and HIF-1 α is stabilized and dimerizes with ARNT to activated transcription of target genes.



expression is significantly increased under hypoxia and this pattern is regulated by HIF (Forsythe et al. 1996). Lysyl oxidase (LOX) is involved in tumor metastasis in response to hypoxia (Erler et al. 2006). Prolyl hydroxylase domain protein 2 (PHD2) exerts tumor-suppressive activity in pancreatic cancer, osteosarcoma, melanoma, and lung cancer. (Metzen et al. 2005; Ameln et al. 2011; Su et al. 2011). Urokinase-type plasminogen activator receptor (u-PAR) is part of the plasminogen activator system (PAS), which contributes to the metastasis and angiogenesis of malignant tumors (Oszajca et al. 2008; Halamkova et al. 2011). Glycolytic enzymes are important targets for anticancer therapy (Semenza et al. 1994; Zawacka-Pankau et al. 2011). Therefore, studying HIF targets gives us better understanding of the hypoxic tumor microenvironment and its contribution to tumor progression.

Hypoxia and Epigenetic Regulation

In addition to directly regulating transcription through HIFs, hypoxia can also modify gene expression epigenetically. It may alter DNA methylation, which directly influences gene expression (Cedar 1988; Chawla et al. 1996). It can also affect a series of post-translational modifications on histones, such as acetylation (addition of an acetyl group), methylation (addition of one or more methyl group), phosphorylation (addition of a phosphate group), ubiquitination (addition of ubiquitin tags for degradation), and glycosylation (addition of a carbohydrate), as reviewed by Mimura et al. (Tian and Fang 2007; Mimura et al. 2011). Among these modifications, histone methylation is one of the more complex phenomena. It is involved in several fundamental processes including transcriptional regulation, heterochromatin formation, and DNA repair (Lachner and Jenuwein 2002; Margueron et al. 2005; Tian and Fang 2007).

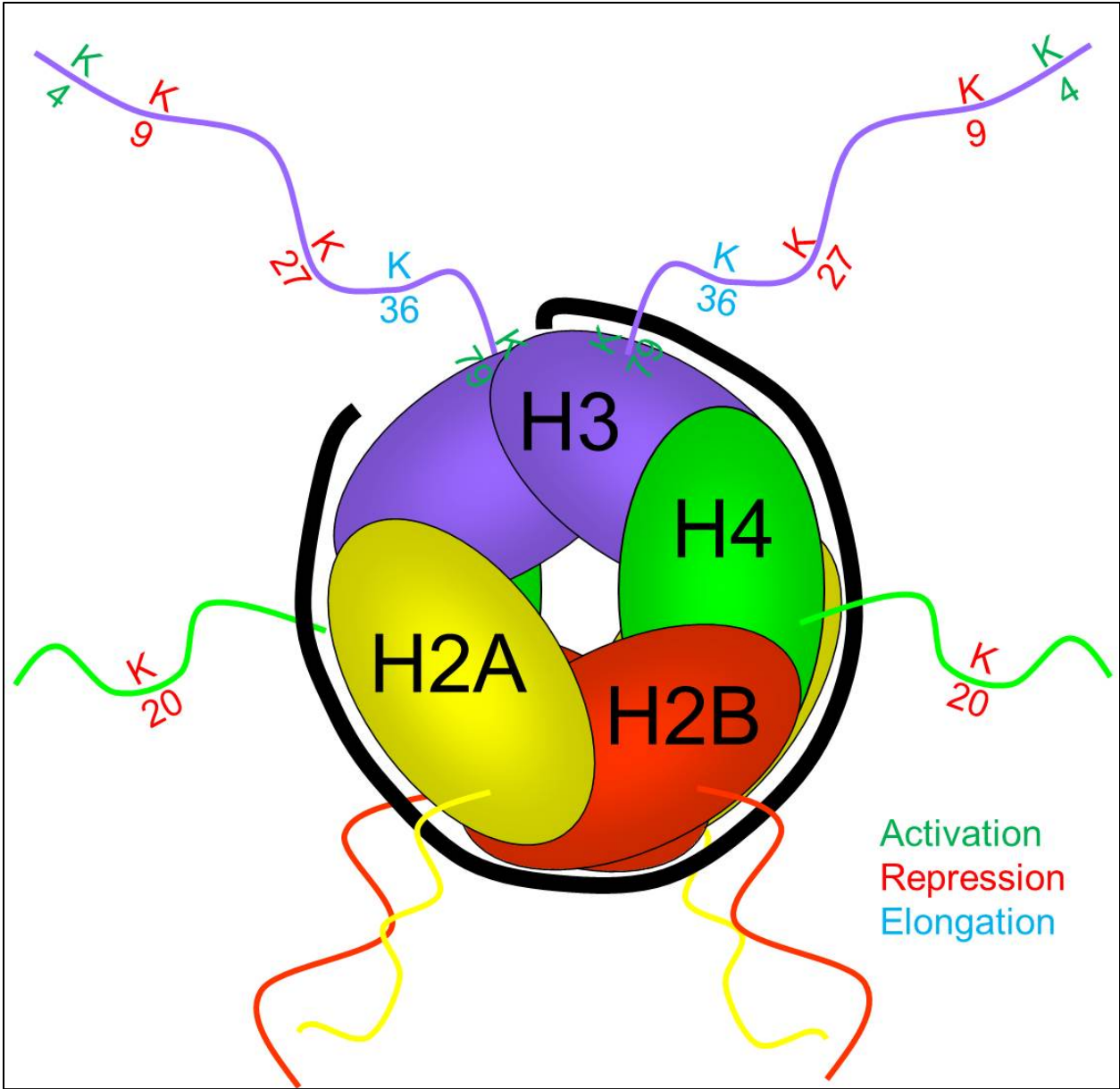
The Nucleosome

DNA transcription is tightly regulated by histone modifications. As part of the condensation mechanism, approximately every 145-147 base pairs of DNA wraps around a core of histone octamer with two of each histone protein, H2A, H2B, H3, and H4 (Figure 1.3), to form a nucleosome (Luger et al. 1997). The protein octamer may be divided into two H3-H4 and two H2A-H2B histone pairs. The two H3-H4 dimers form a central tetramer through a 4-helix bundle between the two H3 histones. A homologous 4-helix bundle between each H2A and H4 connects the H2A-H2B pairs with the tetramer to form the histone octamer (Luger et al. 1997). The unstructured N-terminal “tail” of each histone protein protrudes to interact with DNA. Modifications on these “tails” may influence DNA replication and gene transcription.

Histone Methylation

Histone “tails” can be methylated on the lysine (K) residue or on the arginine (R) residue. The arginine residues of histones can be mono- or di-methylated (symmetric or asymmetric). Histone arginine methylation is generally related to gene activation (Cheng 2014). Histones can take up to three methyl groups on lysine residues H3K4, H3K9, H3K27, H3K36, H3K79, and H4K20 (Figure 1.3). H3K4, H3K36 and H3K79 tri-methylation are often found in transcriptionally active regions, whereas H3K9me3/me2, H3K27me3 and H4K20me3 can lead to gene repression (Kouzarides 2002; Tian and Fang 2007; Pedersen and Helin 2010; Lu et al. 2011; Ma et al. 2011). While once considered to be an irreversible modification, histone lysine methylation was recently found to be reversible. Methyl groups can be removed by histone demethylases through

Figure 1.3. Schematic Diagram Showing The Basic Structure Of The Histone Core, With Depiction of Lysine Methylation. Green, methylated lysine residue is usually found in actively transcribed gene promoter regions. Red, methylated lysine residue is normally found in repressed gene promoters. Blue, methylated residue is often found in the gene body, indicating a possible role in transcription elongation.



enzymatic hydroxylation (Shi et al. 2004; Cloos et al. 2006; Klose et al. 2006; Tsukada et al. 2006; Whetstine et al. 2006; Yamane et al. 2006).

Histone Demethylases

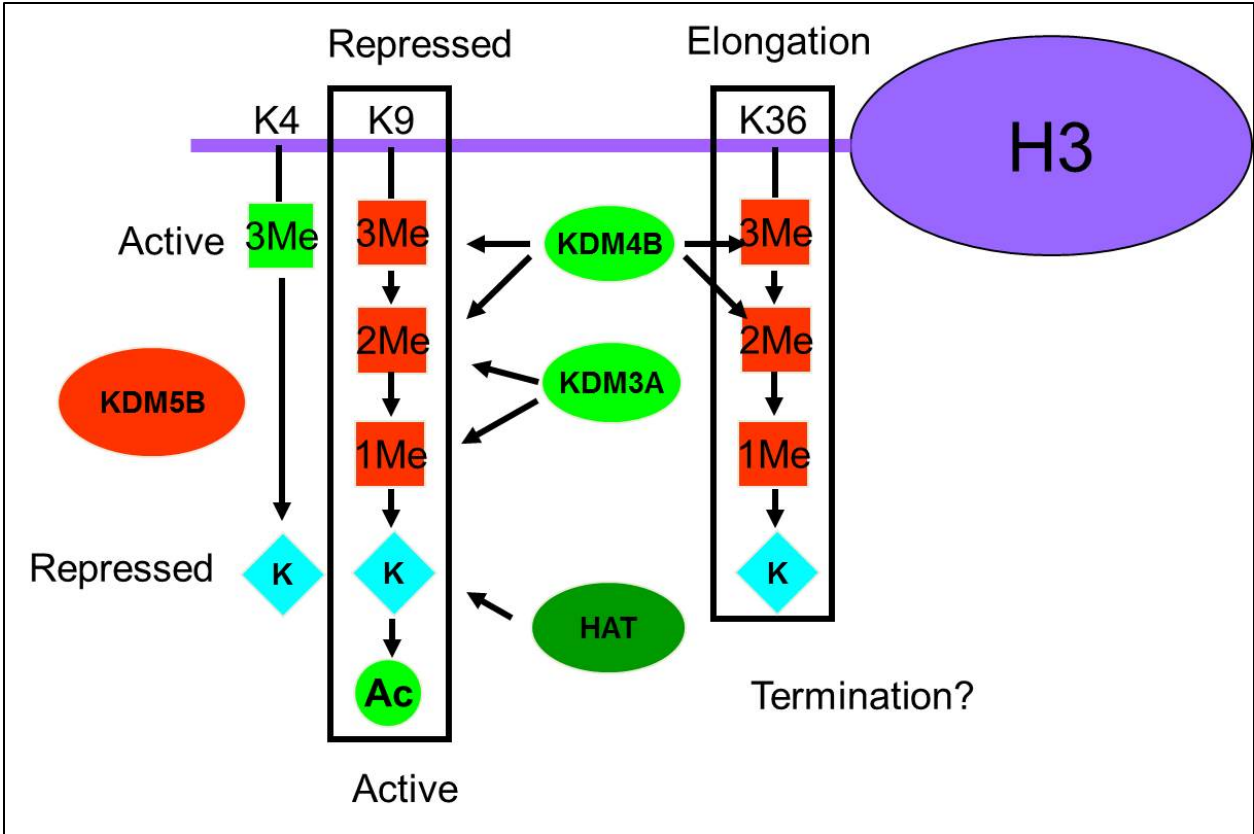
Histone lysine-specific demethylases are enzymes that remove methyl groups from lysine residues on histone “tails”. The first lysine-specific demethylase identified was KDM1 (LSD1) (Shi et al. 2004). It is a FAD (flavin adenine dinucleotide)-dependent enzyme that uses molecular oxygen to demethylate histone H3K4 and H3K9 depending on its co-factor (Shi et al. 2004; Metzger et al. 2005). Another family called JmjC domain-containing histone demethylases are dioxygenases whose activities require oxygen, Fe (II) and 2-oxoglutarate (alpha-ketoglutarate) (Tsukada et al. 2006). There are approximately 30 different JmjC domain-containing histone demethylases (Pedersen and Helin 2010), among which KDM3A, KDM4B and KDM5B are well known HIF1 targets that are regulated by hypoxia (Beyer et al. 2008; Pollard et al. 2008; Xia et al. 2009; Krieg et al. 2010) (functions depicted in Figure 1.4). A few other JmjC domain-containing proteins, including KDM3B, KDM4C, KDM5A, KDM5C, KDM7, and JMJD6, can also be regulated by hypoxia in certain conditions (Pollard et al. 2008; Yang et al. 2009). These hypoxia regulated histone demethylases demonstrate a link between the hypoxic tumor microenvironment and epigenetic regulation, thus may play important roles in cancer progression.

Histone Demethylases in Cancer

The histone demethylases display diverse functions in cancer (Johansson et al. 2014). Subfamily members may not always play similar roles. For example, in the KDM3 subfamily, KDM3A is induced by hypoxia and is overexpressed in multiple

Figure 1.4. Schematic Diagram Showing The Enzymatic Functions Of Selected

Hypoxia-Inducible Histone Demethylases. The N-terminus of histone H3 can be methylated on lysine 4, lysine 9, lysine 27 and lysine 36. H3K4 methylation is often found in the promoter region of actively transcribed genes, whereas H3K9 and H3K27 are usually repressive marks. H3K36 methylation has been shown to be involved in elongation. KDM3A demethylates di- and mono-methylated H3K9, thus activating gene expression. KDM4B demethylates tri- and di-methylated H3K9 and H3K36, leading to activation of gene expression or inhibiting elongation, respectively. KDM5B demethylates tri-methylated H3K4, leading to gene repression. Once all three methyl groups are removed by KDM4B and KDM3A, H3K9 can further be acetylated by histone acetyltransferase (HAT), leading to further activation of gene expression.



cancers, including bladder, lung, hepatocellular, prostate, colorectal and renal cell carcinoma, whereas KDM3B and KDM3C have demonstrated tumor suppressing roles in breast cancers (Hu et al. 2001; Wolf et al. 2007; Qi et al. 2010; Uemura et al. 2010; Guo et al. 2011; Kim et al. 2012i; Tang et al. 2012; Yamada et al. 2012; Osawa et al. 2013). The KDM5 and KDM6 subfamily members are mostly tumor suppressors, except that KDM5B and KDM6B have also demonstrated oncogenic roles (Lu et al. 1999; Agger et al. 2009; Barradas et al. 2009; Roesch et al. 2010; Anderton et al. 2011; Li et al. 2011a; Pereira et al. 2011; Ramadoss et al. 2012; Kuzbicki et al. 2013; Wouters et al. 2013).

The KDM4 subfamily members are overexpressed in many cancer types and are generally considered oncogenes, as reviewed by several groups (Cloos et al. 2008; Hojfeldt et al. 2013; Johansson et al. 2014).

The KDM4 subfamily comprises four members, KDM4A, KDM4B, KDM4C, KDM4D, and two potential pseudo-genes, KDM4E and KDM4F (Berry and Janknecht 2013). KDM4A-C are more closely related and have very similar structures with a JmjN domain, a JmjC domain, two PHD domains and two TUDOR domains, whereas KDM4D only has the JmjN and JmjC domains (Johansson et al. 2014). These enzymes are able to demethylate H3K9me3/me2 and H3K36me3/me2, with a higher efficiency for the H3K9me3, which is associated with gene repression (Johansson et al. 2014). KDM4A-C are increased in prostate cancer and are coactivators of the androgen receptor (Berry and Janknecht 2013; Coffey et al. 2013). They have also been shown to be important regulators in estrogen receptor positive (ER+) breast cancers (Yang et al. 2010; Kawazu et al. 2011; Berry and Janknecht 2013). Compared to KDM4A-C, not much is

known about KDM4D function in cancer. More recently, a study showed that KDM4D was rapidly recruited to DNA damage sites in a PARP-dependent manner, thus promoting DNA double-strand break repair in cells (Khoury-Haddad et al. 2014). Being a direct HIF target and up-regulated in multiple cancer types, KDM4B shows intriguing importance in regulating cancer progression.

KDM4B Function in Cancer

KDM4B plays a significant role in tumorigenesis, driving cancer cell proliferation (Yang et al. 2010; Kim et al. 2012a), manipulating cell cycle (Kawazu et al. 2011; Shi et al. 2011; Zhu et al. 2012) and inducing chromosomal instability (Kops et al. 2005; Slee et al. 2011; Young et al. 2013). KDM4B is regulated by the estrogen receptor, HIF, and p53 (Krieg et al. 2010; Yang et al. 2010; Zheng et al. 2013). Several studies have shown that KDM4B is overexpressed in ER+ breast cancer and acts as a co-activator with ER α to regulate downstream signaling pathways (Yang et al. 2010; Kawazu et al. 2011; Shi et al. 2011). A separate study showed that KDM4B may also regulate the expression of *ER* and *FOXA1* genes, which together control the estrogen-dependent breast cancer phenotype (Gaughan et al. 2013). KDM4B can also regulate the expression of the *androgen receptor (AR)* in prostate cancer and act as a co-activator with AR in downstream signaling (Coffey et al. 2013).

Elevated levels of KDM4B has been detected in several cancer types, including ER+ breast cancer (Yang et al. 2010), malignant peripheral nerve sheath tumor (MPNST) (Pryor et al. 2011), gastric-cancer (Li et al. 2011b), bladder cancer, lung cancer (Toyokawa et al. 2011), prostate cancer (Coffey et al. 2013), colorectal cancer (Fu et al. 2012), and osteosarcoma (Li and Dong 2015). Several KDM4B downstream

pathways have been identified. KDM4B promotes breast and gastric cancer proliferation by regulating cell cycle genes such as CCND1, CCNA1, WEE1, CDK6, and oncogenes such as MYB and MYC (Yang et al. 2010; Kawazu et al. 2011; Toyokawa et al. 2011; Kim et al. 2012a). In gastric and colon cancers, KDM4B promotes epithelial-mesenchymal transition (EMT) by cooperating with β -catenin (Kim et al. 2012a; Zhao et al. 2013a). KDM4B, along with KDM4C, mediates tumorigenesis of osteosarcoma by inducing fibroblast growth factor 2 (FGF2) (Li and Dong 2015). KDM4B also plays a role in colon cancer cell apoptosis and DNA damage repair (Chen et al. 2014; Sun et al. 2014). Besides its direct functions in cancer, KDM4B has also shown importance in stem cell generation and differentiation. Human KDM4B is necessary for the self-renewal of embryonic stem cells and induces pluripotent stem cell generation (Kato and Katoh 2007; Das et al. 2014). It also plays critical roles in osteogenic commitment of mesenchymal stem/stromal cells by promoting *distal-less homeobox 2 (DLX2)* expression (Ye et al. 2012; Qu et al. 2014). Since various steps of embryonic morphogenesis and wound healing involve EMT, a process also involved in early metastasis, these findings indicate a potential role of KDM4B in cancer cell progression (Hanahan and Weinberg 2000). In a study of DNA damage response, KDM4A and KDM4B also showed a demethylase-independent function in DNA double-strand-break (DSB) repair (Mallette et al. 2012). KDM4A/B binds to H4K20me₂, preventing recruitment of 53BP1, an important factor for DSB repair. In response to DNA damage, RNF8 and RNF168 are recruited to the damage site, ubiquitinating and degrading KDM4A/B. Once KDM4A/B is degraded and released from the H4K20me₂ site, 53BP1 accumulates to perform DNA repair (Mallette et al. 2012).

Taken together, KDM4B is overexpressed in multiple cancers and plays an important role in cancer cell proliferation and invasion. However, because of the heterogeneity of cancer, how KDM4B functions in each cancer type may be unique. Detailed mechanism of how KDM4B regulates colorectal cancer is still unclear. No studies have been reported regarding how KDM4B functions in renal cell carcinoma or epithelial ovarian cancer. Systematic studies identifying the genes regulated by KDM4B in these cancers will reveal novel mechanisms that are specific for each cancer type, which may lead to more effective targeting therapy (See Chapter 2).

Heterogeneity of Cancer

The heterogeneity of cancer makes it a difficult disease to treat. Not only are cancers generated from different organs highly distinct, but even patients with the same cancer type frequently have unique disease presentation and therapeutic response (Jamal-Hanjani et al. 2015). Within the same tumor, there are also distinct cellular populations with specific genetic, epigenetic, and phenotypic features (Jamal-Hanjani et al. 2015). The same primary tumor may contain different cellular populations that would generate metastatic lesions at different secondary sites, resulting in heterogeneity among metastases (Jamal-Hanjani et al. 2015). In addition, as cancer progresses, both primary and metastatic lesions can acquire new mutations and evolve independently with each cell division (Jamal-Hanjani et al. 2015). Therefore, finding a common regulatory mechanism among different cancer types may contribute significantly to cancer therapy efficiency by treating several cancers with the same drug.

Colorectal Cancer

Colorectal cancer (CRC) is the second most common cancer in males and the

third most common cancer in females in the United States, with an estimated diagnosis of 71,830 men and 65,000 women and an estimated death of 26,270 men and 24,040 women in the year of 2014 (Siegel et al. 2014a). Consumption of red meat and alcohol, obesity, and a history of inflammatory bowel disease are associated with a higher risk of CRC (Stintzing 2014). Although hereditary syndromes, such as familial adenomatous polyposis and hereditary non-polyposis CRC, and familial clustering are assumed to account for some cases of CRC, the vast majority of CRC are sporadic (about 75%) (Stintzing 2014). Survival rates of CRC depends on its staging, which is classified based on the size of the primary tumor (T stage), the involvement of lymph nodes (N stage), and the occurrence of distant metastases (M stage) (Stintzing 2014). The availability of screening programs and the development of more effective therapies have improved the 5-year survival rates of CRC (all stages) from about 51% in 1977 to about 65% in 2009 when all races are taken together (Siegel et al. 2014d). Patients with Stage I or II tumor (Union for International Cancer Control (UICC)) have an excellent 5-year survival rate after surgery alone, whereas 5-year survival rates of Stage IV patients remain low at about 15%, even with modern improved surgical techniques and targeted therapies (Kopetz et al. 2009).

Genetic alterations considered responsible for CRC development are *APC*, *TP53*, and *KRAS* mutations (Vogelstein et al. 1988). The canonical adenoma-carcinoma development of CRC is classified by Wnt pathway dysregulation (He et al. 1998). CRC may also develop through serrated polyps with early *BRAF* mutations (Noffsinger 2009). The Cancer Genome Atlas Network study with next-generation sequencing on 97 colorectal tumors has revealed a complex network of genetic alterations leading to the

dysregulation of multiple pathways in CRC (Cancer Genome Atlas 2012).

Currently, the most effective chemotherapy combination for malignant CRC treatment consists of a fluoropyrimidine with irinotecan or oxaliplatin (de Gramont et al. 2000; Douillard et al. 2000; Saltz et al. 2000). However, the benefit of oxaliplatin on patient overall survival is restricted to younger patients (<70 years) and is not well established for older patients (≥70 years) (McCleary et al. 2013). Targeted therapies using antibodies against VEGF (bevacizumab) or EGFR (cetuximab) have recently shown some efficacy in combination with chemotherapies (Stintzing 2014).

KDM4B plays important roles in CRC tumorigenesis and proliferation. Fang's laboratory has discovered that induction of KDM4B by HIF-1 α contributes to the malignant phenotype of CRC by regulating some proliferative and metastatic genes (Fu et al. 2012). They then went on to demonstrate that KDM4B silencing induced DNA damage and cell apoptosis (Chen et al. 2014; Sun et al. 2014). With a more detailed mechanism, Berry et al. showed that KDM4B contributed to CRC tumorigenesis by interacting with the key regulator in its canonical developmental pathway, β -catenin, in its central amino acids 353-740 (Berry et al. 2014). The complex formed by KDM4B, β -catenin, and the DNA-binding protein TCF4, which is the main factor recruiting β -catenin to chromatin in the intestine, contribute to the expression of β -catenin/TCF4 downstream oncogenes, such as JUN, MYC and Cyclin D1 (Berry et al. 2014). These findings indicate KDM4B may be an interesting target for CRC therapy. However, with only four studies published regarding the contribution of KDM4B to CRC development, more investigation is still necessary for a better understanding of its therapeutic potential.

Renal Cell Carcinoma

Another cancer that is influenced by HIF signaling is renal cell carcinoma (Gudas et al. 2014). The estimated diagnosis of renal cell carcinoma (RCC) is 39,140 for men and 24,780 for women in the year of 2014. It was estimated that 8,900 men and 4,960 women would die of RCC in 2014 (Siegel et al. 2014d). The 5-year survival rates of RCC has improved from 50% in 1977 to 73% in 2009 due to improved surgical management of the primary tumor and increased understanding of the molecular biology and genomics of the disease (Siegel et al. 2014d). RCC may be classified into three types, clear cell RCC (most common, 70% of all kidney cancers), papillary RCC (Type I and Type II), and chromophobe RCC (lowest-risk of developing metastases) (Jonasch et al. 2014). The most common genetic feature associated with clear cell RCC is loss or mutation of the *von Hippel-Lindau (VHL)* tumor suppressor gene, which is identified in 60-90% of sporadic cases. The loss of this protein results in stabilization of the HIFs, transactivating genes involved in angiogenesis, cell migration, and metabolism.

Other genetic events closely associated with RCC include inactivated *PBRM1*, *BAP1*, and *SETD2*, and mutations in a variety of additional histone modifiers (*KDM5A*, *ARID1A*, and *UTX*) (Dalgliesh et al. 2010; Varela et al. 2011; Jonasch et al. 2012; Penallapis et al. 2012). RCC patient survival is also correlated to its staging. The five-year survival rate for patients with stage I and II RCC (American Joint Committee on Cancer (AJCC) staging system) is approximately 80-95%, if tumors invade the urinary collecting system, survival is reduced to approximately 60%, similar to the five-year survival rate of Stage III patients (Elmore et al. 2003; Verhoest et al. 2009). With the development of

targeted agents, the overall survival of Stage IV patients has increased from 10 months to beyond two years since the 1980s (Motzer et al. 1999; Gore and Larkin 2011). The current standard practice for RCC is cytoreductive nephrectomy followed by treatment with a chosen combination of immunotherapeutic drugs, antiangiogenic agents, and mTOR inhibitors (Jonasch et al. 2014). However, despite the improvement in therapeutic effectiveness, mortality rate of RCC remains high at an average of 37% (Siegel et al. 2014a). Better treatments are clearly needed.

KDM4B overexpression has been reported in RCC cells (Beyer et al. 2008; Krieg et al. 2010). However, no study has ever demonstrated its function and regulatory mechanism in RCC. KDM4B may play important roles in RCC, yet much more study is needed for a thorough understanding of the potential of using KDM4B as a target for RCC therapy.

HIF and Ovarian Cancer

The Hypoxia Inducible Factor 1 (HIF1) is associated with poor prognosis of ovarian cancer as well as other cancer types. In response to hypoxia, HIF1 induces genes that promote ECM remodeling, migration and metastasis in ovarian cancer (Rankin et al. 2010; Horiuchi et al. 2012; Ji et al. 2013). Birner et al. showed that although HIF-1 α overexpression alone was not a prognostic indicator, it became a strong prognostic marker in combination with mutation of the *TP53* tumor suppressor (Birner et al. 2001). Lee et al. suggested that tumor hypoxia might play a role in conferring chemoresistance in ovarian clear cell carcinoma by HIF-1 α nuclear localization (Lee et al. 2007). Wong et al. demonstrated a higher expression of VEGF and HIF-1 α in epithelial ovarian cancer cells compared to normal ovarian tissue and a

strong correlation between the two factors, indicating high level of HIF-1 correlates to higher angiogenesis (Wong et al. 2003). Moreover, Osada et al determined that nuclear HIF-1 α might represent an important biological marker in the evaluation of the prognosis of patients with ovarian carcinoma by showing that nuclear expression of HIF-1 α was significantly higher in tumors of Stages III and IV (International Federation of Gynecology and Obstetrics (FIGO)) than in those of FIGO stages I and II (Osada et al. 2007). Studies have also shown that the hypoxic microenvironment upgrades the stem-like properties of ovarian cancer cells and promote ovarian CSC expansion (Liang et al. 2012; Nozawa-Suzuki et al. 2015). Therefore, HIF-1 α expression and localization appear to play an important role in ovarian cancer progression.

Epithelial Ovarian Cancer

Epithelial ovarian cancer (EOC) represents 80% of all ovarian cancers (Lengyel 2010). It is the 10th most common cancer among women and the fifth leading cause of mortality, making it the most deadly of gynecologic cancers. Approximately 21,300 new cases of ovarian cancer will be diagnosed in 2015, accompanied by 14,180 patient deaths (ACS 2015). EOC is a highly heterogeneous disease, generally stratified by the aggressiveness of growth, with slower growing Type I tumors having better prognosis than more rapidly growing Type II tumors (Vang et al. 2009). Type I EOC classifies low-grade carcinomas that develop in a stepwise manner from an atypical proliferative tumor through a noninvasive stage (LMP) before becoming invasive, with frequent mutations in *KRAS*, *BRAF*, or *ERBB2* genes, whereas Type II EOC includes high-grade, less differentiated, malignant cancers that are characterized by mutations and/or loss of heterozygosity in *TP53* and *BRCA* loci (Vang et al. 2009).

EOC is also categorized into four pathological subtypes: serous, endometrioid, mucinous, and clear-cell carcinoma (Lengyel 2010). Histology of the well or moderately differentiated serous adenocarcinoma resembles the papillary surface epithelium of the fallopian tube, which is why the fallopian-tube-origin of EOC was hypothesized. Endometrioid carcinoma resembles endometrioid carcinomas of the uterus. The more well-differentiated areas of mucinous carcinomas resemble either endocervical glands or gastrointestinal epithelium. Clear-cell carcinoma of the ovary is a rare subtype that shares morphological features with both serous and endometrioid ovarian carcinoma.

The majority of Type II EOC patients are diagnosed at an advanced FIGO stage (Stage III or IV), with widespread dissemination of metastatic tumors throughout the peritoneal cavity (Naora and Montell 2005; Vang et al. 2009; Lengyel 2010). Of the 4 general pathological subtypes that comprise EOC, the majority of the Type II (or high grade) EOC are high grade serous adenocarcinoma (HGSA), which represent 70% of the total EOC cases (Vang et al. 2009; Lengyel 2010).

The origin of HGSA has been debated over the years. The ovarian surface epithelium (OSE) has been accepted as the origin of HGSA for over 40 years. However, histologic characteristics of HGSA resembles that of mullerian-like tissues, whereas the OSE is derived from the coelomic epithelium next to the gonadal ridge. One study by Dr. Naora's laboratory demonstrated that expression of the HOX genes can lead undifferentiated transformed mouse ovarian surface epithelial cells to undergo differentiation and form tumors that histologically resemble serous carcinomas, endometrioid-like or mucinous-like ovarian carcinomas, confirming the possibility of dedifferentiation and re-commitment of cancer cells during tumorigenesis (Naora and

Montell 2005; Lengyel 2010). Recent genomic analyses have demonstrated that the majority of HGSA patients have mutations in the tumor suppressor *TP53*, with significant proportions also containing mutations in *BRCA1*, *BRCA2*, and the *pRB* pathways (Cancer Genome Atlas Research 2011). Recent studies suggest that additional sites of origin exist and a substantial proportion of cases may arise from precursor lesions located in the fallopian tubal epithelium (Perets et al. 2013). This hypothesis is based on the detection of early lesions, namely serous tubal intraepithelial carcinomas (STIC), found in the fallopian tubes of both women at high-risk for developing serous carcinomas as well as patients with disseminated HGSCs (Perets et al. 2013).

Current Therapies for HGSA

The front-line therapy for HGSA consists of surgical debulking followed by treatment with platinating agents and taxol derivatives (Lengyel 2010). The initial response of patients to the combination of carboplatin and paclitaxel is generally effective, however resistant tumors typically recur within 2-4 years (Lengyel 2010). This rapid recurrence is caused by re-growth of residual, chemoresistant cancer cells residing in the peritoneal cavity. Moreover, this rapid re-establishment of tumor growth suggests that a process inherent to EOC progression facilitates adaptation to the respective stresses imposed by the metastatic process, surgery, and chemotherapy.

Over more than 40 years, the five-year survival rate of ovarian cancer in all races has increased only slightly, from 36% to 44%. However, when dividing the patients into categories, it increased from 35% to 44% in the white population but decrease from 42% to 36% in the black population (Siegel et al. 2014d). Therefore, a more thorough

understanding of the molecular mechanisms driving EOC metastasis is still very important for improving our ability to prevent recurrence.

Research Objectives: KDM4B Function and Regulatory Mechanism in Cancer

The discovery of the regulation between hypoxia and histone demethylases has uncovered an interesting aspect in cancer biology. As reviewed above, several histone demethylases, such as KDM3A, KDM4B, KDM4C, and KDM5B, are regulated by hypoxia. These histone demethylases have demonstrated important functions in promoting or suppressing tumor growth. These findings have made histone demethylases, especially the KDM4 subfamily interesting targets for cancer treatment. However, the mechanism of how KDM4B regulates tumor progression is still not clear, especially in CRC, RCC, and EOC. Some of the clear remaining questions include: 1. As a universally expressed histone demethylase, how general is the regulation by KDM4B in different cancer types and what are its downstream pathways in these cancer types? 2. Is it also overexpressed in EOC and if so, what are the functional roles of KDM4B in EOC? 3. How well can the JmjC domain function at low oxygen tension, since its enzymatic activity also requires oxygen?

In this study, **I hypothesize that KDM4B regulates general tumorigenic mechanisms that are shared by different cancer types as well as mechanisms that are specific for individual cancer types. KDM4B expression is induced by hypoxia in EOC cells and may regulate genes and pathways that contribute to EOC tumorigenesis and progression.**

To test this hypothesis, I proposed the following aims:

Aim 1. Identify potential common and tissue-specific target genes and pathways

regulated by KDM4B in three cancer types. Hypothesis: KDM4B regulates distinct genes and pathways in different cancer types by demethylating H3K9me3/me2 in target gene promoters.

- a. Identify potential target genes and pathways regulated by KDM4B in three cancer cell lines through microarray analysis.
- b. Characterize the regulation of important KDM4B downstream targets in ovarian cancer progression and validate target gene expression and KDM4B demethylation through qRT-PCR, western blot and ChIP.

Aim 2. Determine the functional role of KDM4B in regulating the progression of ovarian cancer. Hypothesis: KDM4B contributes to ovarian cancer proliferation and/or metastasis both *in vitro* and *in vivo*.

- a. Study the role of KDM4B in mediating cancer progression using *in vitro* functional analysis of OVCAR cell lines, including cell proliferation, migration, invasion, and attachment-free growth.
- b. Explore the functional role of KDM4B *in vivo* through intraperitoneal tumor xenograft growth of OVCAR cell lines in nude mice.

Experimental findings related to Specific Aim 1 are presented in Chapter 2 and those associated with Specific Aim 2 are presented in Chapter 3.

Significance of the study: KDM4B expression is induced by HIF-1 α in hypoxia (Beyer et al. 2008; Krieg et al. 2010). Elevated levels of KDM4B have been detected in many cancer types, yet its regulation is poorly understood in CRC, and has never been demonstrated in RCC or EOC. By studying its downstream pathways in these three

cancers, we will have a more fundamental understanding in how KDM4B contributes to the progression of each cancer. By studying its functional role in ovarian cancer progression, we may bring better understanding of the complex network contributing to ovarian cancer metastasis, which is one of the main reasons for the high mortality rate of HGSA. Characterizing KDM4B function in HGSA metastasis will be important for the development of more effective therapies.

CHAPTER 2:

**KDM4B REGULATES DISTINCT PATHWAYS IN THREE DIFFERENT CANCERS
AND IN DIFFERENT OXYGEN CONDITIONS**

ABSTRACT

Solid tumors contain hypoxic regions due to their unchecked proliferation. This hypoxic microenvironment induces expression of genes involved in metastasis and angiogenesis to promote tumor survival. The hypoxia-inducible factors (HIFs) are the primary regulators of the hypoxic response, inducing genes involved in important tumor progression pathways. The lysine (K)-specific demethylase KDM4B is a direct target of HIF, creating an intriguing link between the hypoxia tumor microenvironment and downstream gene expression beyond the direct actions of HIF stabilization. The findings that hypoxia-inducible KDM4B overexpression occurs in multiple cancer types suggests a general mechanism for KDM4B to regulate gene expression in these cancers. However, our current knowledge on KDM4B function in each cancer type seems to rely on a tissue-specific pathway. In a microarray analysis using transient knockdown of KDM4B, we identified a set of potential KDM4B targets with clear associations to tumor cell growth, migration, and metastasis. Microarray data from HCT116 colon carcinoma cells, SKOV3ip.1 ovarian cancer cells and RCC4 renal cell carcinoma cells identified numerous genes specifically regulated in each cell type, as well as 16 common targets shared by all three cell lines. Through Ingenuity Pathway Analysis, we found that not only did KDM4B regulate distinct targets in different cancer types, it also regulated different pathways under different oxygen conditions. In general, KDM4B regulated proliferation-related genes in normoxia, and migration-related genes in hypoxia. We have also demonstrated that KDM4B regulated these target genes by binding and demethylating near the promoter regions of these genes. Our findings suggest that KDM4B regulates pathways specific to each cancer type and tumor microenvironment

to support cancer cell survival.

INTRODUCTION

Hypoxia, or low oxygen tension, is a common feature of solid tumors. In response to hypoxia, cells manipulate their gene expression to promote survival (Chan and Giaccia 2007). This is not only important for normal development but is also critical for tumor progression. Hypoxia has been reported to contribute to metastasis, glycolysis, and angiogenesis, which correlates to poor prognosis and patient outcome (Chan and Giaccia 2007).

A key regulator of the hypoxic gene expression pattern is the HIF family of transcription factors (Krieg et al. 2010). Downstream HIF targets play important roles in various pathways, including glycolysis, tissue remodeling, viability, proliferation, migration, and angiogenesis (Krieg et al. 2010). One of these known HIF targets is lysine (K)-specific demethylase 4B (KDM4B, also known as JMJD2B) (Krieg et al. 2010). KDM4B catalyzes the demethylation of H3K9me3/me2, leading to gene activation (Fodor et al. 2006). Its amplification has been detected in multiple cancer types, including ER+ breast cancer, colon cancer, renal cell carcinoma, gastric cancer, prostate cancer, and osteosarcoma (Beyer et al. 2008; Krieg et al. 2010; Kawazu et al. 2011; Li et al. 2011b; Fu et al. 2012; Berry et al. 2014; Chu et al. 2014; Li and Dong 2015). In several cancer types, KDM4B promotes cancer cell proliferation by regulating cell cycle genes and oncogenes, inhibiting cell apoptosis, and promoting DNA damage repair (Yang et al. 2010; Kawazu et al. 2011; Toyokawa et al. 2011; Kim et al. 2012a; Chen et al. 2014; Sun et al. 2014; Li and Dong 2015). KDM4B contributes to gastric and

colon cancer metastasis through the Wnt signaling pathway (Kim et al. 2012a; Zhao et al. 2013a). However, its molecular mechanism is still unclear in most cancer types.

There is only limited understanding of KDM4B-dependent regulation in colon cancer. To date, no study has been reported regarding the function of KDM4B in ovarian cancer or renal cell carcinoma.

Colorectal cancer (CRC) is the second most common cancer in males and the third most common cancer in females (Siegel et al. 2014a). Late-stage CRC survival remains low even though all-stage survival has been improved by the implementation of screening programs in combination with the development of more effective therapies. (Kopetz et al. 2009). Genetic alterations considered responsible for CRC development are *APC*, *TP53*, and *KRAS* mutations (Vogelstein et al. 1988). The most effective chemotherapy combination, a fluoropyrimidine with irinotecan or oxaliplatin, is not applicable to all patients due to its high toxicity. Therefore, novel therapies with less toxicity need to be developed to improve patient outcome of CRC. KDM4B has demonstrated some promising roles in CRC tumorigenesis through mediating proliferative pathways, preventing apoptosis, and promoting DNA damage repair, indicating it may be an interesting target for CRC therapy (Fu et al. 2012; Berry et al. 2014; Chen et al. 2014; Sun et al. 2014).

The most common genetic feature associated with clear cell renal cell carcinoma is loss or mutation of the *von Hippel-Lindau (VHL)* tumor suppressor gene, which leads to constitutively active HIF signaling. Although improvement of surgical methods and the application of targeted therapies have improved the survival rate of RCC, its mortality rate remains high and better treatments are clearly needed (Motzer et al. 1999; Gore

and Larkin 2011). Studies have shown that KDM4B is overexpressed in RCC, yet its function in RCC has not been reported at this time. Therefore, understanding the pathways regulated by KDM4B in RCC may lead to novel targets that would improve RCC therapies.

Epithelial ovarian cancer (EOC) is the most deadly of gynecologic cancers. The main reason for its high mortality rate is late diagnosis, at which time the cancer has often disseminated throughout the peritoneal cavity and ascites fluid has developed. Although current surgical and chemotherapeutic approaches may successfully remove primary and metastatic tumors, recurrence typically occurs within five years. This poor prognosis of EOC has not been improved over the past 40 years (Siegel et al. 2014d). Therefore, a more thorough understanding of the molecular mechanisms driving EOC metastasis is still very important for improving our ability in preventing recurrence. Although little has been reported regarding KDM4B expression or function in EOC, the hypoxia-inducible expression of KDM4B and its contribution to other cancer types indicate it may also play an important role in EOC proliferation and progression.

In this study, we identified the genes regulated by KDM4B in normoxia and hypoxia in the HCT116 colon carcinoma cells and SKOV3ip.1 ovarian cancer cells using microarray analysis and quantitative PCR. We also conducted parallel studies using RCC4 renal cell carcinoma cells, which do not have functional VHL thus leading to a “pseudo-hypoxic” phenotype. By comparing the microarray data of the three cell lines, we found 16 common targets, as well as many tissue-specific targets that were down-regulated by knockdown of KDM4B. Two of the 16 common targets are LOXL2 and ERO1L, which are involved in ECM remodeling and VEGF secretion, respectively,

indicating KDM4B plays an important role in regulating target genes that are involved in general cancer progression (May et al. 2005; Barker et al. 2011). By comparing KDM4B targets in normoxia and hypoxia in each cell line, we have also found that KDM4B regulates distinct pathways in different oxygen conditions, where it regulates proliferative pathways in normoxia and metastatic pathways in hypoxia. These studies have defined a hypoxia-induced metastatic pathway regulated by KDM4B, confirming the importance of histone demethylation as a mechanism for promotion or maintenance of the hypoxic cancer phenotype. Understanding this regulatory mechanism of KDM4B in the hypoxic tumor microenvironment is therefore important for possible discovery of new cancer therapies.

MATERIALS AND METHODS

Cell Lines and Culture Conditions

HCT116 and RCC4 cell lines were maintained in Dulbecco's Modified Eagle Medium (DMEM, Invitrogen) supplemented with 10% heat-inactivated fetal bovine serum (HI-FBS) and 1% Penicillin Streptomycin (Pen Strep, Invitrogen). OVCAR cell lines SKOV3ip.1 and OVCAR8 were maintained in RPMI-1640 (Invitrogen) supplemented with 10% heat-inactivated fetal bovine serum (HI-FBS) and 1% pen-strep (Invitrogen). HCT116 and RCC4 cells were obtained from Dr. Amato Giaccia (Stanford University). SKOV3ip.1 cells were acquired from Dr. Erinn Rankin (Stanford University) with permission from Dr. Gordon Mills (M.D. Anderson Cancer Center). OVCAR8 cells were purchased from the NCI repository by Dr. Adam Krieg and Dr. Katherine Roby. Upon receipt, cells were expanded in culture to establish early passage stocks. After transducing with lentiviral constructs containing shRNA, as will be described later in

more details, cells were used for experiments within 1-2 months to minimize cell drift or contamination. For transient knockdown of KDM4B, SKOV3ip.1 cells were transfected with a pool of small interfering RNAs (siRNAs) targeting specifically to KDM4B (siK4B, Dharmacon siGenome Smartpool, Thermo Scientific) using Dharmafect 1 transfection reagent according to manufacturer's protocol (Thermo Scientific). Scrambled siRNA (siCon, Dharmacon SiControl 2, Thermo Scientific) was used as the control group. For long-term stable knockdown of the gene, cells were transduced with lentivirus containing short hairpin RNA (shRNA) retroviral constructs against KDM4B (Open Biosystems; shKDM4B-1-puro (shK-1, TRCN0000018014) and shKDM4B-2-puro (shK-2, TRCN0000018016)) and selected in puromycin for 2 days. For short-term hypoxia treatment (16-24 hours), cells were incubated in Ruskinn InVivo300 glove-box hypoxic incubators (Baker) in which oxygen levels were maintained at 0.5% or 2% for 16-24 hours depending on specific experimental needs. For longer duration experiments (i.e. *in vitro* proliferation assays), cells were cultured in HeraCell150 incubators set to the indicated oxygen tension (Thermo Fisher Scientific, Inc.).

QRT-PCR.

Quantitative real-time PCR (qRT-PCR) was conducted using a modification of previously described methods (Krieg et al. 2010). Briefly, total RNA was isolated from 3×10^5 cells with TRiReagent (Sigma-Aldrich) according to the manufacturer's protocol. 500 ng of total RNA was reverse transcribed with MMLV reverse transcriptase (Life Technologies) and 5 μ M random primers (Life Technologies) according to the manufacturer's instructions. Approximately 0.5% of each reverse transcription reaction mixture was added to each reaction containing 5 μ L 2X SYBR green master mix (Life

Table 2.1. Primers Used For Qrt-PCR.

Gene	Forward (5'-3')	Reverse (5'-3')
hsKDM4B	ggactgacggcaacctctac	cgctctcaaactccacctg
hsKDM4A	gccgctagaagtttcagtgag	gcgcccttgacttcttatt
hsKDM4C	aggcgccaagtgatgaag	gagaggtttcgccaagact
hsKDM4D	ggacaagcctgtaccactgag	ctgcacccagaagccttg
shCLDN12	gctgttttgaactgtcaggta	ttccacacaggaaggaaagg
shLUZP6	ggagacttgatgaggtgaaag	caccttctagtgtccggttga
shSEPT2	tctgaagctgagaacctatgc	cataatgaaggctctgggtcac
shMMD	tcttttctatctcacaatgggatt	ctgaagtcctcgggtgtgtt
hsLOXL2	tgacctgctgaacctcaatg	tggcacactcgtaatcttctg
shOSMR	tgtctggagaattgtgagcttg	catgcagtttgataatggcttc
shPALLD	aacaccagctgtcctgcttt	ggccttctttggaaatcctagt
hsERO1L	ggagacagcggcacagag	caatggttcaacatcacaggt
shUSP6NL	tgaggaggagctcccagat	ttcaatttccagggtgcttttg
shELAVL1	cctcgtggatcagactacaggt	ctgggggtttatgaccattg
shBACE2v1	tccatctacctgagagacgaga	tgggctgaatgtaaagctga
shTWSG1	gtgagcaaatgcctcattca	cactccttacagcaggagcaa
shZAKv2	tgacagagcagccaacacc	gacatgacatctctgcactgttt
hsBRCA2	cctgatgcctgtacacctctt	gcaggccgagtactgttagc
hsSKAP2	tggagcttttctgatgagttgt	tctcctaccaccagccata
hsCEP70	gctgatcccagcctaacct	cccaacgagtctcatgtctg
hsUCK2	tccagatccccgtgatgac	acgtctgcgggatagacagt
hsMAP3K2	tctggctcaggaagttgtcc	agctctgagccctaggcatt
hsMAP3K5	cacgtgatgacttaaaatgcttg	agtcaatgatagccttccacagt
hsMAP4K3v1	agctttggattgcatggag	ttctgacagaggtccagttacg
hsMAP4K4v2	caggacaagctcactgctaattg	tctgggtctataaaagggtgtaaag
hsMEF2Av1	tgatgcggaatcataaaatcg	tggaactgtgacagacattgaa
hsMEF2Av2	tgaagatagtgattttatttcaaacg	gtgacagacattgaaaagttctgag
hsRAB31	gctgcagctgttatcgtgatg	ggccattacaatgttttctgg
hsTRAF1a	ctgtgcaggctgtctctctg	cggcttctgggcttatag
hsTNFSF14	agcgaaggctctcacgaggt	cggcaagctggagttgg
hsLPP	cactgcattgaggactcca	caaagccacaatacggacag
hsITGB8	gcattatgtcgaccaaactca	gcaaccaatcaagaatgtaact

hsFGFRL1	cagcctgagcgtcaactaca	ctctcctccctgggcta
hsITGB5	ggagtttgcaaagttcagagc	tgtgctggagataggctt
hsPDGFBv1	ctggcatgcaagtgtgagac	cgaatggtcacccgagtt
hsPDGFBv2	ctggcatgcaagtgtgagac	cgaatggtcacccgagtt
hsMYD88	ttctcgaaagcgaaagc	attgtctgccagcgcttc
hsTLR3	agagttgtcatcgaatcaaattaaag	aatctccaattgctgaaaa
hsTLR5	ctgtccgaacctggagaca	tctgagactataggaatctcatcac
hsIL8	agacagcagagcacacaagc	atggttcctccggtgt
hsSMAD3	tagctcccggtagaggatca	aaggctgggaaaagaagagg
hsIRAK2	aactgtggacctcctgtgc	ccggttccagttcaggat
hsIL6	gatgagtacaaaagtcctgatcca	ctgcagccactggttctgt
hsIL6ST	aggaccaaaagatgcctcaac	gaatgaagatcgggtggatg
hsIL1 β	ctgtcctgctgttgaaaga	ttgggtaattttgggatctaca
hsIL1R1	ccaagaagaatataaaagtggtactca	ttcttcacgtccttgattt
hsIL1R2	cagaaagagcttctgaaggaagac	acacgggaagtggaggact
hsIGFBP1	aatggattttatcacagcagacag	ggtagacgcaccagcagagt
hsLCN2	ctccacctcagacctgatcc	acataccacttcccctggaat
shLOXv1	ggatacggcactggctactt	gacgcctggatgtagtaggg
shLOXv2	tgggaatggcacagttgtc	aaactgctttgtggccttc
shTGFB1	actactacgccaaggaggtcac	tgcttgaactgtcatagatttcg
shMIR31	tctatatcagcatccacaacctt	gaccccatTTTTCTGGAA
18S rRNA	gcccgaagcgttactttga	tccattattcctagctgcggtatc

Technologies) and 50 nM forward and reverse primers specific for the genes of interest in a total volume of 10 uL. Real-time PCR detection was performed using an ABI VIIA sequence detection system using 18S rRNA as an internal control. PCR primers (Table 2.1) were designed using the Roche Universal Probe Library design Tool (<http://lifescience.roche.com/shop/products/universal-probelibrary-system-assay-design>). Melt curve analysis confirmed formation of single amplicons of the expected size.

Microarray Analysis.

HCT116, SKOV3ip.1, and RCC4 cells were transiently transfected with siRNA to KDM4B (siK4B, Dharmacon siGenome Smartpool, Thermo Scientific) or scrambled siRNA (siCon, siControl 2, Thermo Scientific) for 32 hours before exposure to 21% (all three lines) or 0.5% oxygen (HCT116 and SKOV3ip.1 only) for an additional 16 hours. All experiments were performed in triplicate. A total of 100 ng RNA from each experimental replicate was profiled using Affymetrix GeneChip® Human Exon 1.0 ST exonic transcript arrays (Affymetrix). Each array consists of 1.4 million probe sets, of which 289,961 are core exon probes supported by putative full-length mRNA (RefSeq and full-length GenBank annotated alignments). These core probe sets map to approximately 18k genes with high confidence. These genes were the focus of the current study. The exon-arrays were RMA-background corrected, quantile-normalized and gene-level summarized using the Median Polish algorithm (Irizarry et al. 2003). The resulting log (base 2) transformed signal intensities (expression values) were used for downstream analysis. The 2-way ANOVA model: $Y_{ijk} = \mu + \text{HYPOXIC}_i + \text{Scan Date}_j + \epsilon_{ijk}$ was used to calculate the significance in differential expression in genes in different

hypoxic conditions of ovarian cancer cells, where the intercept μ models the common effect of the whole experiment and ϵ represents the random error assumed to be normally and independently distributed with mean 0 and fixed variance for all measurements. The categorical variable 'HYPOXIC' models the hypoxic state of the cells and the categorical variable 'Scan Date' models the random effect attributed to the different days in which the experiments were performed. P-values were corrected for multiple-hypothesis testing by the Benjamini and Hochberg method (Benjamini and Hochberg 1995). The analysis was done on tissue samples obtained from biological triplicates. All computations were performed in the Partek Genomic suite (v 6.5, Partek Inc.).

Potential KDM4B target genes were classified as those genes with >1.4 fold significant up- or down-regulation by siK4B knockdown ($P < 0.05$) compared to the siCon transfected cells. Hypoxia-induced genes were classified as those genes with >1.4 fold significant up-regulation comparing siCon in hypoxia (0.5% oxygen) to siCon in normoxia (21% oxygen). GeneVenn (<http://www.bioinformatics.org/gvenn/>) was employed to identify overlapping expression between different oxygen tensions and knockdown constructs. Specific Pathways influenced by KDM4B were identified using Ingenuity Pathway Analysis (Ingenuity Systems). Microarray data was deposited under accession number GSE66894 in the NCBI's Gene Expression Omnibus (Edgar et al. 2002).

ImmunoBlotting.

Cells were lysed in SDS lysis buffer (125 mM Tris-PH6.8, 1% SDS, 10 mg/ml Sodium Deoxycholate, 1 mM EDTA, 5 mM DTT) with protease inhibitor cocktail (Sigma-

Table 2.2. Dilution information of antibodies used in Immunoblotting.

Antigen	Supplier	Product NO.	Discription	Dilution
KDM4B	Cell Signaling	8639	Rabbit mAb	1:1,000
KDM4A	Cell Signaling	5328	Rabbit mAb	1:500
KDM4C	Novus	NB110-38884	Rabbit pAb	1:1,500
KDM4D	Novus	NBP1-03357	Rabbit pAb	1:2,000
histone H3	Abcam	ab1791	Rabbit pAb	1:2,000
H3K9me3	Abcam	ab8898	Rabbit pAb	1:4,000
LCN2	R&D	MAB1757	Rat mAb	1:1,000
LOX	Novus	NB100-2527	Rabbit pAb	1:2,000
α -Tubulin	Thermo	MS-581-PABX	Mouse mAb	1:2,000
Rabbit IgG (H+L)	KPL	474-1516	Goat secondary Ab	1:5,000
Mouse IgG (γ)	KPL	474-1802	Goat secondary Ab	1:5,000
Rat IgG (H+L)	KPL	474-1612	Goat secondary Ab	1:5,000

Aldrich). Following SDS-PAGE, proteins were transferred to nitrocellulose and probed with the indicated primary and horseradish peroxidase conjugated secondary antibodies (Table 2.2). Chemiluminescent signal was detected with ECL Prime reagent (GE Healthcare) using a Bio-Rad Molecular Imager ChemiDoc XRS+ equipped with Image Lab Software (Bio-Rad).

Chromatin Immunoprecipitation Assay.

Chromatin Immunoprecipitation was performed as described previously (Krieg et al. 2010), with minor modifications. Hypoxia-treated cells were fixed within the chambers to avoid reoxygenation. Fixed cells were then lysed with SDS lysis buffer and sonicated with either a Diagenode Bioruptor 300 with a chilling water bath or an Active Motif Q800AMS Sonicator[®] with an Oasis 180 Chiller with similar results. DNA concentration and sonication efficacy (DNA fragmented to less than 1000 bp, with an average length of 300 bp) from representative aliquots of input DNA were verified by spectrophotometry and gel electrophoresis, respectively. Depending on the antibody, 8~50 µg of sonicated DNA per immunoprecipitation was incubated with 1~5 µg antibody (See Table 2.3 for more specific information). Enrichment to specific regions was measured using qRT-PCR. Primers to promoters and control regions were designed using Primer Express software (Life Technologies). See Table 2.4 for a complete list of primers used. Results were normalized to input to determine relative enrichment.

Modified Histone Peptide Array.

Histone H3K9me3 antibody specificity was tested with MODified[™] Histone Peptide Array (ActiveMotif). Briefly, the array slide was blocked with 5% non-fat dried milk in TBST for one hour and then incubated with Rabbit anti-H3K9me3 antibody

Table 2.3. Antibody Dilution Used in Chromatin IP.

Antigen	Supplier	Product NO.	Discription	Dilution
KDM4B	Cell Signaling	8639	Rabbit mAb	1:100
H3K9me3	Abcam	ab8898	Rabbit pAb	2-4 µg per 25 µg chromatin
IgG Control	Cell Signaling	3900S	Rabbit mAb	560 ng/ml as control for KDM4B; 2 µg per CHIP as control for H3K9me3

Table 2.4. Primers Used in Chromatin IP.

Gene	Forward (5'-3')	Reverse (5'-3')	Genomic coordinates
ERO1L-1	ggctagtgccactgtattagaca	cctcacttcttaggcctgttct	chr14:53,163,046-53,163,127
ERO1L-2	cacctctgtgccgctgtct	gccggagctgcaatgg	chr14:53,162,096-53,162,211
LOXL2-1	agcgctcgtaaaagtgt	gctacagctgatccaatctga	chr8:23,260,663-23,260,733
LOXL2-2	tgcttgccacctcctatcc	aacactttcattcggcagcttt	chr8:23,261,969-23,262,053
PDGFB-1	gagccctccgcttaacc	cagccaggcgcaggaa	chr22:39,638,710-39,638,763
PDGFB-2	cctggcactcgggagctt	tccaggtgaggctagatgga	chr22:39,641,397-39,641,470
PDGFB-3	ggaagctggatggcaaagg	tctggcctcagcacacttct	chr22:39,637,081-39,637,147
LCN2	aagtgttccgcaggagttg	gggatctagggtgggtgat	chr9:130,911,623-130,911,702
LOX	actgagcgcaggaacttctc	cactggtccaagctggcta	chr5:121,413,216-121,413,314
DESERT-C16D8	gagcaagcagaccctaatgc	ctgtccactcaggagccttc	chr16:62,316,298-62,316,449

(Abcam; Cat# ab8898) for two hours at room temperature. The slide was then incubated with secondary antibody (KPL; Cat# 474-1516) for 30 minutes and detected with the Amersham ECL Prime Western Blotting Detection Reagent (GE Healthcare Life Sciences). Antibody specificity was analyzed with manufacturer's Array Analyze Software (Active Motif).

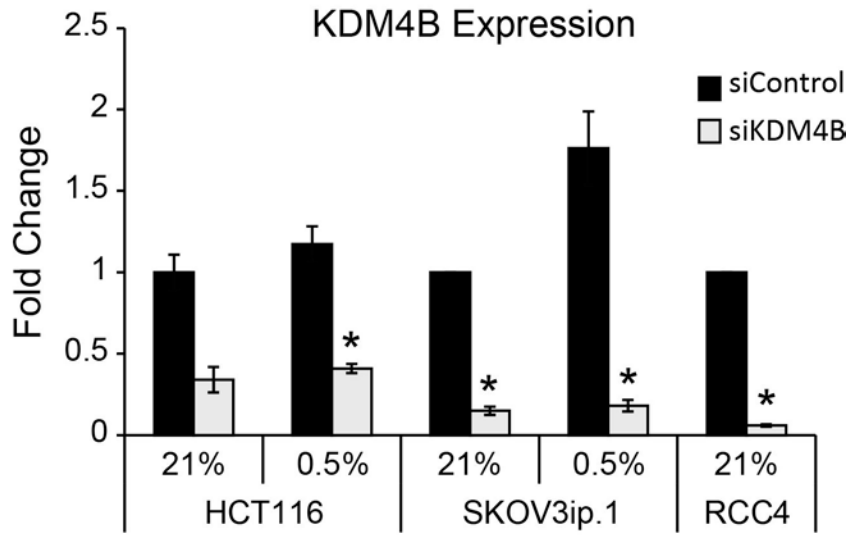
RESULTS

KDM4B Regulates Common and Tissue-Specific Targets in Three Cancer Types

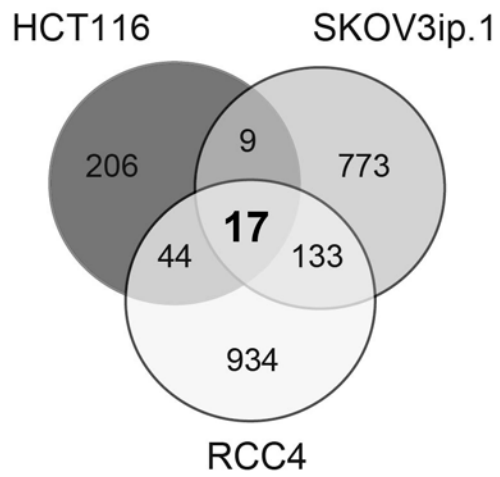
KDM4B has demonstrated functional contribution in multiple cancer types, as reviewed in Chapter 1. To determine whether the KDM4B-dependent regulation is general for multiple cancer types or specific for each cancer, we identified genes regulated by KDM4B in SKOV3ip.1 ovarian carcinoma, HCT116 colon carcinoma, and RCC4 renal cell carcinoma cell lines. SKOV3ip.1 is an epithelial ovarian cancer cell line sub-cultured from ascites cells generated by intra-peritoneal injection of SKOV3 parental cells, which do not express p53 (Yu et al. 1993; O'Connor et al. 1997). HCT116 is an epithelial colon carcinoma cell line that expresses wild type p53 (el-Deiry et al. 1994). RCC4 is a VHL-deficient renal cell carcinoma cell line that displays a "pseudo-hypoxia" phenotype (Maxwell et al. 1999). Cells were transiently transfected with siRNA to KDM4B (siK4B) or an irrelevant control (siCon), achieving robust knockdown in both standard growth condition (21% oxygen or normoxia) and hypoxia (0.5% oxygen) in all cell lines tested (Fig. 2.1A). RCC4 cells were only tested in normoxic condition since HIF-1 α is constitutively active due to its VHL-deficiency. Genes dependent on KDM4B in SKOV3ip.1 and HCT116 cells in 0.5% oxygen and in RCC4 cells in 21% were identified by microarray analysis (fold change of -1.4 or less, relative to siCon transfected cells in

Figure 2.1. Identification of common KDM4B target genes in HCT116 colon carcinoma, SKOV3ip.1 ovarian cancer and RCC4 renal cell carcinoma cell lines. A, HCT116 colon carcinoma, SKOV3ip.1 ovarian cancer, and RCC4 renal cell carcinoma cells were transfected with siRNA to KDM4B (siK4B) and control siRNA (siCon). HCT116 and SKOV3ip.1 cells were exposed to normoxia (21% O₂) and hypoxia (0.5% O₂) for 16 hours, whereas RCC4 cells were only exposed to normoxia (21% O₂). QPCR with primers to KDM4B confirmed knockdown in all three cell lines. Data represents average fold change ± SEM from three independent experiments measured in triplicate. *, p<0.05, determined by Two-tailed Paired Student's T Test. **B,** Venn Diagram showing the number of genes overlapped in the three cell lines and those that are distinct for each cancer type. RNA was profiled using Affymetrix Human Exon ST1.0 arrays in the KUMC Microarray Facility and analyzed in the KUMC Bioinformatics core using Partek RMA analysis. Genes significantly decreased in expression with siK4B (absolute decrease of or greater than 1.4 fold, p<0.05) in HCT116 cells under hypoxia are depicted in dark gray (top left), genes significantly decreased in expression with siK4B in SKOV3ip.1 cells under hypoxia are shown in light gray (top right), and genes significantly decreased in expression with siK4B in RCC4 cells are shown in white (bottom). The numbers of genes in the overlap regions are depicted.

A



B



either condition, $P < 0.05$) and compared by GeneVenn. A total of 932, 276, and 1,128 gene probes were dependent on KDM4B in SKOV3ip.1, HCT116, and RCC4, respectively. Among these gene probes, only 17 genes were commonly regulated in all three cell lines (Fig. 2.1B, Table 2.5), among which two probes represent the same gene, *SEPT2*. A majority of these targets are involved in tumorigenesis- and/or metastasis-related pathways (Table 2.5). For example, genes like claudin-12 (CLDN12), leucine zipper protein 6 (LUZP6/MPD6), septin-2 (SEPT2), monocyte to macrophage differentiation-associated (MMD), and DENN/MADD domain containing 5A (DENND5A) are involved in tumorigenesis and proliferation (Wang et al. 2006; Xiong et al. 2006; Grone et al. 2007; Morita et al. 2008; Li and He 2014), whereas lysyl oxidase-like 2 (LOXL2), oncostatin M receptor (OSMR), palladin (PALLD), endoplasmic reticulum oxidoreductin 1-like (ERO1L), and USP6 N-terminal-like protein (USP6NL/RN-tre) play important roles in cancer metastasis and are usually associated with malignancy and poor prognosis (Goicoechea et al. 2009; Barker et al. 2011; Fossey et al. 2011; Kutomi et al. 2013; Palamidessi et al. 2013). Embryonic Lethal, Abnormal Vision, Drosophila-Like 1 (ELAVL1/HuR) promotes cancer cell resistance to chemotherapy drugs or apoptosis by binding to the 3'-UTR of WEE1 or caspase 2L mRNA, respectively (Licata et al. 2010; Lal et al. 2014; Winkler et al. 2014). ZAK, ZDHHC2 and DAZAP2 appear to have tumor suppressing potential. For example, ZAK plays a role in leading cells to cell cycle arrest (Yang 2002). Reduced ZDHHC2 expression is associated with lymph node metastasis and predicts a poor prognosis of gastric cancer (Yan et al. 2013). Not much is known about the role of DAZAP2 in cancer but it has been shown to be downregulated in human multiple myeloma (Shi et al. 2007; Luo et al. 2012).

Table 2.5. List of the 16 Genes Commonly Regulated by KDM4B in Three Cancer Cell Lines.

Gene Symbol	Description	Fold change			Cell process	Citation
		CRC	EOC	RCC		
<i>CLDN12</i>	claudin 12	-1.52	-2.24	-1.7	Tumorigenesis	(Grone et al. 2007)
<i>LUZP6</i>	myotrophin; leucine zipper protein 6	-1.53	-1.44	-1.49	Myeloproliferative disease-associated antigen	(Xiong et al. 2006)
<i>SEPT2</i>	septin 2	-1.46	-1.97	-2.24	Cell division, cell proliferation; carcinogenesis	(Yu et al. 2009; Liu et al. 2010)
<i>MMD</i>	monocyte to macrophage differentiation-associated	-1.63	-4.4	-5.49	Macrophage maturation, Erk and Akt activation	(Liu et al. 2012)
<i>LOXL2</i>	lysyl oxidase-like 2	-1.62	-3.18	-3.28	Cell migration, metastasis	(Barker et al. 2011)
<i>OSMR</i>	oncostatin M receptor	-1.52	-1.61	-1.73	Angiogenesis, cell migration	(Fossey et al. 2011)
<i>PALLD</i>	palladin, cytoskeletal associated protein	-1.58	-1.47	-1.78	Cytoskeletal remodeling, metastasis	(Goicoechea et al. 2009)
<i>ERO1L</i>	ERO1-like (S. cerevisiae)	-1.43	-3.38	-2.85	Disulfide bond formation in ER	(Cabibbo et al. 2000; May et al. 2005)
<i>USP6NL</i>	USP6 N-terminal like	-1.49	-1.48	-1.82	Focal adhesion remodeling	(Palamidessi et al. 2013)
<i>ELAV1</i>	embryonic lethal, abnormal vision, Drosophila-like 1 (Hu	-1.45	-1.6	-1.63	Regulation of RNA stability	(Licata et al. 2010; Lal et al. 2014; Winkler et al. 2014)

	antigen R)					
<i>BACE2</i>	beta-site APP-cleaving enzyme 2	-1.4	-1.81	-1.8	Cleaves Amyloid-beta-precursor protein	(Farzan et al. 2000; Xie et al. 2007)
<i>TWSG1</i>	twisted gastrulation homolog 1 (Drosophila)	-1.45	-1.94	-2.39	BMP agonist	(Oelgeschlager et al. 2000)
<i>ZAK</i>	sterile alpha motif and leucine zipper containing kinase AZK	-1.54	-1.65	-1.64	Cell cycle checkpoint, proapoptotic	(Yang 2002)
<i>ZDHHC2</i>	zinc finger, DHHC-type containing 2	-1.49	-1.53	-2.06	Palmitoyl-acyltransferase, tumor suppressor	(Zhang et al. 2008)
<i>DENND5A</i>	DENN/MADD domain containing 5A	-1.4	-1.62	-2.6	Intracellular trafficking and cell cycle progression	(Li et al. 2014)
<i>DAZAP2</i>	DAZ associated protein 2	-1.52	-2.5	-3.73	TCF4 binding factor and coactivator; downregulated in multiple myeloma	(Lukas et al. 2009; Luo et al. 2012)

QPCR results showed that knocking down KDM4B significantly impaired expression of these targets, confirming the accuracy of Microarray analysis (Figure 2.3-2.6). Two independent experiments were conducted with HCT116 cells to achieve better hypoxic induction (KDM4B knockdown from HCT116 experiments were validated in Figure 2.2). Although the decrease in the expression of some targets by siK4B was not statistically significant, which was most likely due to small sample size of the experimental replicates and low expression level of some target genes, the trend of regulation of these genes by KDM4B was consistent (Figure 2.3-2.6). SKOV3ip.1 and RCC4 seemed to share more KDM4B targets (113), whereas HCT116 shared fewer common targets with each line (44 with RCC4 and only 9 with SKOV3ip.1). The majority of targets regulated by KDM4B in each cell line were specific for the line (206 for HCT116, 773 for SKOV3ip.1, and 934 for RCC4), indicating the primary regulatory mechanisms mediated by KDM4B in different cancers are distinct.

KDM4B Regulates Distinct Pathways in Different Oxygen Conditions in HCT116 and SKOV3ip.1

By comparing KDM4B targets in normoxia and hypoxia, we found that less than 10% of these targets overlapped in HCT116 cells and less than 15% overlapped in SKOV3ip.1 cells (Figure 2.7 A-B). KDM4B regulated only 3% and 11% of the hypoxia-inducible genes in HCT116 and SKOV3ip.1, respectively (Figure 2.7 C-D). A majority of KDM4B targets in hypoxia were not hypoxia-induced, suggesting KDM4B regulated genes independent from HIF or there might be other compensatory or inhibitory regulators involved.

Figure 2.2. KDM4B expression in HCT116 cells. HCT116 cells were transfected with siRNA to KDM4B (siK4B) and control siRNA (siCon). Cells were exposed to normoxia (21% O₂) and hypoxia (0.5% O₂) for 16 hours. QPCR with primers to KDM4B confirmed knockdown. Data represents average fold change ± SEM from two independent experiments measured in triplicate. *, p<0.05, determined by Two-tailed Paired Student's T Test.

KDM4B Expression

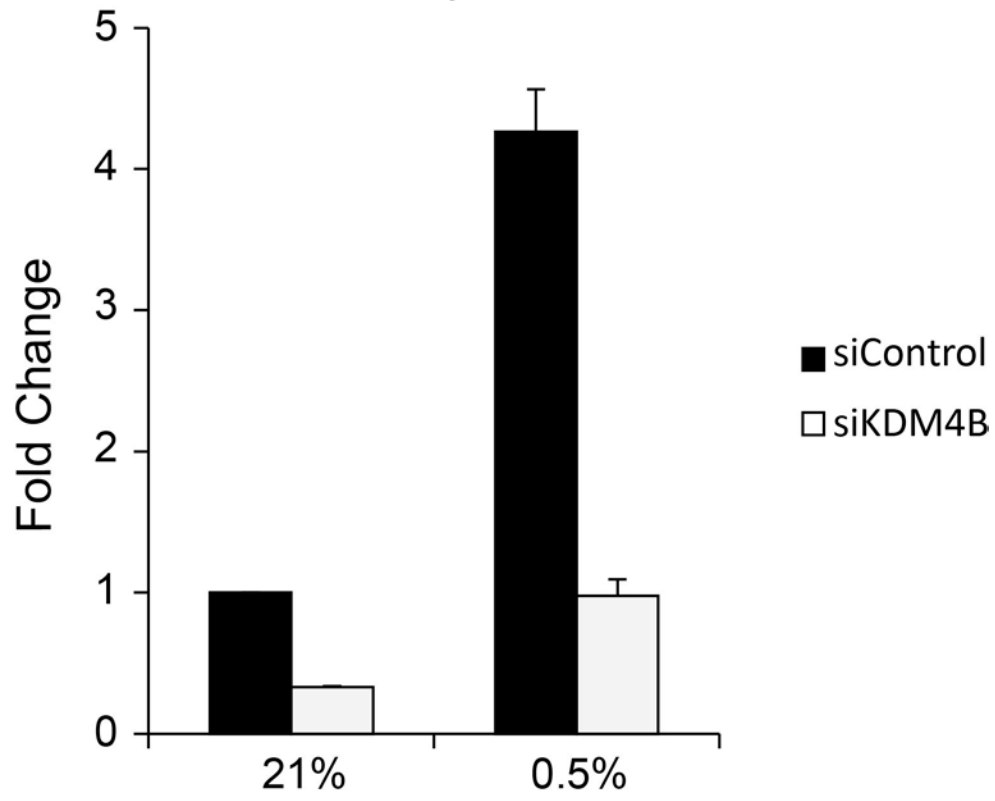
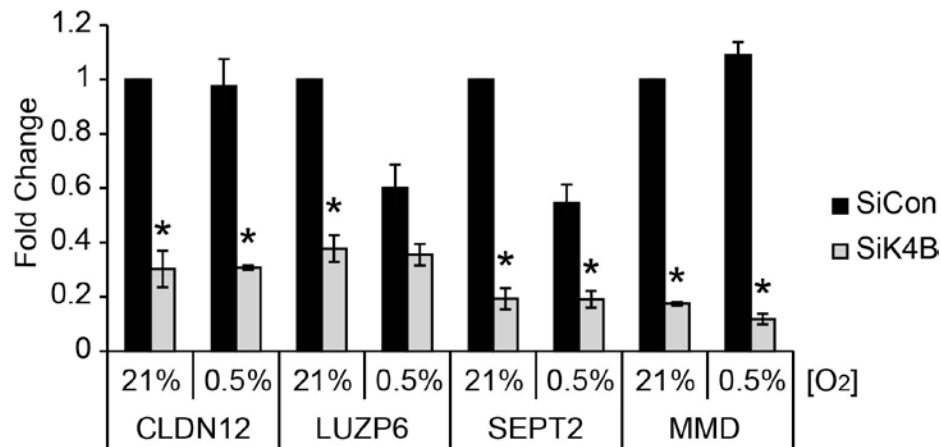
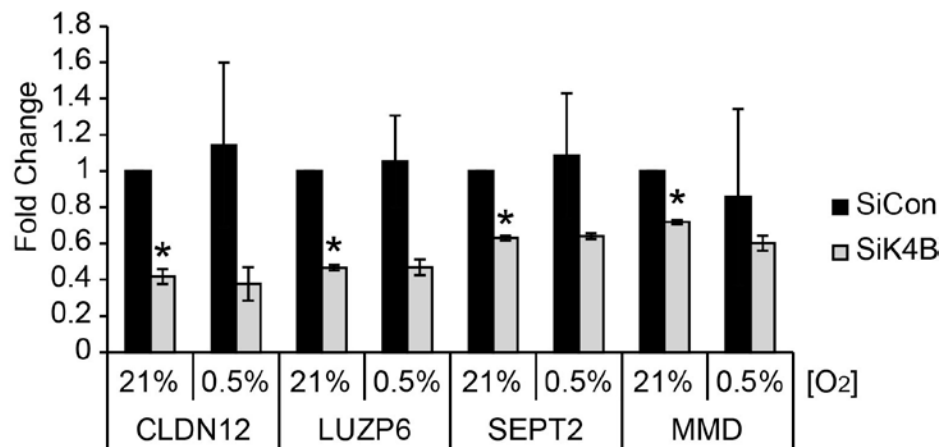


Figure 2.3. Common KDM4B targets in the SKOV3ip.1, HCT116 and RCC4 that are involved in tumorigenesis and proliferation pathways. **A**, SKOV3ip.1 RNA samples were used for QPCR. Data represent average fold change \pm SEM from three independent experiments measured in triplicate. *, $P < 0.05$, determined by Two-tailed Paired Student's T Test. **B**, HCT116 RNA samples were used for QPCR. Data represent average fold change \pm SEM from two independent experiments measured in triplicate. *, $P < 0.05$, determined by Two-tailed Paired Student's T Test. **C**, RCC4 RNA samples were used for QPCR. Data represent average fold change \pm SEM from three independent experiments measured in triplicate. *, $P < 0.05$, determined by Two-tailed Paired Student's T Test.

A Tumorigenesis/Proliferation - SKOV3ip.1



B Tumorigenesis/Proliferation - HCT116



C Tumorigenesis/Proliferation - RCC4

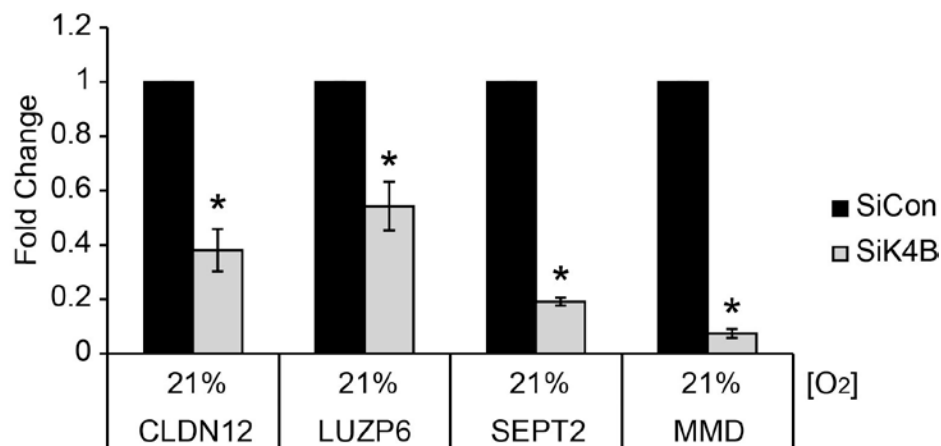


Figure 2.4. Common KDM4B Targets in the SKOV3ip.1, HCT116 and RCC4 that are involved in migration and metastasis pathways. **A**, SKOV3ip.1 RNA samples were used for QPCR. Data represent average fold change \pm SEM from three independent experiments measured in triplicate. *, $P < 0.05$, determined by Two-tailed Paired Student's T Test. **B**, HCT116 RNA samples were used for QPCR. Data represent average fold change \pm SEM from two independent experiments measured in triplicate. *, $P < 0.05$, determined by Two-tailed Paired Student's T Test. **C**, RCC4 RNA samples were used for QPCR. Data represent average fold change \pm SEM from three independent experiments measured in triplicate. *, $P < 0.05$, determined by Two-tailed Paired Student's T Test.

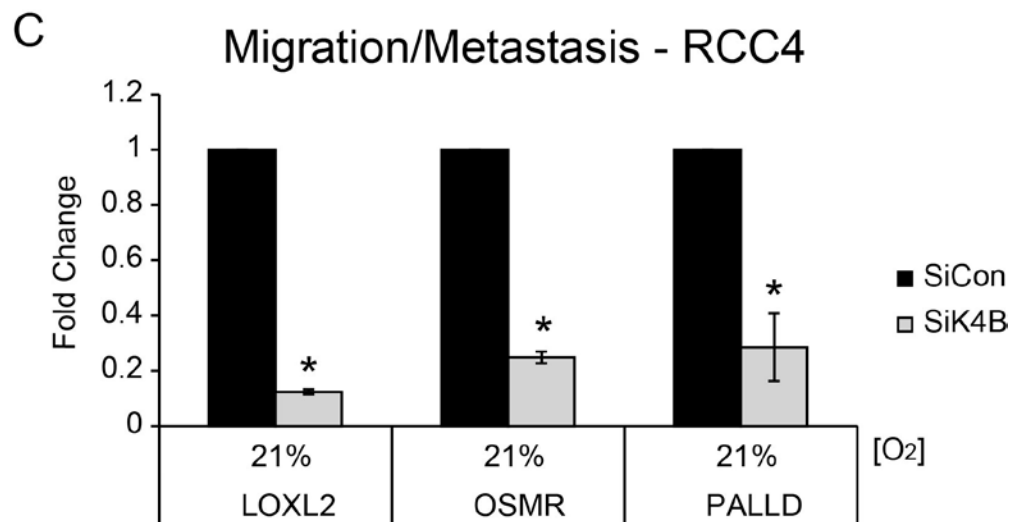
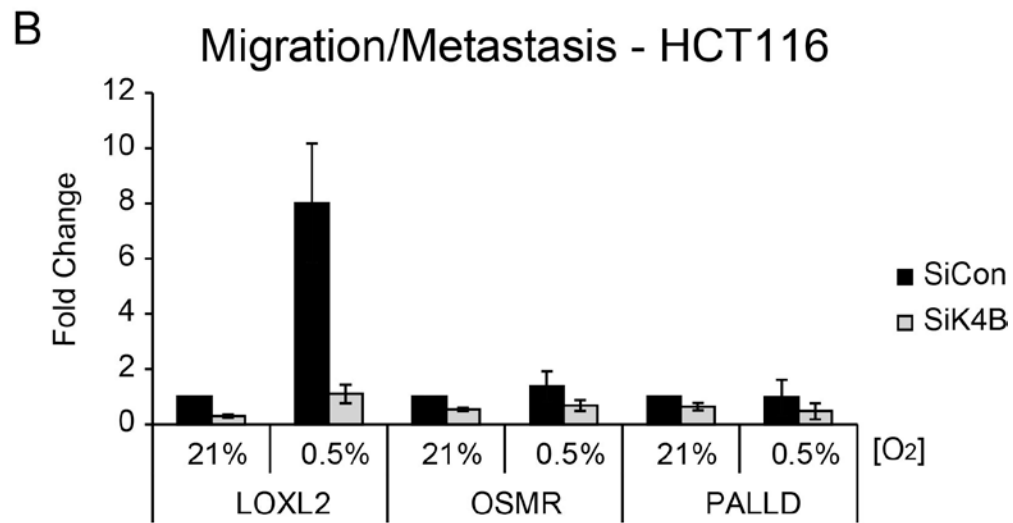
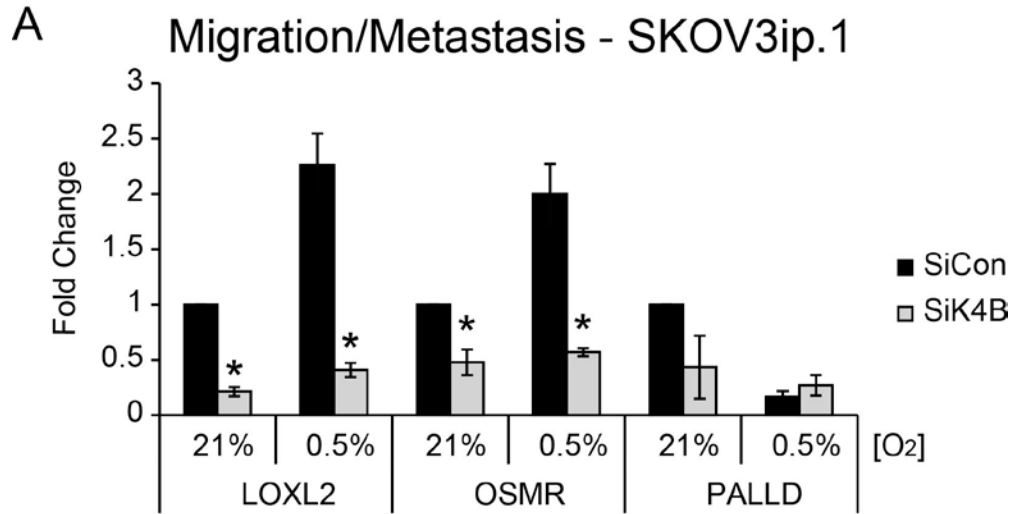


Figure 2.5. Common KDM4B Targets in the SKOV3ip.1, HCT116 and RCC4 that are involved in protein folding and processing and RNA processing. A, SKOV3ip.1 RNA samples were used for QPCR. Data represent average fold change \pm SEM from three independent experiments measured in triplicate. *, $P < 0.05$, determined by Two-tailed Paired Student's T Test. **B, HCT116** RNA samples were used for QPCR. Data represent average fold change \pm SEM from two independent experiments measured in triplicate. *, $P < 0.05$, determined by Two-tailed Paired Student's T Test. **C, RCC4** RNA samples were used for QPCR. Data represent average fold change \pm SEM from three independent experiments measured in triplicate. *, $P < 0.05$, determined by Two-tailed Paired Student's T Test.

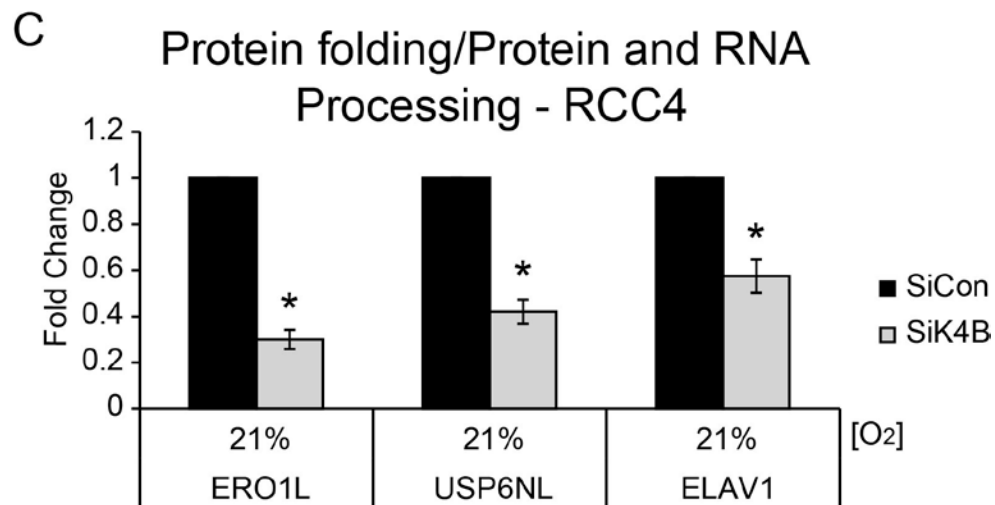
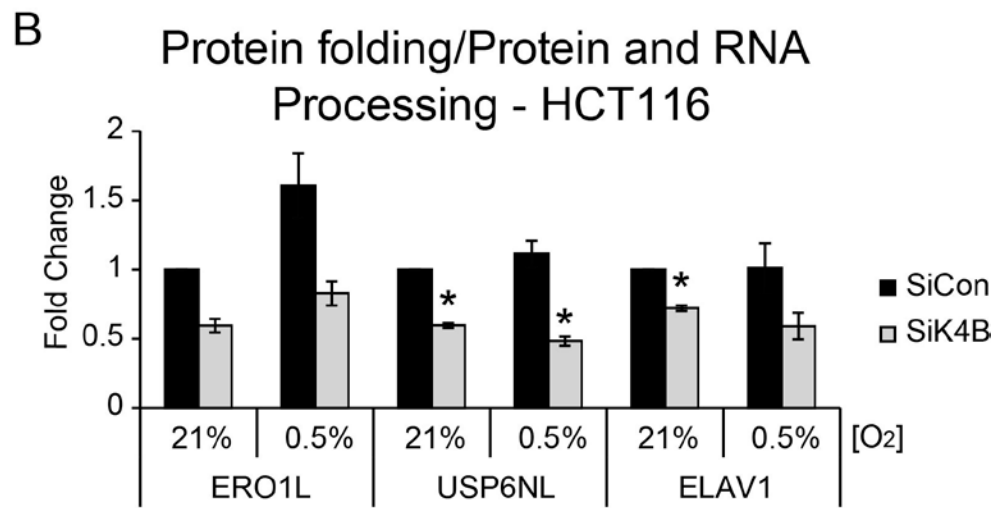
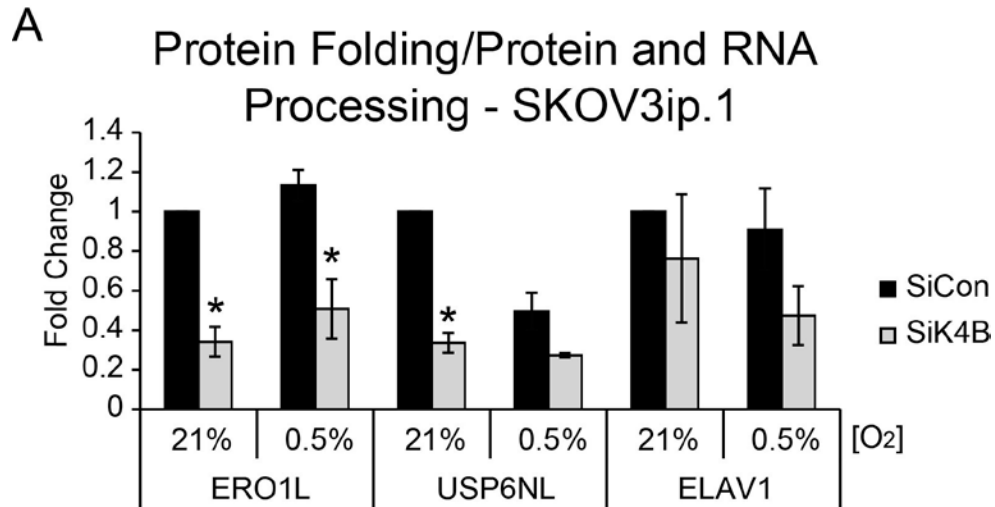


Figure 2.6. Common KDM4B Targets in the SKOV3ip.1, HCT116 and RCC4 that are involved in amyloid protein precursor cleavage, ion metabolism, and apoptosis. A, SKOV3ip.1 RNA samples were used for QPCR. Data represent average fold change \pm SEM from three independent experiments measured in triplicate. *, $P < 0.05$, determined by Two-tailed Paired Student's T Test. **B,** HCT116 RNA samples were used for QPCR. Data represent average fold change \pm SEM from two independent experiments measured in triplicate. *, $P < 0.05$, determined by Two-tailed Paired Student's T Test. **C,** RCC4 RNA samples were used for QPCR. Data represent average fold change \pm SEM from three independent experiments measured in triplicate. *, $P < 0.05$, determined by Two-tailed Paired Student's T Test.

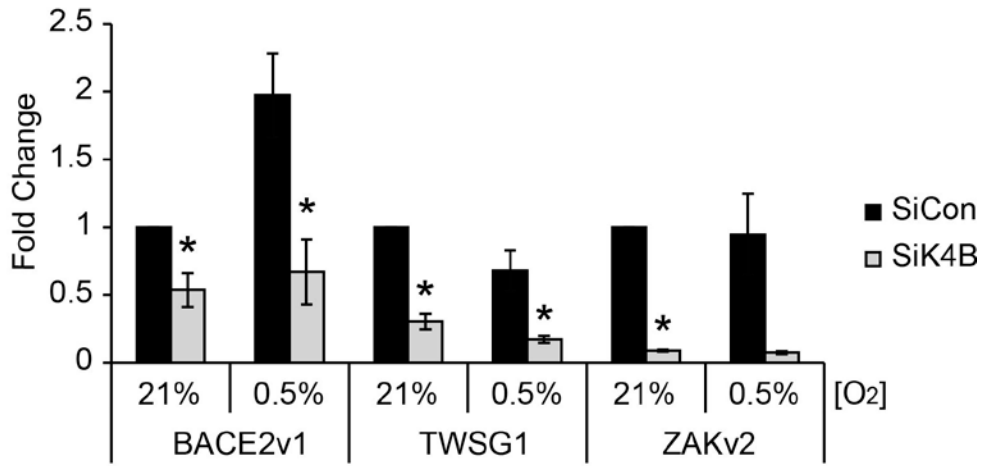
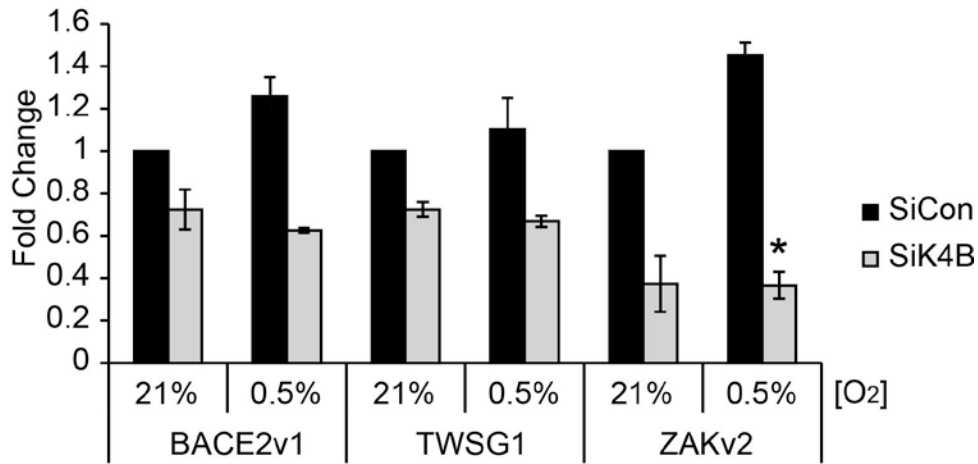
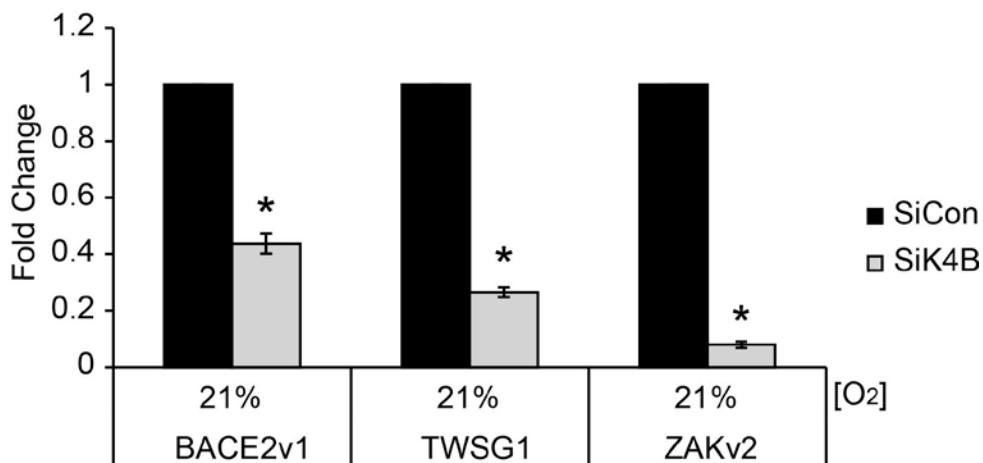
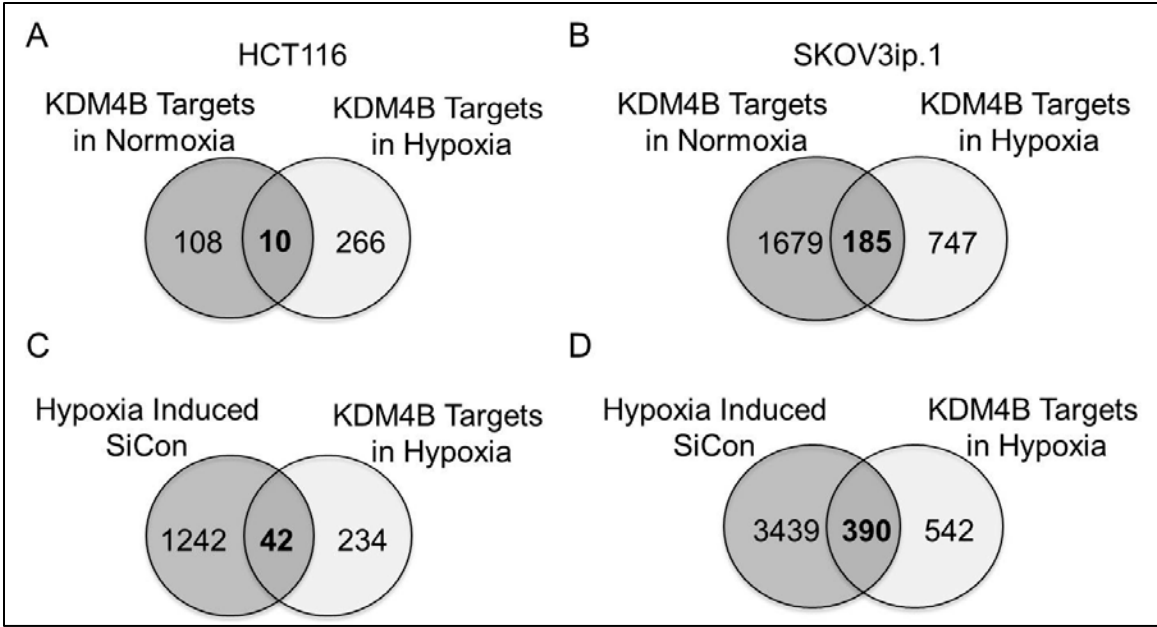
A**Miscellaneous - SKOV3ip.1****B****Miscellaneous - HCT116****C****Miscellaneous - RCC4**

Figure 2.7. Identification of KDM4B target genes in HCT116 colon carcinoma cells and in SKOV3ip.1 ovarian cancer cells. A, Venn diagram showing the overlap between genes down-regulated greater than 1.4 fold by siK4B in normoxia (left circle) and hypoxia (right circle) in HCT116 colon carcinoma cells. **B,** Venn diagram showing the overlap between genes down-regulated greater than 1.4 fold by siK4B in normoxia (left circle) and hypoxia (right circle) in SKOV3ip.1 cells. **C,** Venn diagram showing the overlap between genes induced greater than 1.4 fold in hypoxia (left circle) and genes down-regulated greater than 1.4 fold by siK4B in hypoxia (right circle) in HCT116 colon carcinoma cells. **D,** Venn diagram showing the overlap between genes induced greater than 1.4 fold in hypoxia (left circle) and genes down-regulated greater than 1.4 fold by siK4B in hypoxia (right circle) in SKOV3ip.1 ovarian cancer cells.



Ingenuity Pathway Analysis determined that the predominant pathways regulated by KDM4B in each oxygen condition were distinct in SKOV3ip.1 cells (Table 2.6-2.7). In atmospheric oxygen, genes involved in cancer, cell cycle (including DNA replication, recombination, and repair), and cell death pathways were influenced most significantly by KDM4B. In contrast, genes involved in inflammatory response, cellular development, and cellular movement were predominantly represented in hypoxia, implying a role in metastasis. Cell proliferation and metastasis are known to be the most critical pathways manipulated in cancer to promote survival during early (usually without hypoxic stress) and late (promoted by HIF-signaling) stages of cancer development, respectively. By regulating OVCAR cell proliferation in normoxia and metastasis in hypoxia, KDM4B may play crucial roles in promoting ovarian cancer progression.

Similar differential regulation by KDM4B was also detected in HCT116 cells, although to less extent. In HCT116 cells, KDM4B regulated cellular assembly, cellular movement and cellular development in both normoxia and hypoxia (Table 2.6). However, the effect was more significant and more genes were involved in these pathways in hypoxia. Moreover, cell morphology and cell-to-cell signaling pathways were also regulated by KDM4B in hypoxia, whereas cellular function and maintenance and molecular transport were influenced in normoxia. Cancer was still among the top diseases influence by KDM4B in normoxia, whereas metabolic disease and endocrine system disorders were the major diseases affected in hypoxia (Table 2.7). These results suggested a KDM4B-dependent metastatic phenotype in hypoxia and cell maintenance in normoxia in HCT116 cells.

Table 2.6. Molecular and Cellular Functions Regulated by KDM4B in Normoxia or Hypoxia in SKOV3ip.1, HCT116, and RCC4 Cells.

Cell Line/O₂ Condition	Name	P-value	# Molecules
SKOV3ip.1 Normoxia	Cell Cycle	7.00E-15 - 8.16E-04	239
	Cellular Assembly and Organization	6.70E-14 - 7.94E-04	197
	DNA Replication, Recombination, and Repair	6.70E-14 - 8.16E-04	182
	Cell Death	8.00E-14 - 8.19E-04	353
	Post-Translational Modification	1.29E-08 - 7.92E-04	153
SKOV3ip.1 Hypoxia	Cellular Movement	2.51E-10 - 5.57E-03	77
	Cellular Development	8.92E-10 - 4.14E-03	99
	Cell Death	4.59E-07 - 5.57E-03	100
	Cell-To-Cell Signaling and Interaction	8.13E-07 - 5.57E-03	78
	Antigen Presentation	1.00E-06 - 4.46E-03	50
HCT116 Normoxia	Cellular Assembly and Organization	1.63E-04 - 4.55E-02	14
	Cellular Function and Maintenance	1.63E-04 - 3.63E-02	9
	Molecular Transport	1.63E-04 - 4.79E-02	9
	Cellular Movement	1.81E-04 - 4.79E-02	13
	Cellular Development	2.62E-04 - 4.32E-02	15
HCT116 Hypoxia	Cellular Assembly and Organization	8.77E-07 - 9.89E-03	39
	Cellular Movement	2.93E-06 - 9.89E-03	34
	Cell Morphology	3.39E-06 - 9.89E-03	27
	Cell-To-Cell Signaling and Interaction	3.00E-05 - 9.89E-03	28
	Cellular Development	5.03E-05 - 9.89E-03	48
RCC4 Pseudo-Hypoxia	Cell Cycle	2.23E-14 - 3.05E-03	148
	Cellular Assembly and Organization	4.66E-10 - 2.94E-03	143
	DNA Replication, Recombination, and Repair	4.66E-10 - 2.11E-03	100
	Cell Death	5.88E-10 - 3.00E-03	228
	Cellular Growth and Proliferation	1.38E-09 - 3.13E-03	247

Table 2.7. Disease and Disorders Regulated by KDM4B in Different Oxygen Conditions in SKOV3ip.1, HCT116, and RCC4 Cells.

Cell Line/O₂ Condition	Name	P-value	# Molecules
SKOV3ip.1 Normoxia	Cancer	6.37E-20 - 7.63E-04	496
	Gastrointestinal Disease	4.81E-16 - 8.16E-04	422
	Hematological Disease	5.56E-13 - 7.63E-04	141
	Genetic Disorder	2.03E-11 - 7.94E-04	249
	Infectious Disease	9.82E-11 - 6.64E-04	187
SKOV3ip.1 Hypoxia	Inflammatory Response	1.64E-12 - 5.57E-03	97
	Inflammatory Disease	5.53E-05 - 4.52E-03	90
	Renal and Urological Disease	5.53E-05 - 3.50E-03	29
	Respiratory Disease	1.46E-04 - 2.11E-03	22
	Hematological Disease	1.48E-04 - 3.26E-03	8
HCT116 Normoxia	Neurological Disease	5.84E-05 - 4.56E-02	17
	Cancer	9.25E-05 - 4.09E-02	20
	Renal and Urological Disease	9.25E-05 - 4.56E-02	5
	Cardiovascular Disease	1.27E-04 - 4.56E-02	11
	Gastrointestinal Disease	2.32E-04 - 3.07E-02	12
HCT116 Hypoxia	Neurological Disease	1.05E-06 - 9.89E-03	61
	Metabolic Disease	1.73E-06 - 9.89E-03	57
	Endocrine System Disorders	3.68E-06 - 9.89E-03	52
	Gastrointestinal Disease	3.68E-06 - 9.89E-03	81
	Genetic Disorder	3.68E-06 - 9.89E-03	108
RCC4 Pseudo-Hypoxia	Cancer	4.02E-21 - 3.13E-03	305
	Gastrointestinal Disease	6.68E-14 - 2.98E-03	303
	Reproductive System Disease	6.33E-11 - 3.13E-03	184
	Genetic Disorder	2.17E-10 - 2.98E-03	271
	Hematological Disease	6.43E-07 - 2.49E-03	84

KDM4B Differentially Regulates Gene Expression in Atmospheric and Hypoxic Growth Conditions in Ovarian Cancer Cell Lines

Since the differential regulation of pathways by KDM4B in different oxygen conditions was most obvious in SKOV3ip.1 cells, further studies continued with this cell line to demonstrate the potential mechanism of this regulation. Immunoblot showed that siRNA robustly knocked down KDM4B protein expression in SKOV3ip.1 cells and global H3K9me3 level was not influenced by KDM4B knockdown (Figure 2.8). The expression of targets from the proliferation, inflammatory response, and metastasis networks were validated by QPCR (Figure 2.9). Proliferative genes like *BRCA2*, *CEP70*, *SKAP2*, *MAP4K3* and *MAP4K4* displayed robust dependence on KDM4B in normoxic conditions, with lesser effect in hypoxia (0.5% siCon) (Figure 2.9A). Many inflammation-associated genes exhibited robust dependence on KDM4B in both conditions, (*SMAD3*, *IL-1B*, *IL-8*, *IL-6ST*, Figure 2.9B). Similarly, several genes associated with metastatic pathways (*LOXL2*, *ERO1L*, *PDGFB*, *TRAF1a*, *FGFRL1*, *LPP*, *ITGB5*, Figure 2.9C) were also dependent on KDM4B in both oxygen tensions.

In order to establish a more robust experimental system for the study of KDM4B in functional and mechanistic assays, SKOV3ip.1 and OVCAR8 cells were stably transduced with two shRNA constructs targeting KDM4B (shK-1 and shK-2, see Materials and Methods for description). SKOV3ip.1 is an EOC cell line sub-cultured from ascites cells of an intra-peritoneal xenograft model injected with SKOV3 parental cells (Yoneda et al. 1998). It is a commonly used ovarian cancer model for *in vitro* and *in vivo* studies. OVCAR8 is an undifferentiated ovarian carcinoma that lacks p53 (Hamilton et al. 1984). Compared to an irrelevant control shRNA (shGFP), shK-1 and

Figure 2.8. H3K9 tri-methylation in SKOV3ip.1 transfected with siK4B. SKOV3ip.1 cells were transfected with siRNA to KDM4B (siK4B) and control siRNA (siCon). Cells were exposed to normoxia (21% O₂) and hypoxia (0.5% O₂) for 16 hours. Antibodies were used to validate KDM4B expression and H3K9 trimethylation level. Tubulin serves as control for protein loading of the KDM4B blot. Histone H3 serves as controls for protein loading of H3K9me₃, probed on a separate blot loaded with the same aliquots of protein samples. Images were taken from one representative experiment.

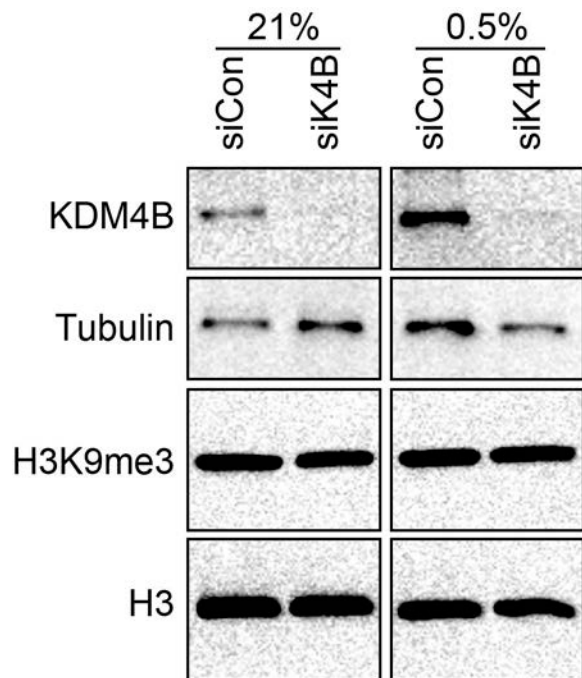
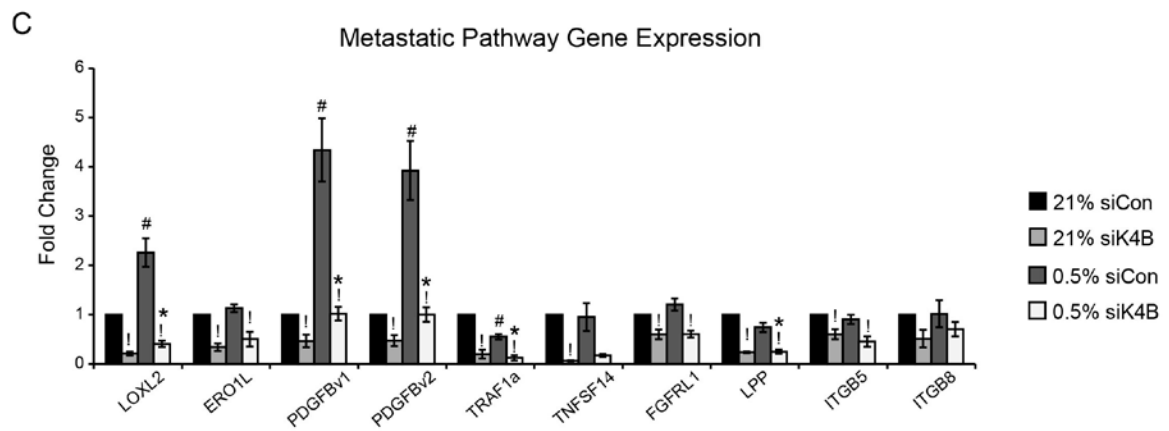
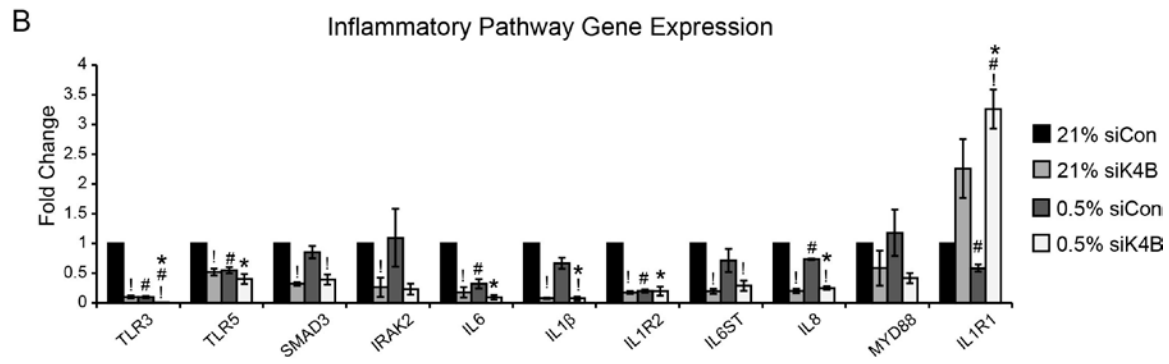
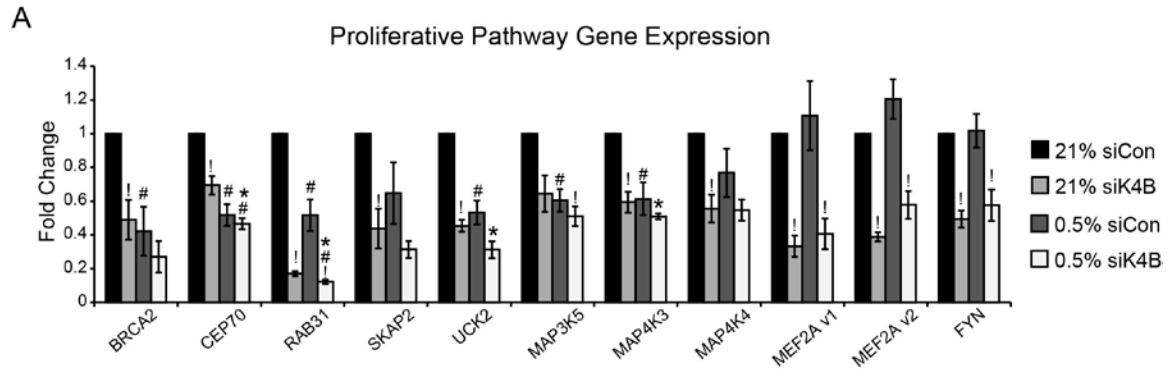


Figure 2.9. KDM4B regulates proliferative, inflammatory, and metastatic genes in SKOV3ip.1 cells. **A**, Quantitative RT-PCR validation of selected proliferation-associated genes regulated by KDM4B. **B**, Quantitative RT-PCR validation of inflammation-associated genes regulated by KDM4B. **C**, Quantitative RT-PCR validation of metastasis-associated genes regulated by KDM4B. Data in represent mean Fold Change \pm S.E.M. normalized to 18S rRNA, calculated relative to siCon in 21% O₂ (black bars). Results were averaged from three independent experiments, measured in triplicate. Significance of differences was calculated using two-tailed paired Student's T-test (!, P<0.05 for siK4B compared to siCon,; #, P<0.05 for hypoxia compared to normoxia) or two-way ANOVA (*, P<0.05).



shK-2 significantly suppressed expression of KDM4B protein and RNA in 21% and 0.5% oxygen in both cell lines (Figure 2.10). Most importantly, hypoxic induction was robustly attenuated to levels less than or equivalent to the shGFP control at 21%.

Two other KDM4 family members, KDM4A and KDM4C, are structurally similar to KDM4B (Whetstine et al. 2006; Berry and Janknecht 2013), and a third family member KDM4D has been shown to have overlapping functions in other systems (Iwamori et al. 2011). Expression of these other members of the KDM4 family was measured by qRT-PCR and immunoblotting to determine if any compensatory expression was induced following suppression of KDM4B (Figure 2.10). Our qRT-PCR results suggested that there was no biologically significant change in KDM4A and KDM4C expression at the mRNA or protein level with suppression of KDM4B. However, KDM4D mRNA and protein were both upregulated in cells expressing shRNA to KDM4B, particularly in OVCAR8 cells transduced with construct shK-1. Similar to what has been reported in other systems (Beyer et al. 2008), knockdown of KDM4B did not increase H3K9 trimethylation in whole cell extracts (Fig. 2.8 and 2.11, anti-H3K9me3 antibody specificity was demonstrated in Figure 2.12). There may have been a decrease in methylation, indicating that any regulation of target genes by demethylation is through specific recruitment to regulatory regions and not global changes in the epigenetic environment.

The hypoxic induction of the putative target gene *platelet derived growth factor beta* (*PDGFB*, a potent angiogenic, lymphangiogenic, and transformative factor (Schito et al. 2012)) was attenuated by approximately 30% in hypoxic SKOV3ip.1 cells expressing shRNA to KDM4B (Figure 2.13B), with a decrease of 50% in OVCAR8 cells

Figure 2.10. Expression of KDM4 subfamily members in SKOV3ip.1 and OVCAR8 cells expressing shRNA to KDM4B. **A**, Quantitative RT-PCR measurement of *KDM4A*, *KDM4B*, *KDM4C*, and *KDM4D* in SKOV3ip.1 cells expressing shRNA to KDM4B (shK-1, dark grey and shK-2, light grey) in 21%, 2%, and 0.5% oxygen. Data represent mean three independent experiments \pm S.E.M measured in triplicate, normalized to shGFP control at 21% oxygen. *, $P < 0.05$, determined by two-tailed paired Student's t-test. **B**. Immunoblot of KDM4B, KDM4A, KDM4C, and KDM4D in SKOV3ip.1 cells in Panel A. Tubulin serves as a loading control. **C**, Quantitative RT-PCR measurement of *KDM4A*, *KDM4B*, *KDM4C*, and *KDM4D* RNA in OVCAR8 cells expressing shRNA to KDM4B as in Panel A. **D**, Immunoblot of KDM4B, KDM4A, KDM4C, and KDM4D in OVCAR8 cells, as in Panel B.

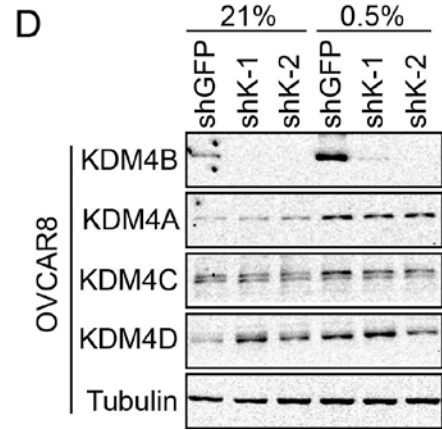
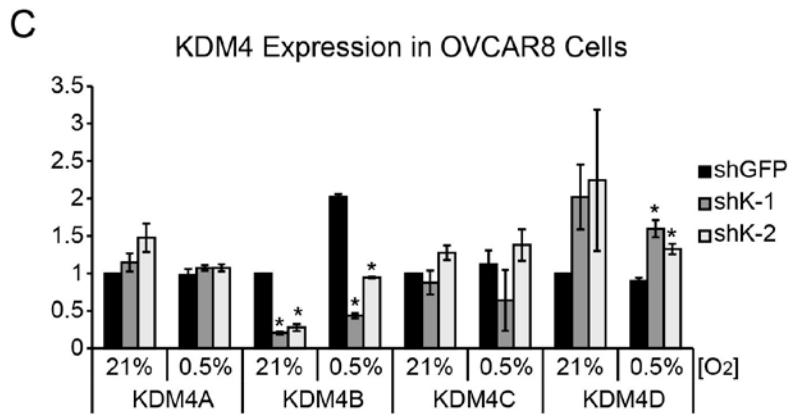
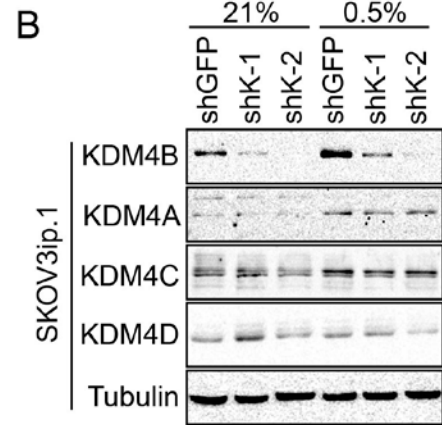
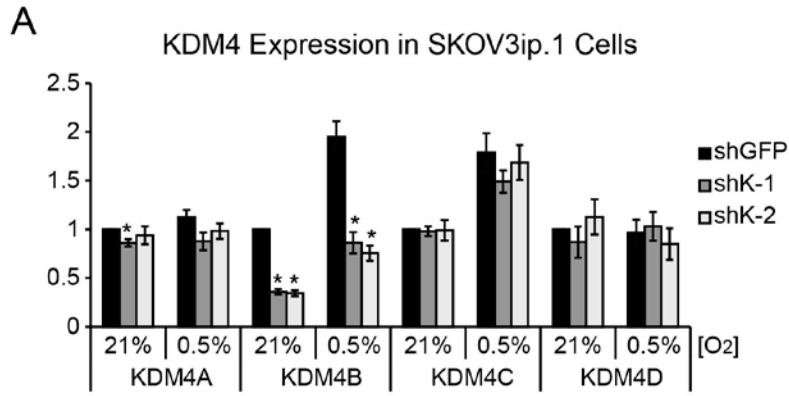
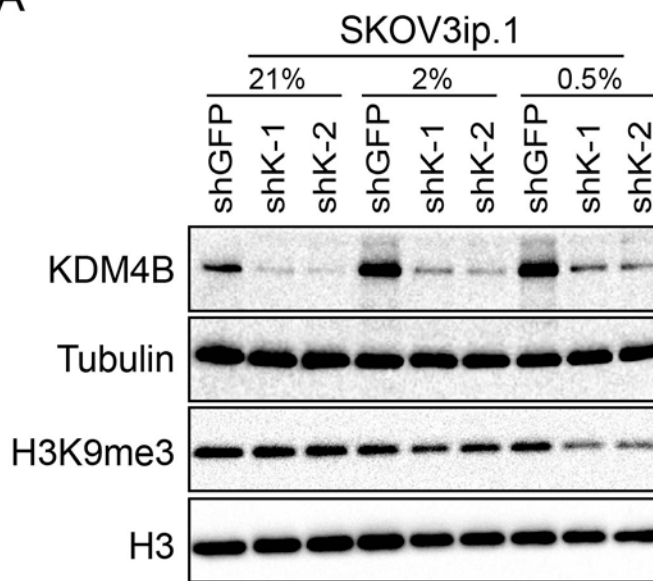


Figure 2.11. H3K9me3 Level in SKOV3ip.1 and OVCAR8 ovarian cancer cell lines.

A. Immunoblot measurement of KDM4B and H3K9me3 in SKOV3ip.1 cells expressing shRNA targeting KDM4B (shK-1 and shK-2) or GFP (control) in 21%, 2%, and 0.5% O₂. Tubulin and histone H3 serve as loading controls. **B.** Immunoblot of OVCAR8 cells, treated as in Panel A.

A



B

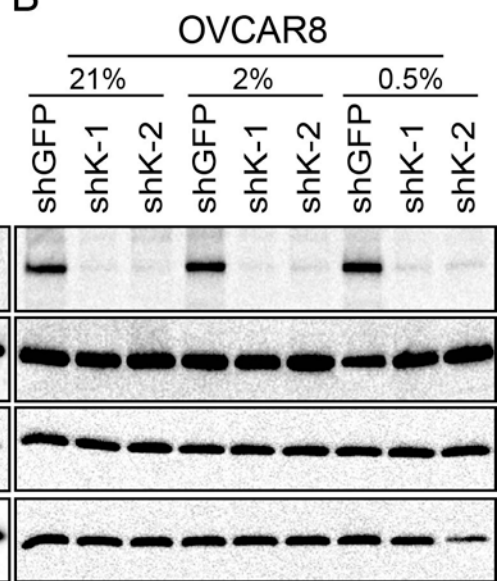
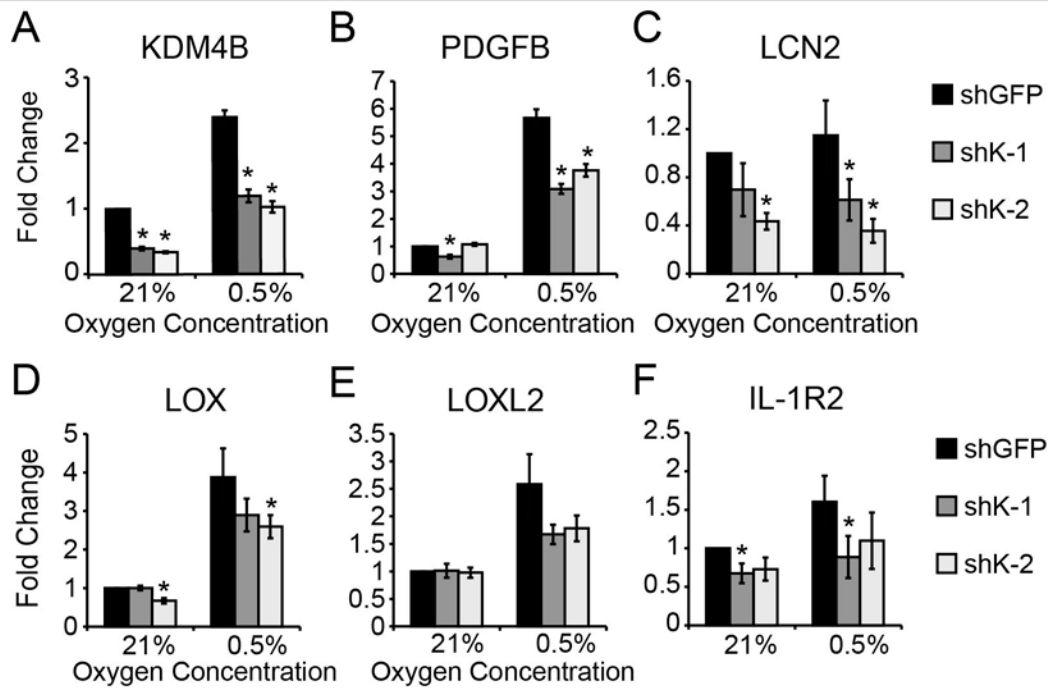


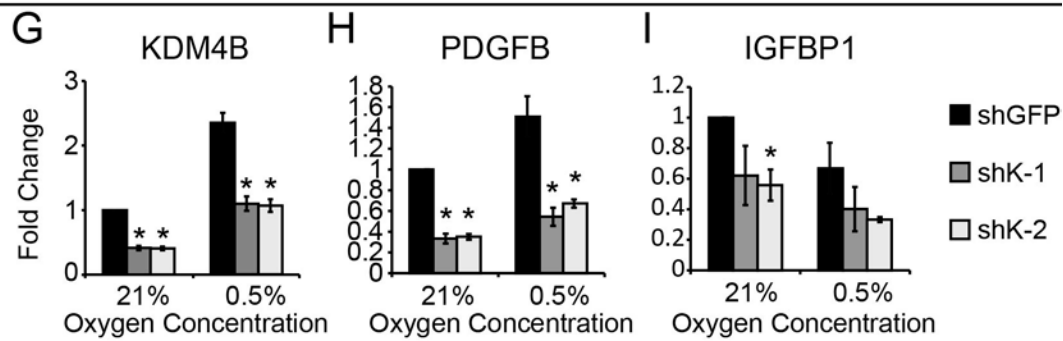
Figure 2.12. Modified Histone Peptide Array. **A**, Specificity Plot demonstrating that the H3K9me3 antibody (Abcam ab8898) used for immunoblotting and ChIP was more specific for H3K9me3 than other modifications, including H3K27me3. **B**, Reactivity Plot for Abcam ab8898, demonstrating preferential reactivity with H3K9me3. Data was analyzed and figures generated with Array Analyze Software (Active Motif).

Figure 2.13. Expression of KDM4 target genes in SKOV3ip.1 and OVCAR8 cells expressing shRNA to KDM4B. **A-F**, Quantitative RT-PCR measurement of KDM4B target genes in SKOV3ip.1 cells expressing shRNA to KDM4B (shK-1, dark grey and shK-2, light grey) in 21%, 2%, and 0.5% oxygen. Data represent mean \pm S.E.M, normalized to shGFP control at 21% oxygen. Results were averaged from two to four independent experiments, measured in triplicate. *, $P < 0.05$, determined by two-tailed paired Student's t-test. **G-I**, Quantitative RT-PCR measurement of KDM4B target genes in OVCAR8 cells expressing shRNA to KDM4B (shK-1, dark grey and shK-2, light grey) in 21%, 2%, and 0.5% oxygen. Data represent mean \pm S.E.M, normalized to shGFP control at 21% oxygen. Results were averaged from four independent experiments, measured in triplicate. *, $P < 0.05$, determined by two-tailed paired Student's t-test.

SKOV3ip.1 Cells



OVCAR8 Cells



in all oxygen tensions tested (Figure 2.13H). Other candidate genes from the metastatic (*LOX* and *LOXL2*) and inflammatory (*IL-1R2*) pathways also displayed attenuated induction with KDM4B knockdown in SKOV3ip.1 cells, although with less significance, which may be due to compensation from KDM4D (Figure 2.13D-F). KDM4B also regulates normoxic and hypoxic expression of genes not induced under hypoxia, such as *LCN2* in SKOV3ip.1 cells (Figure 2.13C) and *IGFBP1* in OVCAR8 cells (Figure 2.13I).

Combined, this data suggest that KDM4B preferentially regulates distinct functions in different oxygen tensions, providing multiple avenues to affect EOC tumor growth.

KDM4B Binds and Demethylates Regulatory Regions of Target Genes to Promote Expression

KDM4B is primarily thought to regulate gene expression by demethylating tri- and di-methylated lysine 9 of histone H3 (H3K9me3 and H3K9me2), altering the chromatin environment to favor transcription by removing a modification associated with repression (Mosammamaparast and Shi 2010). In order to investigate this mechanism in EOC cells, SKOV3ip.1-shGFP and SKOV3ip.1-shK-2 cells were exposed to 21% and 0.5% oxygen for 16 hours, and the formaldehyde-fixed cells processed for chromatin immunoprecipitation (ChIP) using antibodies against KDM4B and H3K9me3.

In SKOV3ip.1-shGFP cells, KDM4B was localized to regions near the transcription start sites of *PDGFB*, *LCN2*, *LOX* and *LOXL2*, which have been shown to play important roles in cancer metastasis (Figure 2.14). PDGFB is one of the secreted factors involved in promoting the recruitment of pericytes along the vascular endothelial cells, a process required in tumor angiogenesis (Chantrain et al. 2006). Studies have

Figure 2.14. Chromatin IP demonstrating that KDM4B binds and demethylates its target gene promoters.

A, Map of ChIP-qPCR primers sets used to measure KDM4B

association and demethylation at or near target gene promoters. **B**, ChIP assay for

KDM4B near target gene promoters in SKOV3ip.1 cells treated with normoxia (21%

oxygen) or hypoxia (0.5% oxygen) for 16 hours. QRT-PCR results are shown as fold

change relative to 21% shGFP control. Data represent mean \pm S.E.M of three

independent experiments measured in triplicate. *, $P < 0.05$, determined by two-tailed

paired Student's t-test. **C**, ChIP qPCR analysis of H3K9me3 on selected promoter

regions of target genes following shRNA to KDM4B (shK-2, light grey bars) compared to

shGFP control (black bars). Chromatin was immunoprecipitated with anti-H3K9me3 or

anti-IgG antibodies, and the DNA was analyzed by qRT-PCR using primers specific for

each target gene and normalized to input chromatin subtracting IgG enrichment then

normalized to the desert region. Data represent the average of four independent

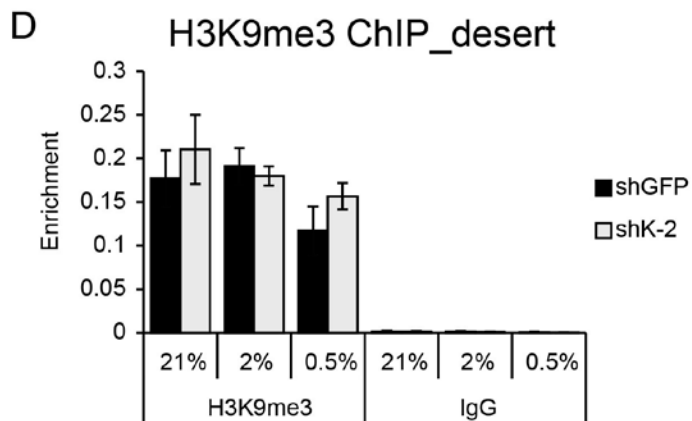
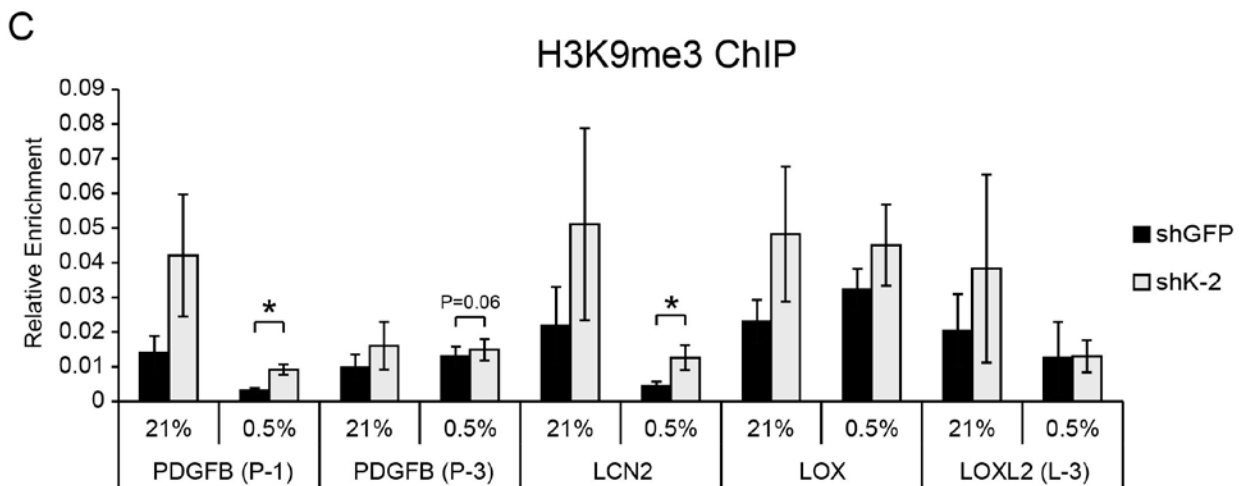
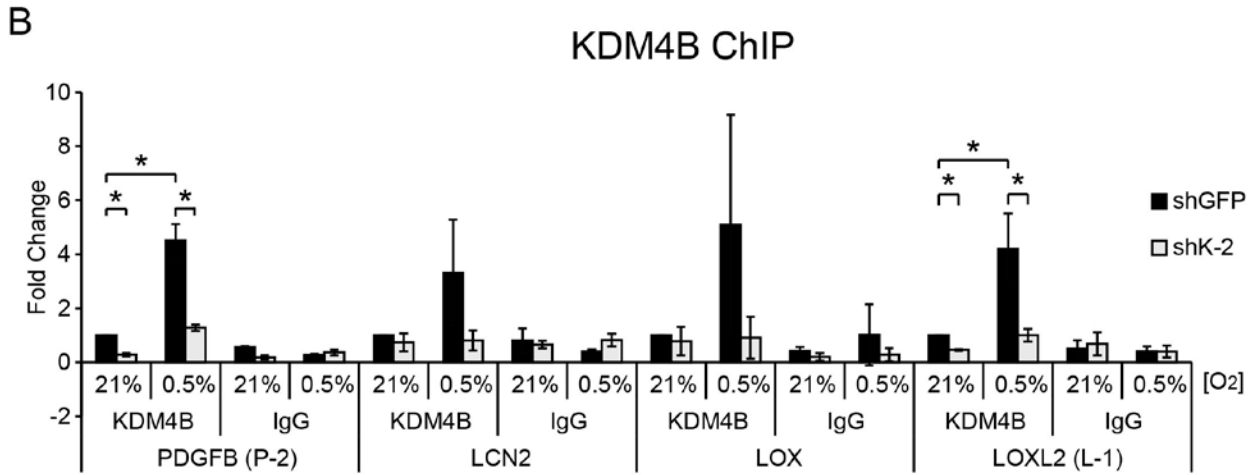
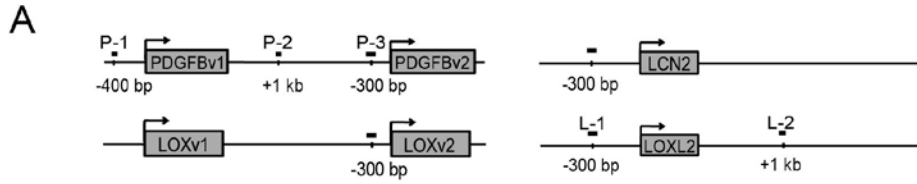
experiments \pm S.E.M. measured in triplicate. Significance for differences relative to

shGFP control was calculated using paired Student's t-test (*, $P < 0.05$). **D**, ChIP qPCR

analysis of H3K9me3 at a desert region on Chromosome 16. Cells were transduced and

chromatin immunoprecipitated as in Panel C. Data represent the average of four

independent experiments \pm S.E.M. measured in triplicate.



also shown that anti-PDGF drugs significantly inhibited tumor growth and metastasis in tumors that express high levels of PDGFB (Hosaka et al. 2013). LCN2 can enhance the gelatinolytic activity of matrix metalloproteinase 9 (MMP9) on ECM (Yan et al. 2001). LCN2 has been shown to have pro-inflammatory functions and regulates cell growth and adhesion (Chakraborty et al. 2012). LOX is involved in extracellular matrix (ECM) remodeling by crosslinking collagen for matrix metalloproteinase 2 (MMP2) cleavage, thus promoting cell invasion and metastasis (Erler et al. 2006). LOXL2 may regulate extracellular and intracellular cell signaling pathways as well as function in ECM remodeling (Decitre et al. 1998). The association of KDM4B to these target gene promoters was increased 2-3 fold with exposure to hypoxia, consistent with the hypoxic induction of KDM4B protein (Figure 2.14B). With expression of shK-2, the most persistent and robust knockdown construct, KDM4B association was reduced to levels comparable to an isotype specific IgG control.

Following knockdown of KDM4B there was increased enrichment of H3K9me3 at the promoters of these targets in 21% oxygen (Figure 2.14C). Although the overall level of H3K9me3 decreased abruptly in hypoxia (2% and 0.5% oxygen) compared to 21% oxygen, H3K9me3 levels at *PDGFB* and *LCN2* promoter regions were significantly increased when knocking down KDM4B (Figure 2.14C). The H3K9me3 level at each target gene promoter was normalized to the enrichment of H3K9me3 on a control “gene desert” region, which was not affected by loss of KDM4B (Figure 2.14D). This suggests that chromatin accessibility was not systematically disrupted in hypoxia or altered by loss of KDM4B. These results demonstrate that KDM4B associates with regulatory regions of target genes, and demethylates the histones at promoters to maximize

hypoxic expression.

Immunoblotting showed that knockdown of KDM4B with shK-2 decreased LCN2 protein expression in both oxygen conditions, whereas the effect of shK-1 was only observed in normoxia (Figure 2.15). The glycosylated pre-pro-LOX peptide, which is made in the cell and then secreted to the extracellular milieu for further processing, was induced in hypoxia and decreased by KDM4B knockdown (Grimsby et al. 2010).

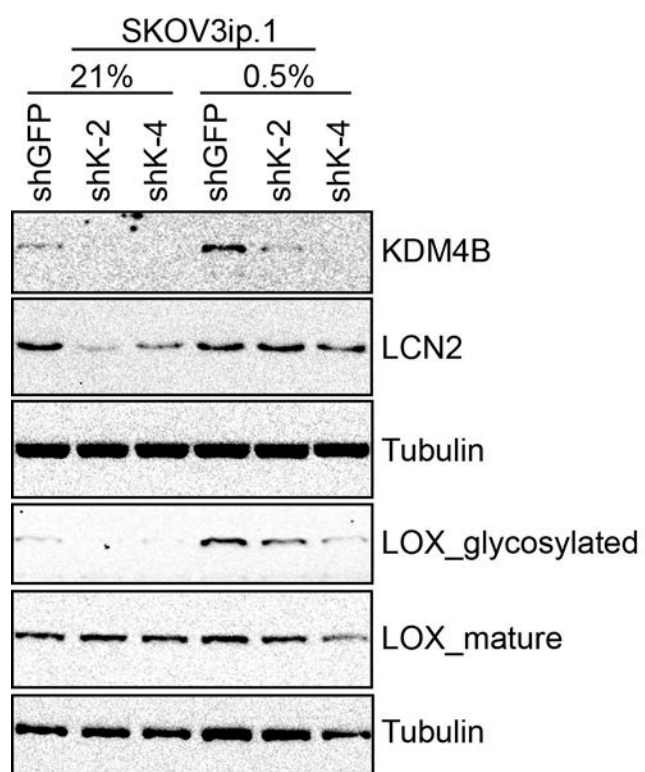
Taken together, our results showed that KDM4B regulated metastatic gene by demethylating their promoters in ovarian cancer cells.

DISCUSSION

KDM4B regulates multiple aspects of cancer progression, including proliferation (Kawazu et al. 2011; Kim et al. 2012a), anti-apoptosis (Sun et al. 2014), DNA damage repair (Mallette et al. 2012; Zheng et al. 2013; Chen et al. 2014), and migration (Zhao et al. 2013e). In this chapter, we have demonstrated that KDM4B may contribute to cancer progression by regulating both general and tissue-specific target genes.

Using microarray analyses, we have identified potential targets of KDM4B in cancer cell lines derived from three different cancer types, including SKOV3ip.1 ovarian cancer, HCT116 colon cancer, and RCC4 renal cell carcinoma. These three cancer types have shown dependence on hypoxic signaling during their development (Birner et al. 2001; Krishnamachary et al. 2003; Gudas et al. 2014). Mechanisms of how KDM4B may contribute to these cancers have not been clearly understood, especially in renal cell carcinoma (RCC) and epithelial ovarian cancer (EOC).

Figure 2.15. Expression of LCN2 and LOX protein in SKOV3ip.1 cells with KDM4B knockdown. SKOV3ip.1 cells were transduced with lentivirus expressing shRNA to KDM4B (shK-1 and shK-2) or control shRNA (shGFP). Cells were incubated in 21% or 0.5% oxygen. LCN2 and LOX protein levels were determined by immunoblotting. Tubulin serves as a loading control. Images were chosen as representative of two independent experiments. Antibody dilution information is listed in Table 2.2.



Using microarray analyses, we have identified potential targets of KDM4B in cancer cell lines derived from three different cancer types, including SKOV3ip.1 ovarian cancer, HCT116 colon cancer, and RCC4 renal cell carcinoma. These three cancer types have shown dependence on hypoxic signaling during their development (Birner et al. 2001; Krishnamachary et al. 2003; Gudas et al. 2014). Mechanisms of how KDM4B may contribute to these cancers have not been clearly understood, especially in renal cell carcinoma (RCC) and epithelial ovarian cancer (EOC).

By comparing KDM4B target genes in these three cell lines, we identified 16 common targets that were regulated by KDM4B in all three cell lines. These genes display a variety of cellular functions, but are mostly related to cancer progression (Table 2.5 and Figures 2.3-2.6). For example, Claudin-12 (CLDN12) is a tight-junction protein that is overexpressed in colon, melanoma cancer cells, and multiple chemo-resistant ovarian cancer cell lines and seemed to play important roles in tumorigenesis (Wang et al. 2006; Grone et al. 2007; Morita et al. 2008). Leucine zipper protein 6 (LUZP6/MPD6) was identified as a tumor antigen in polycythemia vera, chronic myelogenous, and prostate cancer patients (Xiong et al. 2006). Monocyte to macrophage differentiation-associated (MMD) is involved in differentiation from monocyte to macrophage and is important for lung cancer cell proliferation (Li and He 2014). Lysyl oxidase-related enzyme lysyl oxidase-like 2 (LOXL2) expression is correlated with metastasis and decreased survival in patients with aggressive breast cancer (Barker et al. 2011). Oncostatin M receptor (OSMR) was expressed by all human and canine osteosarcoma (OSA) cell lines and canine OSA tumor samples tested by Fossey et al (Fossey et al. 2011). OSM signaling promotes OSA cell invasion

and tumor angiogenesis by inducing STAT3 activation and enhancing the expression/activation of MMP2 and VEGF (Fossey et al. 2011). Paladin (PALLD) is overexpressed in many sporadic pancreas tumors and plays a role in the establishment of the TAF phenotype (Goicoechea et al. 2009). Human endoplasmic reticulum oxidoreductin 1- α (hERO1- α /ERO1L) is a hypoxia-inducible oxidizing enzyme that is overexpressed in cancer cells and is associated with poorer prognosis (Kutomi et al. 2013). USP6 N-terminal-like protein (USP6NL/RN-tre), a GTPase-activating protein (GAP) for Rabs including Rab5 and Rab43, spatiotemporally controls focal adhesion remodeling during chemotactic cell migration (Palamidessi et al. 2013). ELAV (Embryonic Lethal, Abnormal Vision, Drosophila)-Like 1 (ELAVL1/HuR) promotes cancer cell resistance to chemotherapy drugs or apoptosis by binding to the 3'-UTR of related gene mRNA (Licata et al. 2010; Lal et al. 2014; Winkler et al. 2014). Beta-site amyloid β precursor protein (APP)-cleaving enzyme 2 (BACE2) cleaves amyloid- β -precursor protein, which may lead to aggregation of amyloid β and apoptosis (Farzan et al. 2000; Xie et al. 2007). DENND5A is a cancer driver candidate gene that is associated with intracellular trafficking and cell cycle progression (Li et al. 2014). ZAK, ZDHHC2 and DAZAP2 appear to have tumor suppressing potential (Yang 2002; Zhang et al. 2008; Lukas et al. 2009). Given the distinct phenotypes of CRC, RCC and EOC, studying the regulation of these genes may give us a better understanding of the general mechanisms of cancer progression, and may lead to the discovery of novel therapeutic methods targeting multiple cancer types.

Although generally shared mechanisms exist, cancer is also a very heterogeneous disease. Each cancer has its own distinct genetic mutations and progression strategies.

For example, the canonical adenoma-carcinoma development of CRC is classified by Wnt pathway dysregulation (He et al. 1998). The most common genetic feature associated with clear cell RCC is loss or mutation of the *von Hippel-Lindau (VHL)* tumor suppressor gene, which results in stabilization of the HIFs, transactivating genes involved in angiogenesis, cell migration, and metabolism. EOC is the most heterogeneous cancer among the three. The majority of malignant EOC are characterized by mutations and/or loss of heterozygosity in *TP53* and *BRCA* loci (Vang et al. 2009). Our current knowledge of KDM4B function in cancer points to mechanisms that are specific to each cancer type. For example, in breast cancer, KDM4B is regulated by the estrogen receptor and induces expression of pro-proliferative genes like Cyclin D1 (Yang et al. 2010). Androgens regulate KDM4B in prostate cancer, which in turn promotes PSA expression (Coffey et al. 2013). In colon and gastric cancers, KDM4B regulates β -catenin dependent gene expression and WNT signaling to promote attachment-free growth and metastatic behavior (Berry and Janknecht 2013; Zhao et al. 2013a). In this study, we have also shown that the majority of KDM4B targets ($\geq 75\%$) were involved in distinct pathways that were specific for each cancer type, indicating KDM4B may play distinct roles in different cancers (Figure 2.1 and Table 2.6-2.7). The hypoxic tumor microenvironment promotes tumor angiogenesis and metastasis, leading to a more malignant phenotype (Chan and Giaccia 2007; Semenza 2012). In our study, KDM4B showed differential targeting preference in different oxygen conditions, suggesting it may play different roles to support tumor survival in various steps of tumor progression. In normoxia, it preferentially regulated proliferative genes (cell cycle, cellular assembly, DNA replication/recombination/repair, and cell death), maintaining

cell functions to ensure fast growth of the tumor. In hypoxia, it switches to primarily regulating inflammatory and metastatic genes (cellular movement, cellular development, and cell-to-cell signaling), possibly promoting metastasis. This dual function of KDM4B in transcriptional regulation suggests that KDM4B may be an important factor in promoting cancer progression in different tumor microenvironments and may be a potential therapeutic target for cancer treatment.

Because this differential regulation by KDM4B in different oxygen levels was most obvious in SKOV3ip.1 cells, we pursued mechanistic analysis in this cell line. Our microarray experiments suggest that KDM4B regulates the expression of multiple genes contributing to ovarian cancer growth and metastasis. In the case of most proliferative genes identified in the initial screen, this effect was attenuated with stable knockdown. KDM4D is the most likely compensatory enzyme, since we observed a robust increase in protein expression with the shK-1 construct in both cell lines (Figure 2.10). Compensatory Kdm4b expression has been observed in the testes of Kdm4d knockout mice, making it conceivable that our observations represent an inverse effect (Iwamori et al. 2011). Of greater interest is the regulation of genes with clear roles in promoting tumor progression and metastasis. *PDGFB*, *LCN2*, *LOX* and *LOXL2* display dependence on KDM4B for maximum expression, with corresponding changes in histone methylation on their promoters. PDGFB is one of the secreted factors that promote angiogenesis and metastasis (Chantraine et al. 2006; Hosaka et al. 2013). LCN2 can enhance the gelatinolytic activity of matrix metalloproteinase 9 (MMP9) on ECM, thus promoting cell migration (Yan et al. 2001). LOX and LOXL2 both regulate cell migration through extracellular matrix (ECM) remodeling (Decitre et al. 1998; Erlen

et al. 2006).

EOC is typically diagnosed at a late-stage, where metastatic tumors have already disseminated throughout the peritoneal cavity and ascites fluid has developed (Lengyel 2010). For this reason, mortality rate of EOC has not been improved over the past 30 years (Lengyel 2010; Siegel et al. 2014d). After initial surgery and front-line treatment, EOC often recur with chemo-resistant tumors that reseed the peritoneal cavity within 2 to 5 years. Therefore, a thorough understanding of the mechanisms underlying the metastatic behaviors of EOC is crucial for the development of more effective therapeutic methods. Inhibitors against PDGFB, such as sunitinib and sorafenib, have already been developed and used in clinical treatment for cancer, indicating KDM4B regulates important genes that can be targeted for improving cancer therapy (Widmer et al. 2014). Given the large cohort of potential KDM4B targets from the microarray analysis, our study has provided more opportunities to identify important target genes that may be useful for therapeutic treatment.

CHAPTER 3:

**THE HISTONE DEMETHYLASE KDM4B CONTRIBUTES TO PERITONEAL
DISSEMINATION OF OVARIAN CANCER**

ABSTRACT

Epithelial ovarian cancer (EOC) has poor prognosis and rapid recurrence due to widespread dissemination of peritoneal metastases at diagnosis. Multiple pathways contribute to the aggressive growth of EOC, including hypoxic signaling mechanisms. In this chapter, we have determined that the hypoxia-inducible histone demethylase KDM4B is expressed in high grade serous adenocarcinoma and EOC cell lines. KDM4B is expressed in approximately 60% of EOC tumors assayed, including primary, metastatic, and recurrent tumors. Suppressing KDM4B inhibits ovarian cancer cell invasion, migration and spheroid formation *in vitro*. KDM4B is also crucial for seeding and growth of peritoneal tumors *in vivo*, where its expression corresponds to hypoxic regions. Thus, KDM4B is a potent contributor to the seeding and growth of peritoneal tumors, one of the predominant factors affecting prognosis of EOC.

INTRODUCTION

Epithelial ovarian cancer (EOC) is the 10th most common cancer among women and the fifth leading cause of mortality, making it the most deadly of gynecologic cancers. The estimated mortality rate of EOC patients for the year 2015 is 67% (ACS 2015). EOC is a highly heterogeneous disease, generally stratified by the aggressiveness of growth, with slower growing Type I tumors having better prognosis than more rapidly growing Type II tumors (Vang et al. 2009). The majority of Type II EOC patients are diagnosed at an advanced International Federation of Gynecology and Obstetrics (FIGO) stage (stage III or IV), with widespread dissemination of metastatic tumors throughout the peritoneal cavity (Naora and Montell 2005; Vang et al. 2009; Lengyel 2010). Of the 4 general pathological subtypes that comprise EOC (serous, endometrioid, mucinous, and clear cell), the majority of the Type II (or high grade) EOC are high grade serous adenocarcinoma (HGSA), which represent 70% of the total EOC cases (Vang et al. 2009; Lengyel 2010).

Recent genomic analyses have demonstrated that over 90% of HGSA patients have mutations in the tumor suppressor *TP53*, with significant proportions also containing mutations in *BRCA1*, *BRCA2*, and the *pRB* pathways (Cancer Genome Atlas Research 2011). The front-line therapy for HGSA consists of surgical debulking followed by treatment with platinating agents and taxol derivatives (Lengyel 2010). The initial response of patients to the combination of carboplatin and paclitaxel is generally effective, however resistant tumors typically recur within 2-4 years (Lengyel 2010). This rapid recurrence is caused by re-growth of residual, chemoresistant cancer cells residing in the peritoneal cavity. Moreover, this rapid re-establishment of tumor growth

suggests that a process inherent to epithelial ovarian cancer progression facilitates adaptation to the respective stresses imposed by the metastatic process, surgery, and chemotherapy.

The hypoxic tumor microenvironment is a potent contributor to malignancy in multiple cancer types (Semenza 2012). The hypoxia-inducible factors (HIFs) are primary regulators of the hypoxic response, inducing multiple pathways utilized by tumors to promote homeostasis and tumor progression, including metabolic adaptation, self-renewal, angiogenesis, and metastasis (Semenza 2012). Consistent with the aggressively metastatic phenotype of EOC, elevated expression of HIF-1 α hypoxia-induced genes has been linked to poor patient outcome in ovarian cancer (Birner et al. 2001; Chi et al. 2006). Further study of the hypoxic response in EOC may yield other clinically viable effector genes.

Recent studies have determined that HIF-1 α also regulates expression of Jumonji domain histone demethylases (JmjC-KDMs) and other epigenetic regulators (Beyer et al. 2008; Pollard et al. 2008; Wellmann et al. 2008; Krieg et al. 2010). The JmjC-KDMs are non-heme iron-dependent dioxygenases whose activities require oxygen, Fe (II) and 2-oxoglutarate (alpha-ketoglutarate) to demethylate histones and influence gene expression (Klose et al. 2007; Shi and Whetstine 2007; Yang et al. 2009; Mosammaparast and Shi 2010; Okada et al. 2010; Mimura et al. 2011). Among the approximately 30 different JmjC domain-containing histone demethylases (Pedersen and Helin 2010), *KDM3A*, *KDM4B*, *KDM4C* and *KDM5B* are directly regulated by HIF-1 α in response to hypoxia, establishing a compelling link between the hypoxic tumor microenvironment and epigenetic remodeling to support tumorigenesis (Beyer et al.

2008; Pollard et al. 2008; Xia et al. 2009; Krieg et al. 2010).

KDM4B expression is elevated in several cancer types and plays a significant role in tumor growth by driving cancer cell proliferation and inducing chromosomal instability (Yang et al. 2010; Slee et al. 2011; Kim et al. 2012a; Slee et al. 2012).

KDM4B (Lysine-specific histone demethylase 4B, also called JMJD2B), catalyzes the demethylation of tri- and di-methylated histone H3 at Lysine 9 (H3K9me3/me2) and lysine 36 (H3K36me3/me2) (Whetstine et al. 2006). KDM4B regulates expression of cell cycle genes in breast cancer, including *CCND1*, *CCNA1*, *WEE1*, *CDK6*, *MYB*, and *MYC* (Yang et al. 2010; Kawazu et al. 2011). KDM4B also promotes epithelial-mesenchymal transition and metastasis in gastric cancer (Zhao et al. 2013a). Despite the significance of KDM4B in promoting proliferation and metastasis in several cancer types, its role in EOC progression has not been investigated. For this study, we hypothesized that if HIF-1 α and hypoxic signaling contribute to EOC (Chi et al. 2006), then KDM4B would also be expressed in EOC and influence its progression. Using a combination of immunohistochemical analysis of patient samples, *in vitro* functional analyses, and *in vivo* models of peritoneal ovarian cancer metastasis, we have determined that KDM4B is abundantly expressed in EOC tumors, and is a significant contributor to metastatic mechanisms in epithelial ovarian cancer cells, establishing a novel link between hypoxic induction of an epigenetic regulator and peritoneal tumor growth in epithelial ovarian cancers.

MATERIALS AND METHODS

Cell Lines and Culture Conditions

All OVCAR cell lines were maintained in RPMI-1640 (Invitrogen) supplemented with 10% heat-inactivated fetal bovine serum (HI-FBS) and 1% penicillin streptomycin (pen strep, Invitrogen). HIO80 cells were maintained in Medium 199 (Corning) mixed with MCDB 105 Medium (Sigma) at a 1:1 ratio, supplemented with 4% heat-inactivated fetal bovine serum (HI-FBS) and 1% pen strep (Invitrogen). SKOV3ip.1 cells were acquired from Dr. Erinn Rankin (Stanford University) with permission from Dr. Gordon Mills (M.D. Anderson Cancer Center). OVCAR3, OVCAR4, OVCAR5, OVCAR8, and IGROV1 cells were purchased from the NCI repository by Dr. Adam Krieg and Dr. Katherine Roby. OVCAR10 and HIO80 cells were from Dr. Andrew Godwin. Cells were transiently or stably knocked down of KDM4B depending on specific experimental needs as describe in Chapter 2. For overexpression of KDM4B, HIO80 cells were transduced with lentivirus containing either the wildtype KDM4B (WT, containing a silent mutation to escape recognition from shRNA) or the mutant KDM4B (mut, containing both the silent mutation and a catalytic mutation in its active site H189A). Overexpression of lacZ served as a control. For short-term hypoxia treatment (16-24 hours), cells were incubated in Ruskinn InVivo300 glove-box hypoxic incubators (Baker) in which oxygen levels were maintained at 0.5% or 2% for 16-24 hours depending on specific experimental needs. For longer duration experiments (i.e. in vitro proliferation assays), cells were cultured in HeraCell150 incubators set to the indicated oxygen tension (Thermo Fisher Scientific, Inc.).

Antibodies

Antibodies used in this chapter were: KDM4B (Cell Signaling; Cat# 8639, Clone D7E6), HIF-1 α (BD; 610959), β -Actin (Sigma; A1978), PAX8 (Biocare; Cat# ACI 438A, Clone BC12), PDGFB (Santa Cruz; Cat# sc-127, Clone N-30), Ki67 (Thermo; RM-9106-S0), and IgG control (Cell Signaling; Cat# 3900S, Clone DA1E). See Table 3.1 for specific dilutions in each assay of use.

ImmunoBlotting.

Cells were lysed in SDS lysis buffer (125 mM Tris-PH6.8, 1% SDS, 10 mg/ml Sodium Deoxycholate, 1 mM EDTA, 5 mM DTT) with protease inhibitor cocktail (Sigma-Aldrich). Following SDS-PAGE, proteins were transferred to nitrocellulose and probed with the indicated primary and horseradish peroxidase conjugated secondary antibodies (See Table 3.1 for antibody dilution information). Chemiluminescent signal was detected with ECL Prime reagent (GE Healthcare) using a Bio-Rad Molecular Imager ChemiDoc XRS+ equipped with Image Lab Software (Bio-Rad).

Tumor Microarray Samples

Ovarian tissue microarrays (TMAs) were constructed by the KUCC Biospecimen Repository Core Facility. The TMAs were constructed using archival formalin fixed, paraffin embedded samples of primary ovarian carcinoma along with matched metastatic and recurrent tissue samples when available. These samples were identified from the pathology departmental archives of the University of Kansas Medical Center from 1998-2009. The TMA was composed of tumor tissue samples from 48 patients with ovarian cancer: 14 patients with primary, recurrence, and metastatic samples (including one patient with distant metastasis to the brain), 27 patients with primary and

Table 3.1. Antibody Dilutions.

Assay	Antigen	Supplier	Product NO.	Discription	Dilution
Immuno blot	KDM4B	Cell Signaling	8639	Rabbit mAb	1:1,000
	HIF1 α	BD	610959	Mouse mAb	1:1,000
	β -Actin	Sigma	A1978	Mouse mAb	1:2,000
	α -Tubulin	Thermo	MS-581- PABX	Mouse mAb	1:2,000
	Rabbit IgG (H+L)	KPL	474-1516	Goat secondary Ab	1:5,000
	Mouse IgG (Y)	KPL	474-1802	Goat secondary Ab	1:5,000
IHC	KDM4B	Cell Signaling	8639	Rabbit mAb	1:100
	IgG control	Cell Signaling	3900S	Rabbit mAb	1:100
	PDGFB	Santa Cruz	sc-127	Rabbit pAb	1:800
	PAX8	Biocare	ACI438A	Mouse mAb	1:100
	Ki67	Thermo	RM-9106-S0	Rabbit mAb	1:800
	Pimonidazole	Hypoxyprobe, Inc.	70132-50-2	Mouse mAb	1:5000

metastatic samples, and 7 patients with primary and recurrent samples. Based on review of the original pathology reports, the ovarian carcinomas were typed as serous (30 samples), mixed (14 samples; 12 of which included a serous component), carcinosarcoma (1 sample), clear cell (1 sample), papillary carcinoma, not otherwise specified (NOS) (1 sample) and adenocarcinoma, NOS (1 sample). For every sample, hematoxylin and eosin stained slides were reviewed by a board certified pathologist who selected tumor rich areas. Using the semi-automated TMArrayer (Pathology Devices, Inc., Westminster, MD) TMA paraffin blocks were assembled with triplicate 1.0 mm cores using the marked slide as a guide.

Immunohistochemical Analysis

Immunohistochemical (IHC) staining was performed using standard peroxidase/DAB methods (See Table 3.1 for specific antibody dilution information). Deparaffined sections subjected to antigen retrieval by incubating in 10mM Trisodium Citrate buffer, pH 6 at 95°C for 10-30 minutes, depending on the antibody used. Tissue sections were counterstained with hematoxylin and then imaged on a Nikon 80i microscope with a Photometrics CoolSNAP ES camera and a NIS-Elements AR software to assess quality of staining. Isotype specific negative control antibodies were used for all comparisons. Human TMA slides were scanned using an Aperio slide scanning microscope (Leica) at both University of Kansas Medical Center Department of Pathology and the University of California San Francisco Department of Radiation Oncology. Individual spot images were extracted using Aperio TMALab. Stained slides were independently reviewed and evaluated by at least 2 board certified pathologists (authors TK, GT, OT) without prior knowledge of the clinical diagnosis or outcome. For

KDM4B, tumors were scored based on extent of nuclear staining, with extent defined as the percentage of epithelial tumor cells staining positive for KDM4B (negative, 0%-10% of cells expressing; positive, >10% of cells expressing). For CA-IX and PDGFB, tumors were scored on a qualitative scale that integrated both intensity and extent of staining (0 = no staining, 1 = weak staining, 2 = moderate staining, 3 = strong staining). Scores for the triplicate spots from each tumor biopsy were averaged for statistical analysis. SPSS statistical software (IBM) was used to determine significance of coexpression with KDM4B using Bivariate correlation and Mann-Whitney U-test.

QRT-PCR.

Quantitative real-time PCR (qRT-PCR) was conducted as described in Chapter 2. All primers used for RNA analysis used in this chapter are listed in Table 3.2.

Cell Proliferation Assay.

For the short-term assay, approximately 50,000 SKOV3ip.1 cells transiently transfected with either siK4B or siCon were plated in each 6-cm cell culture dish and allowed eight hours to attach to the dish. After the eight-hour incubation at 21% oxygen, one dish of cells from each line (siK4B or siCon) were trypsinized, stained with Trypan blue and counted (as Day 0). Hypoxic treatment began after the Day 0 count and one dish of cells from each group were counted every 24 hours for four days. A long-term proliferation assay was conducted as described previously (Welford et al. 2006), with minor modifications. Briefly, SKOV3ip.1 cells were stably transduced with lentivirus containing shGFP, shK-1 or shK-2 as described in the Cell culture condition section. Approximately 50,000 cells were plated per 6-cm dish. Cells were counted using a hemocytometer every three days and 50,000 cells were plated back into the dish after

Table 3.2. QPCR Primers Used in This Chapter.

Gene	Forward (5'-3')	Reverse (5'-3')
hsKDM4B	ggactgacggcaacctctac	cgtcctcaaactccacctg
hsKDM4A	gccgctagaagtttcagtgag	gcgtcccttgacttcttatt
hsKDM4C	aggcgccaagtgatgaag	gagaggtttcgccaagact
hsKDM4D	ggacaagcctgtaccactgag	ctgcacccagaagccttg

counting each time. Cells were counted in triplicate using five fields per sample. Four independent experiments were recorded and total cell numbers were calculated based on the number of cells from each count and the dilution factor from each passage.

For overexpression experiments, HIO80 cells were stably transduced with lentivirus containing the lacZ, WT or mut KDM4B as described in the Cell culture condition section. Cells were plated and counted the same way as in the SKOV3ip.1 3T3 proliferation assay.

Boyden Chamber Migration and Matrigel Invasion Assay.

For invasion assays, Boyden chambers (BD Falcon, 8 micron pore size) were coated with 100 uL Matrigel (BD Biosciences, diluted to 1 mg/ml in serum free RPMI). Uncoated Boyden chambers were used for migration assays. Fifty thousand cells were distributed to chambers and incubated for 24 hours in 21%, 2% or 0.5% oxygen. Cells that invaded and/or migrated through the membrane were released by trypsinization and quantified using CyQUANT Cell Proliferation Assay Kit (Life Technologies) according to manufacturer's protocol, with modifications developed by Swenson-Fields et al. (Swenson-Fields et al. 2013). DNA content in each group was calculated and the significance of the difference between control and experimental groups were determined using two-tail paired Student's t-test. Cells seeded as monolayers served as controls for any potential proliferation or viability defects resulting from KDM4B knockdown. Aliquots of 50,000 frozen cells also served as internal controls for plating density. Representative membranes were also fixed and stained with Siemens Diff Quik Stain Set (Neobits, Inc.) and imaged using a Leitz LABORLUX12 microscope. Images were captured using LAS EZ software and a Leica EC3 camera.

Soft Agar Assay.

Soft agar assay was conducted according to the established protocol from Gjoerup Lab (Zhao et al. 2003; Cheng et al. 2009), with minor modifications. Briefly, 0.6% agar was coated on the bottom of each well of a six-well tissue culture dish. Approximately 2,500 cells were mixed in growth media containing 0.3% agar and were cultured on top. Two milliliters of growth media was added and replaced every other day to keep sufficient nutrient and moisture. For hypoxic treatment, cells were incubated in a HeraCell150 incubator (Thermo Fisher Scientific, Inc.) set at 2% oxygen. After four to six weeks of incubation, colonies were stained with 0.005% crystal violet. Five representative fields (top, bottom, left, right, and middle) were imaged with a Q-IMAGING camera installed on a Leica MZFLIII dissecting microscope for each well.

Spheroid Formation Assay.

Approximately 600 cells were seeded per well of 96-well ultra-low attachment plates (Corning Incorporated). After four days, spheroids were imaged by brightfield microscopy using a Leica DMI 4000 inverted microscope equipped with a Leica CCD camera (Courtesy of Dr. Michael J. Soares, KUMC). Volume ($V = \frac{4}{3}\pi r^3$) was calculated after measuring the diameter and radius of each spheroid using NIH Image J (Vinci et al. 2012). Differences in average spheroid volume were analyzed by two-tail paired Student's t-test.

Intraperitoneal Tumor Xenografts.

SKOV3ip.1 and OVCAR8 cells were transduced with lentivirus to express firefly luciferase (pLenti PGK V5-LUC Neo (w623-2), a gift from Eric Campeau (Addgene

plasmid # 21471) (Campeau et al. 2009)). Following neomycin selection, KDM4B was knocked down using pLKO.1-puro constructs as described the Cell culture condition section. One million SKOV3ip.1-luc-neo cells or five million OVCAR8-luc-neo cells (in 200 μ l of sterile serum-free RPMI 1640) were injected into the peritoneal cavity of nude mice (Taconic; 4-6 weeks old). Ten mice were injected per group. Each week following injection, each mouse (approximately 20-25 g in weight on average) was injected with 200-250 μ l D-Luciferin (15 mg/mL in sterile PBS, Gold Biotechnology, Inc.) and bioluminescence measured with an IVIS Spectrum *in vivo* imaging system (Perkin Elmer) in the KUMC Center for Molecular Imaging. All mice were euthanized at humane end points for the shGFP control mice (approximately 4.5 weeks and 6.5 weeks post injection for SKOV3ip.1 and OVCAR8 cells, respectively). 30 minutes before euthanasia, animals were injected i.p. with pimonidazole (Hypoxyprobe, HPI) to label hypoxic cells. Significance of KDM4B-dependent changes in bioluminescent signal, tumor mass, and ascites volume were determined using Mann-Whitney U test compared to control (shGFP) mice.

All tumors were dissected, weighed, and flash-frozen or fixed for later analysis. If present, ascites fluid from each mouse was collected and the volume recorded. Frozen tumor samples were homogenized and processed to purify protein and RNA for gene expression analysis by qRT-PCR. Portions of the largest tumors (primarily omental masses) were fixed in 4% Paraformaldehyde in PBS, paraffin-embedded, and sectioned for IHC using antibodies against KDM4B, PAX8, Ki67, and pimonidazole. Representative slide images were captured using a Nikon 80i equipped with a Photometrics CoolSNAP ES camera running NIS-Elements AR image acquisition

software.

RESULTS

KDM4B is Abundantly Expressed in High Grade Ovarian Serous Adenocarcinoma Tumors and OVCAR Cell Lines

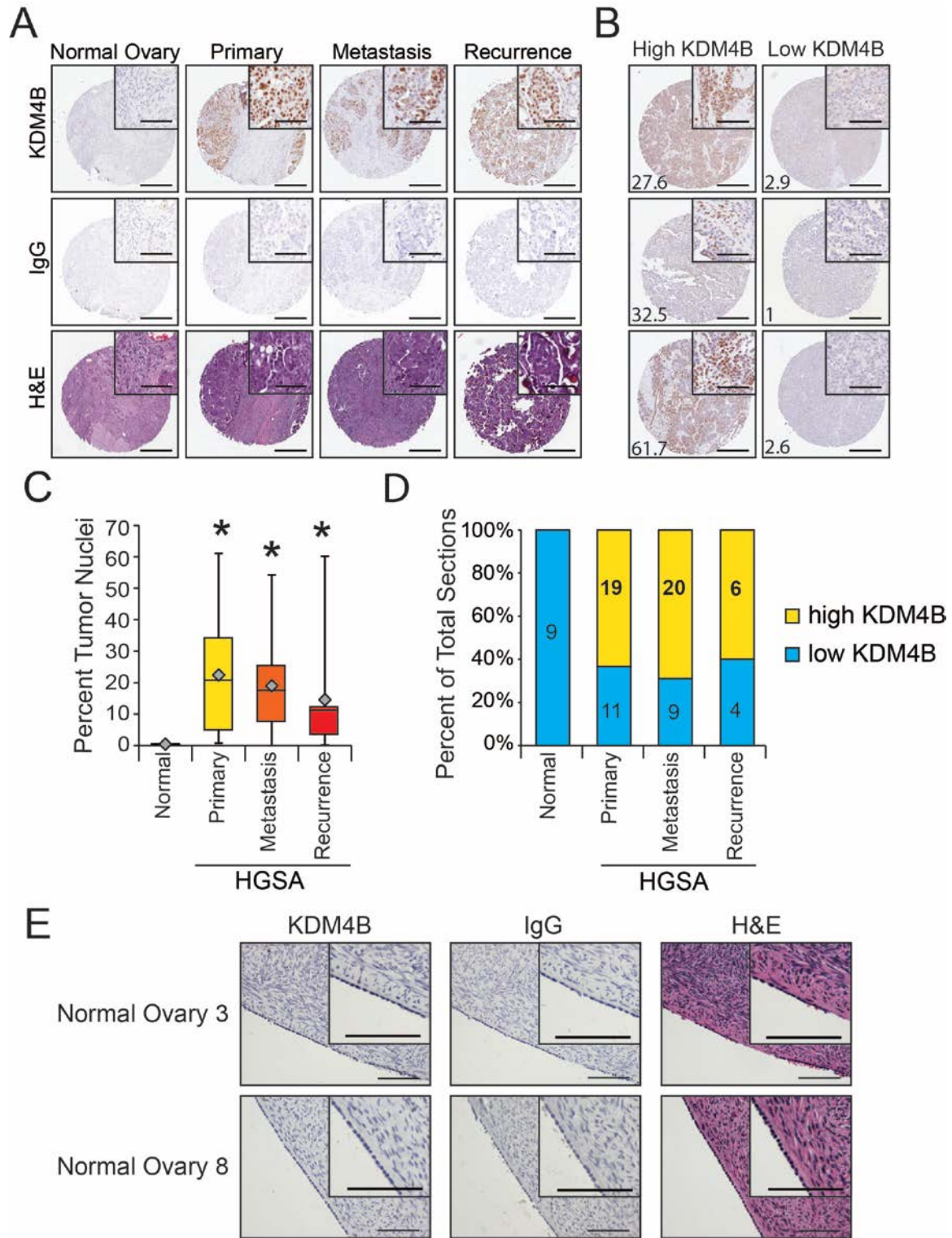
Hypoxic signaling mechanisms contribute to the progression of multiple cancer types, including epithelial ovarian cancers (Chi et al. 2006). Since hypoxic regulation of KDM4B is a common mechanism in many different cancer cell types (Beyer et al. 2008; Wellmann et al. 2008; Xia et al. 2009; Krieg et al. 2010), we hypothesized that KDM4B would also be robustly expressed in EOC, and contribute to tumor growth. In order to test our hypothesis, we obtained ovarian cancer tissue microarrays from the University of Kansas Cancer Center and measured KDM4B expression using immunohistochemistry (See Material and Methods and Table 3.3). These arrays contain representative biopsies from 48 primary EOC tumors with matched metastatic (42) and recurrent ovarian cancer sections (22, as available). Approximately 60% of the total tumor biopsies were collected from high grade serous adenocarcinoma patients (30 primary, 29 matched metastases, with 10 matched recurrent tumors). The remaining 18 tumors displayed combinations of serous, clear cell, endometrioid, and mucinous features (See Materials and Methods and Table 3.3 for a more complete description). KDM4B nuclear staining was significantly over-expressed compared to the normal ovarian sections, with more than 60% of the tumors staining positive for KDM4B (i.e. more than 10% of the tumor epithelium had detectable nuclear staining), while none of the tissues from normal ovarian punches stained positive (Fig. 3.1A-D). KDM4B was

Table 3.3. Analysis of KDM4B expression in normal ovary, and primary EOC tumors with matched metastatic and recurrent tumors.

Samples	Number of samples with High or Low KDM4B expression (% of samples)			% nuclei positive for KDM4B				
	High	Low	Total	Mean	Median	STDEV	Range	
Normal Ovary	0	9 (100)	9	0.4	0.3	0.4	0-1	
High Grade Serous	Primary	19 (63.3)	11 (36.7)	30	22.4	20.8	18.6	0.7-61.1
	Metastases	20 (69)	9 (31)	29	19.0	17.6	13.6	0-54.2
	Recurrence	6 (60)	4 (40)	10	14.5	11.2	17.8	0.2-60.2
	Totals	45 (65)	24 (35)	69	19.8	16.0	16.5	0-61.1
Mixed	Primary	9 (64.3)	5 (35.7)	14	17.5	14.4	15.9	0.4-44.5
	Metastases	3 (37.5)	5 (62.5)	8	10.4	5.1	10.9	1.3-30.2
	Recurrence	6 (54.5)	5 (45.5)	11	10.3	10.8	10.6	0.3-38.5
	Totals	18	15	33	13.4	11.1	13.3	0.3-44.5
Other	Primary	4 (100)	0	4	18.6	18.5	6.9	10.4-27.1
	Metastases	2 (50)	2 (50)	4	19.9	18.5	19.3	1.8-40.7
	Recurrence	0	0	0	NA	NA	NA	NA
	Totals	6 (75)	2 (25)	7	19.3	18.5	13.4	1.8-40.7

Numbers of samples with High or Low KDM4B expression are represented as n (%). Tumors with > 10% nuclei staining positive for KDM4B were considered "high," in a modification of a method described in (Goode, et al. 2011, See materials and Methods). "Mixed" contain various combinations of clear cell, endometrioid, and mucinous characteristics, all with a serous component. Other contains individual tumors with diagnosis of endometrioid, clear cell, or carcinosarcoma.

Figure 3.1. KDM4B is robustly expressed in ovarian cancer tissue and ovarian cancer cell lines compared to normal ovarian surface epithelial cells. A, Representative immunohistochemical detection of KDM4B (top row; brown, DAB; blue, hematoxylin) in Tumor Microarray sections from normal ovary and high-grade ovarian serous adenocarcinoma biopsies with matched primary, metastatic and recurrent tumor sections. IgG (middle) and H&E (hematoxylin and eosin, bottom) serve as controls for non-specific DAB staining and tissue structure controls, respectively. **B,** Representative IHC images of tumor sections with high (left) and low (right) KDM4B. For **A** and **B**, scale bar for entire section, 100 μm ; scale bar for inset, 50 μm . **C,** Box-whisker plot of KDM4B nuclear staining in normal ovary (9), primary HGSA tumors (30), metastases (29), and recurrent tumors (10). Diamond, mean; solid bar, median; top and bottom boxes, 75 and 25 percentile; top and bottom whiskers, high and low. **D,** Percentage of total patient samples in each category (normal, primary, metastasis and recurrence) staining for high or low KDM4B (high > 10% nuclei staining positive for KDM4B). **F,** KDM4B expression in representative normal ovarian surface epithelium. Scale bar, 100 μm .



robustly expressed in multiple ovarian cancer cell lines representing a broad range of EOC genotypes, particularly in response to hypoxia (0.5% oxygen) (Fig. 3.2). In an independent validation using sections derived from normal ovaries from reproductive age women, there was weak KDM4B staining in normal ovarian surface epithelium (OSE, Fig. 3.1E), one potential source tissue for EOC (Lengyel 2010). Additionally, there was weak hypoxic induction of KDM4B in the immortalized OSE cell line HIO80 (Fig. 3.2). Taken together, we conclude that KDM4B is over-expressed in epithelial ovarian cancer cells may be an important factor contributing to progression of HGSA.

KDM4B Regulates *In Vitro* Cell Invasion, Migration, and Anchorage-Independent Growth in Normoxia and Hypoxia

Expression microarray analysis indicated that suppression of KDM4B with transiently transfected siRNA disrupted the regulation of multiple genes with well-described roles in cell proliferation, particularly in normoxic conditions. To determine if regulation of proliferative genes in EOC cells was a significant effect, SKOV3ip.1 cells were transiently transfected with siRNA to KDM4B, and the cells seeded for short-term proliferation assays in 21%, 2%, and 0.5% oxygen (See Materials and Methods, knockdown efficiency was demonstrated in Figure 2.1A and 2.8). By the third day, cell proliferation was significantly reduced in 21% oxygen following KDM4B knockdown compared to the non-silencing control, but not in either 2% oxygen or 0.5% oxygen (Fig. 3.3A-C). These results are consistent with the general decrease in expression of proliferative genes in normoxia described in Figure 2.9A, with little effect of KDM4B in hypoxia. In subsequent experiments using stably integrated shRNA constructs in a long-term proliferation assay, SKOV3ip.1 cells displayed little biologically significant

Figure 3.2. KDM4B protein expression in ovarian cancer cell lines. Immunoblot detection of KDM4B and HIF-1 α in a panel of ovarian cancer cell lines in normoxia (N, 21% oxygen) and in hypoxia (H, 0.5% oxygen). HIO-80 cells serve as non-transformed OSE control. Beta-actin serves as loading control for the KDM4B blot.

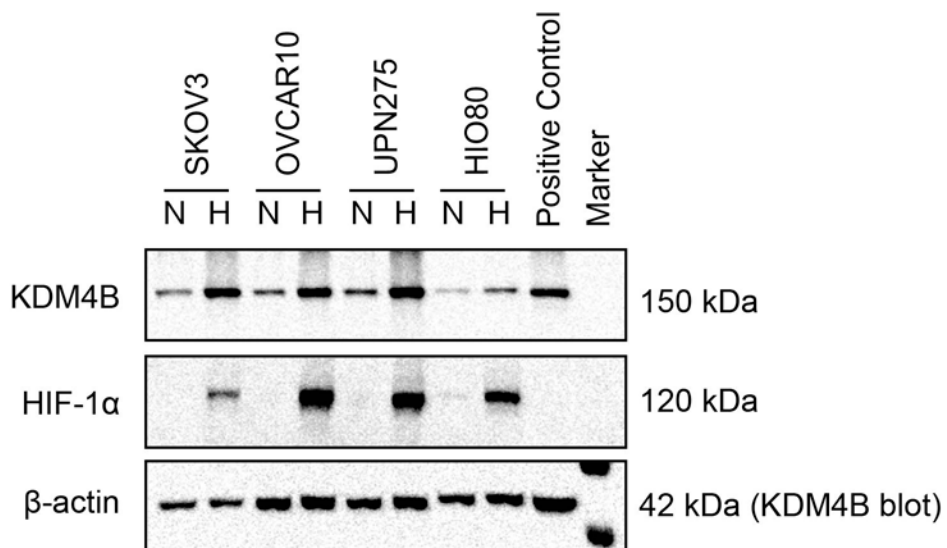
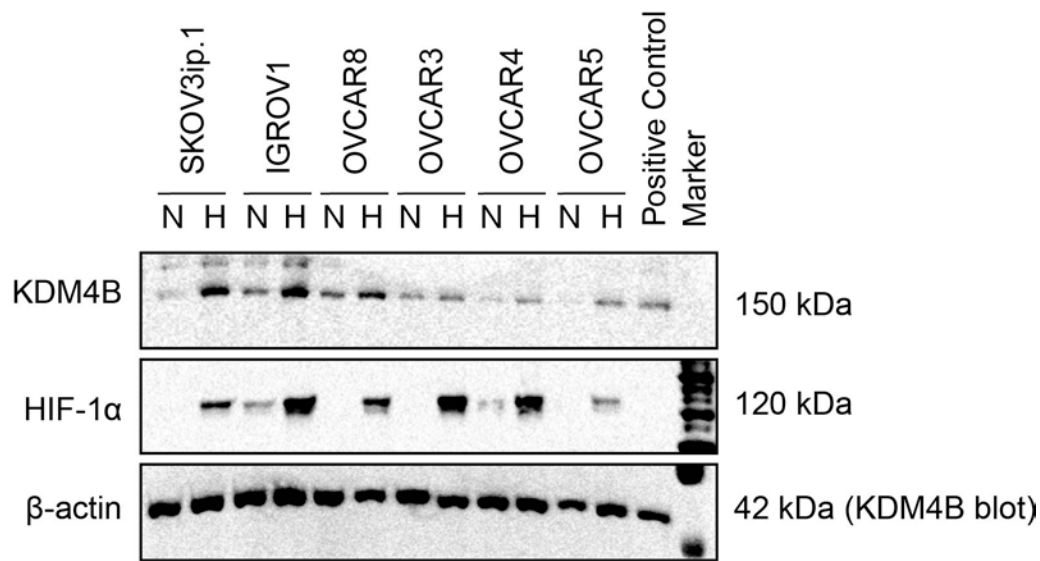
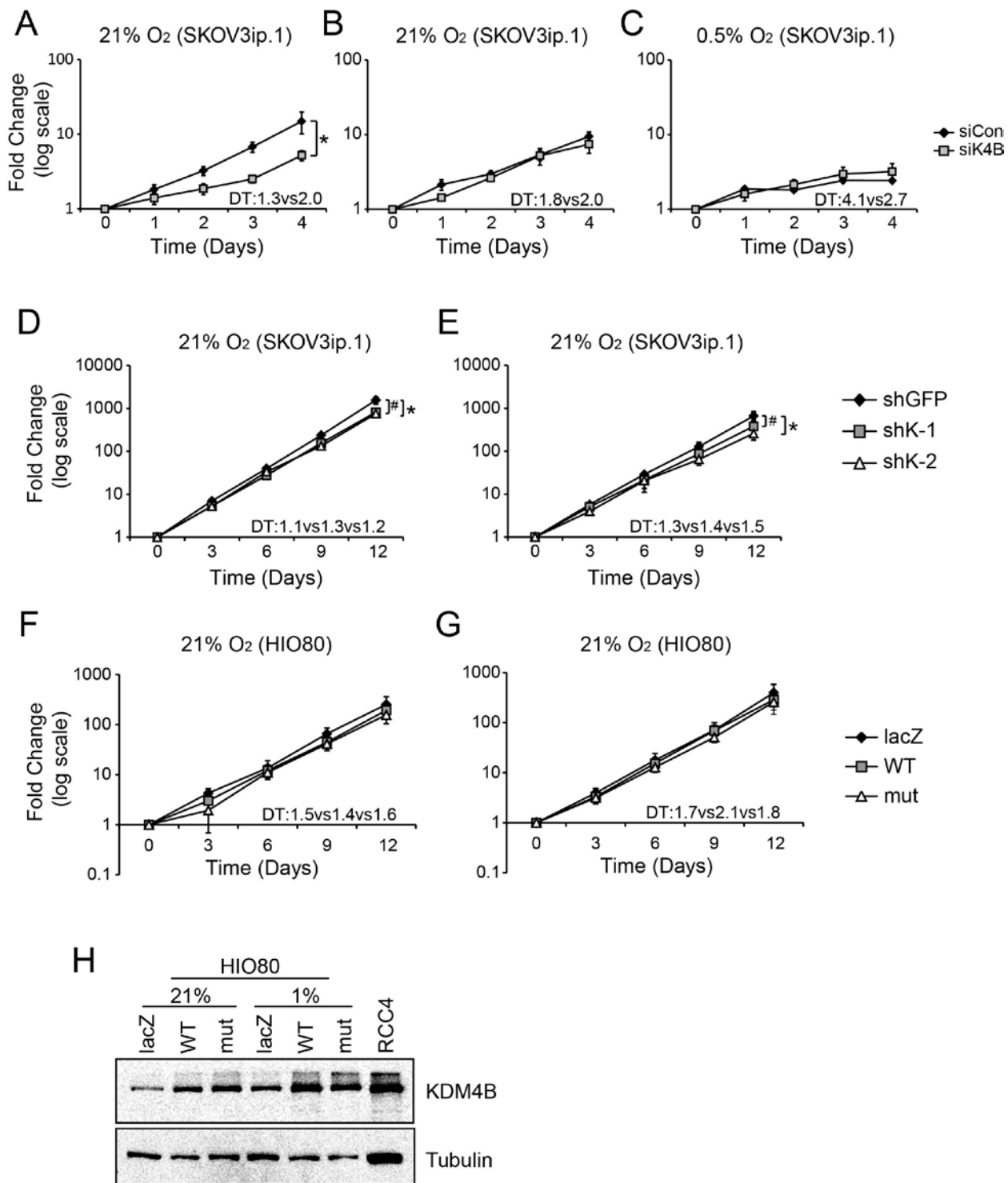


Figure 3.3. Regulation of SKOV3ip.1 cell proliferation by KDM4B. **A-C**, SKOV3ip.1 cells were transfected with siRNA to KDM4B (grey line) or an irrelevant control (black line), seeded for short-term proliferation experiments (See Materials and Methods), and cultured in 21% O₂ (**A**), 2% O₂ (**B**), 0.5% O₂ (**C**). Data represent four independent experiments. *, P<0.05, determined by nonlinear regression. DT, doubling time (days), siCon vs siK4B. **D-E**, Long-term cell proliferation assay. SKOV3ip.1 cells transduced with shRNA to KDM4B (shK-1 and shK-2) were seeded for long-term cell proliferation assays as described in Materials and Methods, and cultured in 21% O₂ (**D**) and 2% O₂ (**E**). Data represent four independent experiments. Significance was determined using nonlinear regression (#, P<0.05, comparing shK-1 to shGFP; *, P<0.05, comparing shK-2 to shGFP). DT, doubling time (days), shGFP vs shK-1 vs shK-2. **F-G**, Long-term cell proliferation assay. HIO80 cells transduced with lentivirus containing wildtype (WT) or H189A mutated (mut) KDM4B were seeded for long-term cell proliferation assays as described in Materials and Methods, and cultured in 21% O₂ (**F**) and 2% O₂ (**G**). Data represent three independent experiments. Significance was determined using two-tailed paired Student's t-test. DT, doubling time (days), lacZ vs WT vs mut. **H**, Immunoblotting showing overexpression of WT and mut KDM4B in HIO80 cells in normoxia (21% O₂) and hypoxia (1% O₂). KDM4B expression in RCC4 cells served as a positive control. Tubulin served as a loading control for the same blot.



dependence on KDM4B for cell growth in any oxygen condition tested (0.1-0.2 day increase in doubling time), although the difference was still statistically significant (Figure 3.3D-E, knockdown efficiency was demonstrated in Figure 2.10), possibly due to compensation from one of the other KDM4 histone demethylases (Figure 2.11). Combined, these results indicate that the regulation of proliferative genes by KDM4B is not the most significant contributing factor to ovarian cancer progression. A separate experiment with the non-transformed cell line HIO80 showed that overexpression of KDM4B did not increase cell proliferation (Figure 3.3F-G, KDM4B expression level validated in Figure 3.3H).

Expression analysis also indicated that KDM4B regulated several metastatic genes and pathways (i.e. *PDGFB*, *LOXL2*, *LOX*, and *LCN2*; Figure 2.9C, 2.13-14). In the case of EOC, metastasis typically occurs as peritoneal dissemination, where the primary tumors shed cancer cells into the peritoneal cavity. Free-floating cells in the peritoneum establish tumors throughout the omentum, visceral fascia, and mesothelial lining of the abdominal cavity (Naora and Montell 2005; Lengyel 2010). This unique mechanism of metastasis restricts most of the relevant mechanisms to invasion, migration, and attachment-free growth. SKOV3ip.1 and OVCAR8 cells expressing shK-1 and shK-2 were seeded to Boyden chamber migration and invasion assays (Figure 3.4 and 3.5). Consistent with the observed alterations in metastatic genes from the microarray expression analysis, both SKOV3ip.1 and OVCAR8 cells demonstrated a dependence on KDM4B for invasion through Matrigel, with at least 60% decrease in invasive capacity for shK-2 in all conditions tested (Figure 3.4A and 3.5A). In SKOV3ip.1 cells, shK-1 is a less effective construct under hypoxia (Figure 3.4A-B), so

Figure 3.4. KDM4B supports SKOV3ip.1 cell invasion and migration. A, SKOV3ip.1 Matrigel Invasion Assay. SKOV3ip.1 cells expressing shRNA to KDM4B (shK-1 and shK-2) were seeded to Boyden Chambers coated with Matrigel and processed as described in Methods. Data represent mean \pm S.E.M for five independent experiments conducted in triplicate. **B,** Migration Assay. SKOV3ip.1 cells were seeded to empty Boyden chambers, cultured and quantified as in Panel A. Data represent mean \pm S.E.M for five independent experiments conducted in triplicate. **C,** SKOV3ip.1 proliferation control for Boyden Chamber Migration and Matrigel Invasion Assay. SKOV3ip.1 cells were grown as monolayers for 24 hours, trypsinized, frozen, and analyzed in parallel with the cells in the migration and invasion groups (**A-B**). Data represent mean \pm S.E.M. Results were averaged from five independent experiments conducted in triplicate. For Panels **A-C**, significance was calculated relative to shGFP control at each oxygen condition, using Mann Whitney U-tests (*, $P < 0.05$; #, $P < 0.005$). **D,** Representative image of SKOV3ip.1 invasion assay. Filters treated in parallel to those in Panel A were fixed and stained, as described in Materials and Methods. 100X magnification, scale bar = 200 μ m.

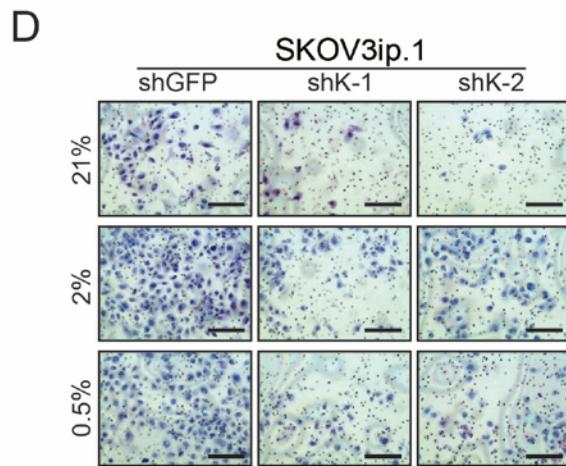
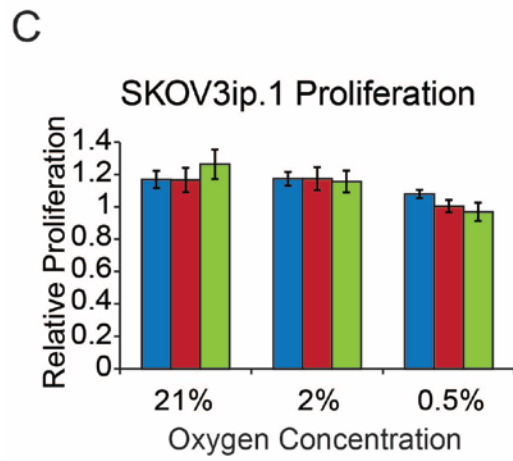
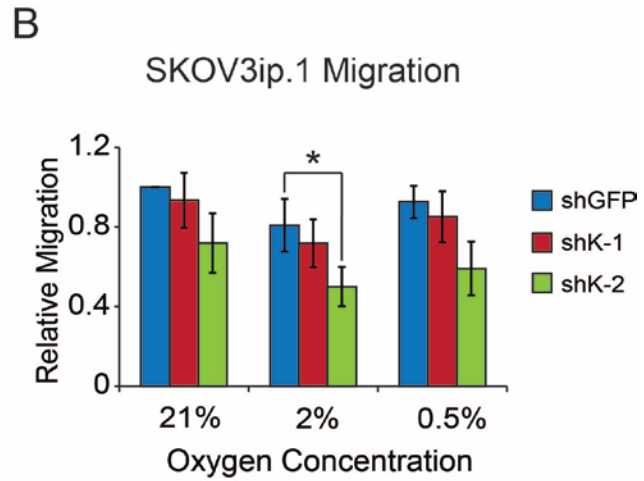
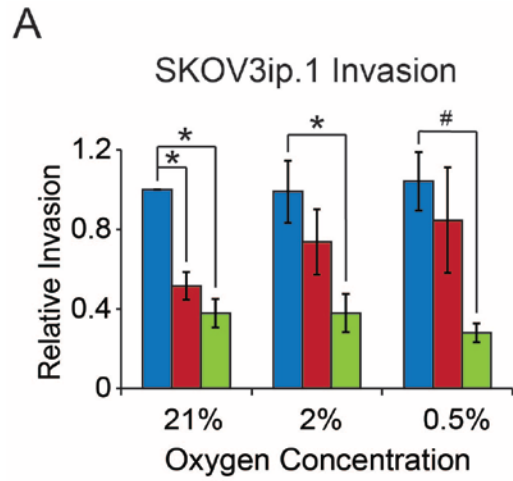
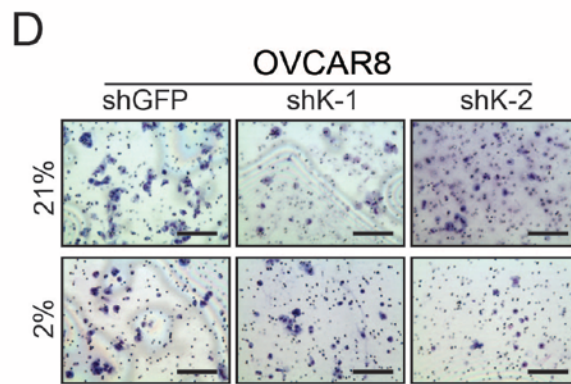
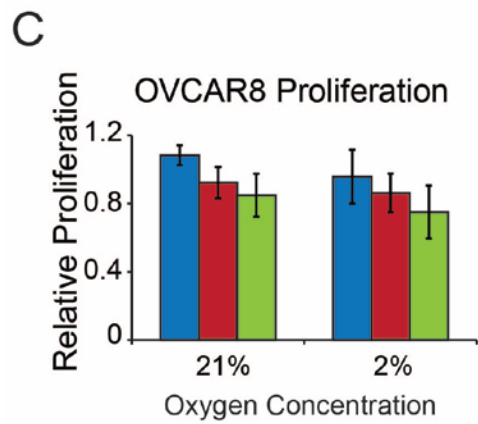
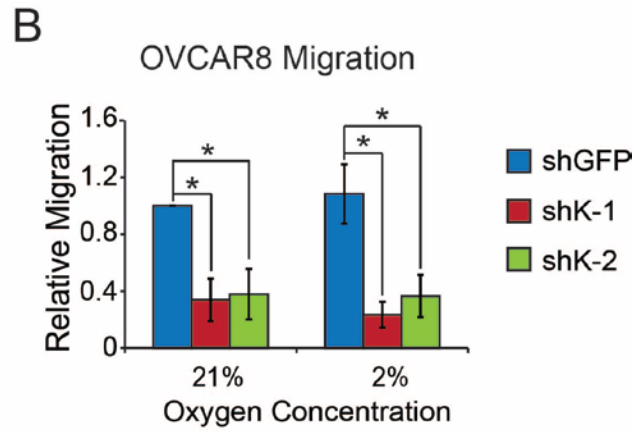
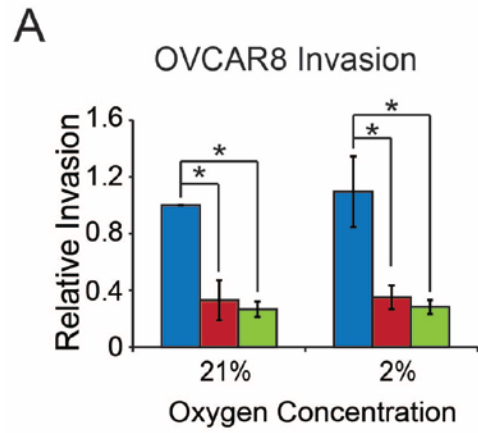


Figure 3.5. KDM4B supports OVCAR8 cell invasion and migration. A, OVCAR8 Matrigel Invasion Assay. OVCAR8 cells expressing shRNA to KDM4B (shK-1 and shK-2) were seeded to Boyden Chambers coated with Matrigel and processed as described in Methods. Data represent mean \pm S.E.M for four independent experiments conducted in triplicate. **B,** Migration Assay. OVCAR8 cells were seeded to empty Boyden chambers, cultured and quantified as in Panel A. Data represent mean \pm S.E.M for four independent experiments conducted in triplicate. **C,** OVCAR8 proliferation control for Boyden Chamber Migration and Matrigel Invasion Assay. OVCAR8 cells were grown as monolayers for 24 hours, trypsinized, frozen, and analyzed in parallel with the cells in the migration and invasion groups (**A-B**). Data represent mean \pm S.E.M. Results were averaged from four independent experiments conducted in triplicate. For Panels **A-C**, significance was calculated relative to shGFP control at each oxygen condition, using Mann Whitney U-tests (*, $P < 0.05$). **D,** Representative image of OVCAR8 invasion assay. Filters treated in parallel to those in Panel A were fixed and stained, as described in Materials and Methods. 100X magnification, scale bar = 200 μ m.



while there was a trend of reduced invasion and migration, attenuation of migration was only significant in 2% oxygen. In OVCAR8 cells, invasion through Matrigel and migration through the empty inserts were severely attenuated with both shRNA constructs (>80%) (Figure 3.5A-B), indicating that while KDM4B was universally important for regulating invasive behavior in either cell line, its effects may be mediated through distinct, but overlapping mechanisms. This effect was not due to defect of cell proliferation, as tested in a paralleled proliferative control experiment (Figure 3.4C and 3.5C).

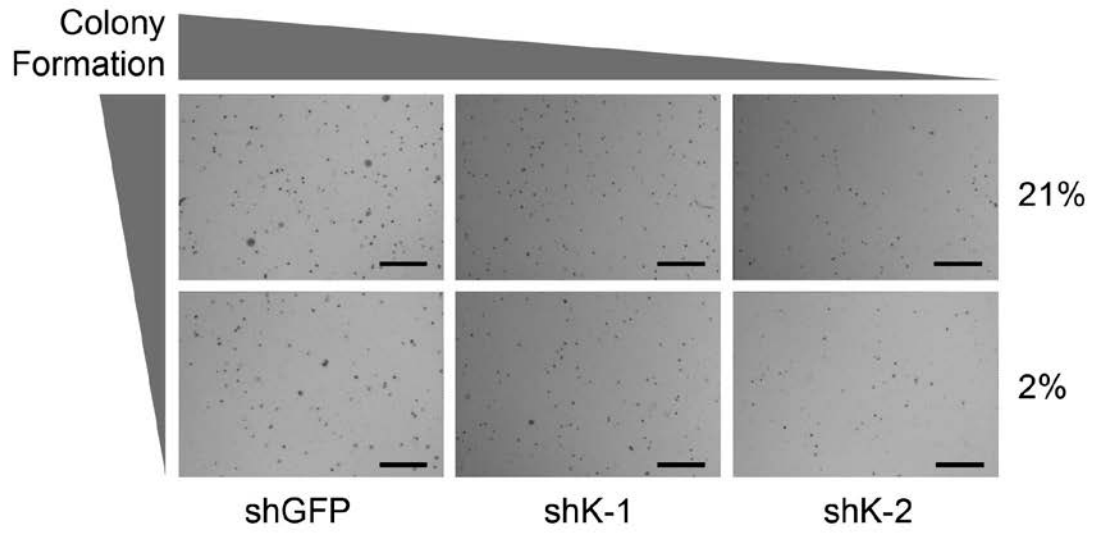
Another characteristic of metastatic EOC cells is the ability to grow as clusters of cells suspended in peritoneal ascites (Lengyel 2010). When SKOV3ip.1 cells were embedded in soft agar, cells transfected with siK4B grew smaller and fewer colonies compared to siCon cells (Figure 3.6A). Using a quantitative assay to measure the formation of single spheroids in ultra-low attachment plates, we determined that loss of KDM4B significantly reduced the size of spheroids by a factor of at least 50% in SKOV3ip.1 cells, with similar results in OVCAR8 cells (Figure 3.6B-C). Additionally, the shapes of the spheroids displayed with the appearance of frayed boundaries in the knockdown groups compared to the shGFP controls (Figure 3.6D-E). Combined, these results indicate that KDM4B may influence ovarian cancer progression by promoting formation of ascites spheroids in the peritoneal cavity and subsequent invasion of these clusters to peritoneal tissues.

KDM4B is Required for Peritoneal Tumor Growth

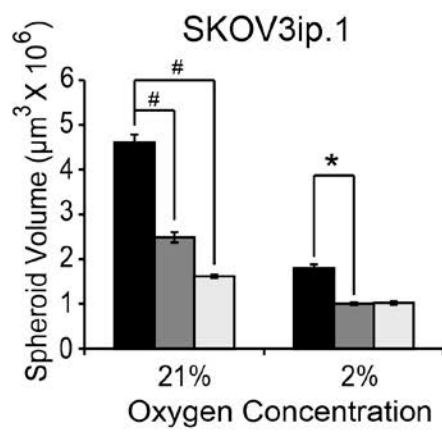
To determine if loss of KDM4B influenced tumor progression *in vivo*, SKOV3ip.1 and OVCAR8 cells were stably transduced with firefly luciferase (See Materials and Methods). KDM4B was knocked down with shRNA, and cells were injected i.p. into

Figure 3.6. KDM4B supports ovarian cancer cell attachment-free growth. A, SKOV3ip.1 soft agar spheroid formation assay. SKOV3ip.1 cells transfected with shRNA to KDM4B were cultured in 0.3% soft agar in tissue culture dish coated with 0.6% soft agar. Cells were incubated in 21% and 2% O₂ as described in Materials and Methods. Images were taken after 2 weeks of incubation. 10X magnification, scale bar = 1 mm. **B,** SKOV3ip.1 spheroid formation assay. SKOV3ip.1 cells transduced with shRNA to KDM4B were cultured in 3D spheroid formation assays in 21% and 2% O₂ as described in Materials and Methods. After four days, spheroid volume was calculated. Data represent mean volume \pm S.E.M. 16 spheroids for each shRNA construct. **C,** Representative images (median volume) of SKOV3ip.1 spheroids. 100X magnification, scale bar = 100 μ m. **D,** OVCAR8 spheroid formation assay, conducted as described for B. **E,** Representative images (median volume) of OVCAR8 spheroids. 100X magnification, scale bar = 100 μ m. For Panels **B** and **D**, significance was calculated relative to shGFP control at each oxygen condition, using Mann Whitney U-tests (*, P<0.05; #, P<0.005).

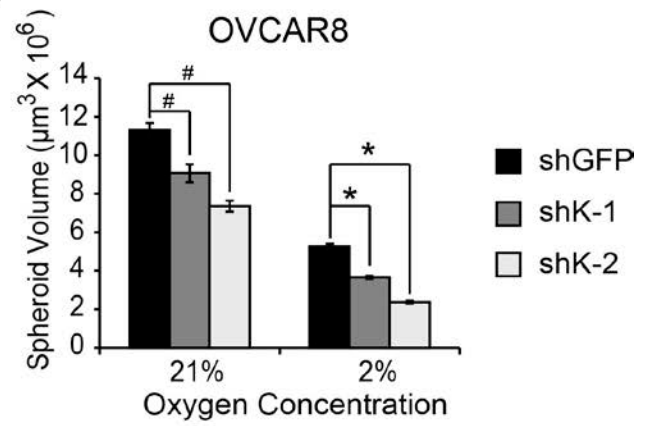
A



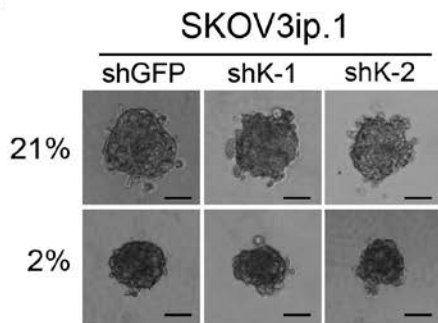
B



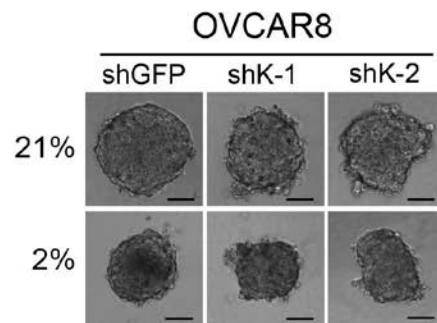
C



D



E



nude mice. Tumor seeding and growth was monitored weekly by bioluminescence. At experimental endpoint, KDM4B knockdown significantly decreased tumor signal in mice (Figure 3.7 and 3.8). Quantitation of the total photon flux revealed a significant decrease in accumulation of tumor burden in cells expressing shRNA to KDM4B (Figure 3.9). This effect was significant for both shK-1 and shK-2 in SKOV3ip.1 cells, whereas shK-2 showed a more significant effect in slowing OVCAR8 tumor growth than shK-1 (Figure 3.9). Total endpoint tumor weight was significantly decreased by at least 50% with both shRNA constructs in SKOV3ip.1 cells and with shK-2 in OVCAR8 cells (Figure 3.10A-B). OVCAR8 cells expressing the shK-2 construct developed significantly less ascites fluid compared to the shGFP control, while shK-1 showed an intermediate decrease in total ascites volume (Figure 3.10C). Terminal necropsy confirmed a general decrease in the size of metastatic nodules in the omentum, viscera, and peritoneal wall. (See representative images, Figure 3.11). Combined, these studies demonstrate a requirement for KDM4B in the establishment and growth of peritoneal tumors.

KDM4B is Expressed in Hypoxic Regions of Tumors

Immunohistochemical detection of KDM4B in xenograft tumors confirmed the stability of knockdown throughout the study (Figure 3.12A-D), while also demonstrating coexpression of KDM4B with tumor hypoxia (Figure 3.12E-L, as measured by pimonidazole and PAX8 staining to detect hypoxia and EOC tumor epithelium, respectively). There was no apparent difference in cell proliferation (Ki-67 staining, Figure 3.12M-P), supporting the *in vitro* observations that stable knockdown of KDM4B had little effect on cell proliferation in monolayers (Figure 3.3). QPCR measurement of *KDM4B*, *KDM4A*, *KDM4C*, and *KDM4D* RNA in both SKOV3ip.1 and OVCAR8 derived

Figure 3.7. KDM4B regulates in vivo peritoneal growth of SKOV3ip.1 cells. Ventral bioluminescent images of nude mice injected with SKOV3ip.1-luc-neo cells transduced with KDM4B shRNA constructs, compared to shGFP control. Images were taken weekly after injection.

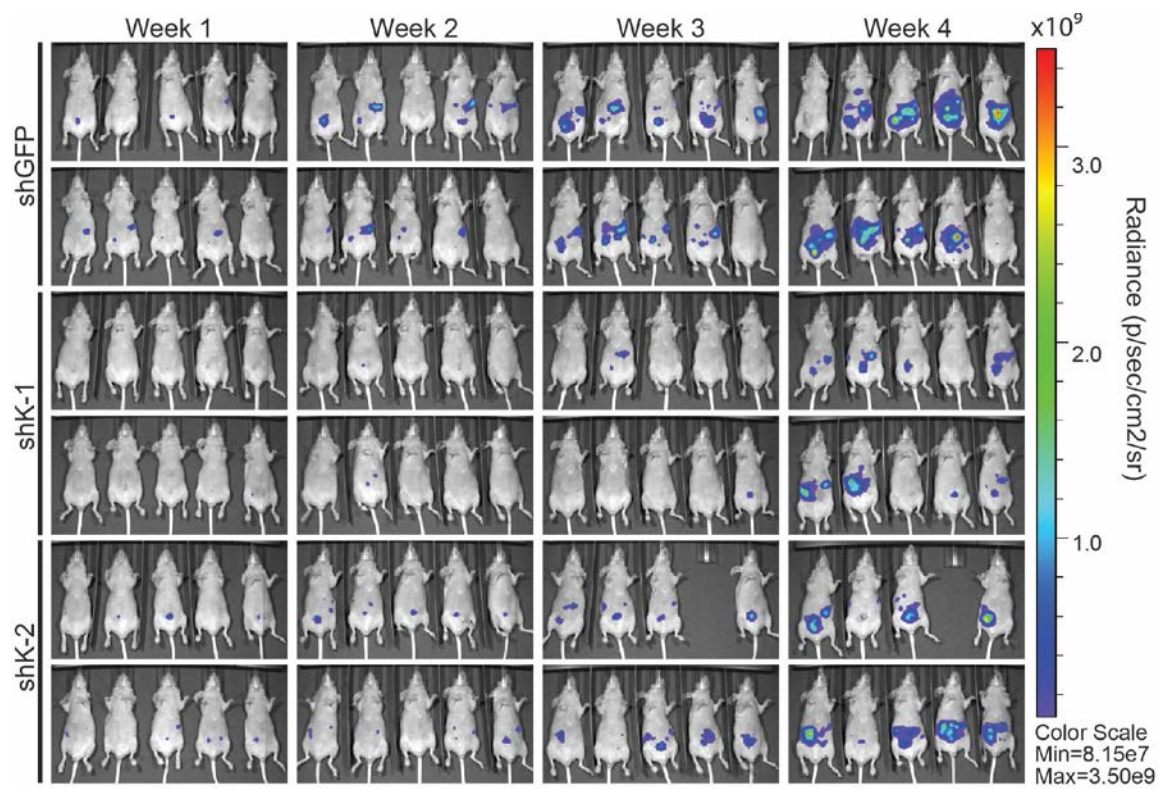


Figure 3.8. KDM4B regulates in vivo peritoneal growth of OVCAR8 cells. Ventral images of mice injected with OVCAR8 cells transduced with the indicated KDM4B shRNA constructs. Images were captured weekly after injection.

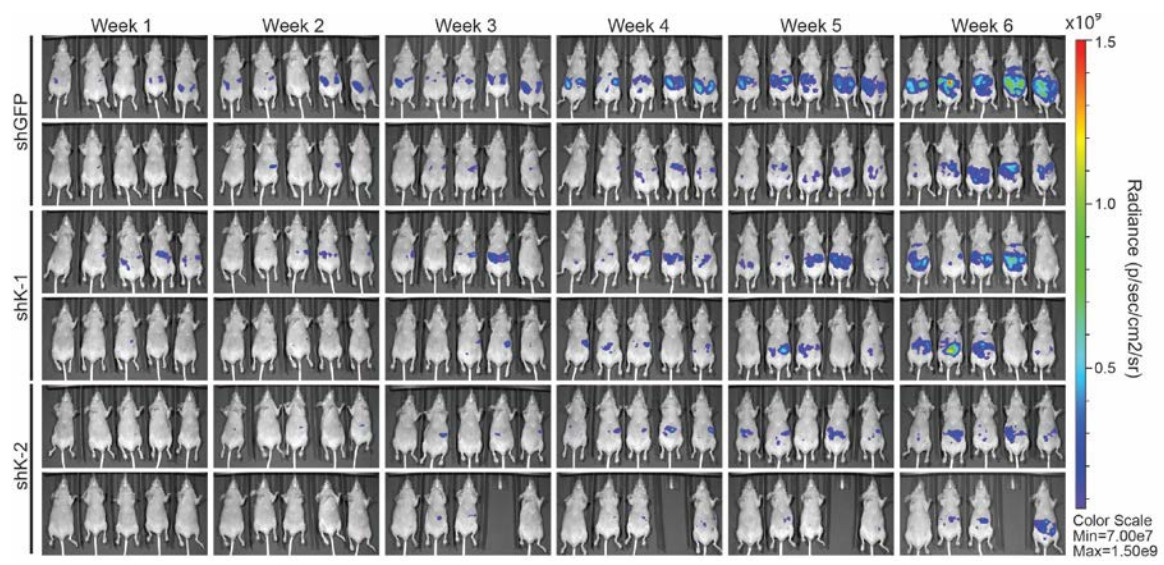


Figure 3.9. KDM4B regulates in vivo peritoneal growth of ovarian cancer cells. A, Longitudinal measurement of ventral bioluminescence for all mice injected with SKOV3ip.1-luc-neo transduced with shGFP control (blue line, n=10), shK-1 (green line, n=10), and shK-2 (red line, n=9). Data represents mean total radiance (photons/sec) for each group \pm SEM. **B,** Longitudinal dorsal bioluminescence for SKOV3ip.1 study, analyzed as in **A**. **C,** Longitudinal measurement of ventral bioluminescence for all mice injected with OVCAR8-luc-neo transduced with shGFP control (blue, n=10), shK-1 (red, n=10), and shK-2 (green, n=10). Data represents mean total radiance (photons/sec) for each group \pm SEM. **D,** Longitudinal dorsal bioluminescence for OVCAR8 study, analyzed as in **C**. Statistics were calculated by Kruskal Wallis and Mann Whitney U-tests (*, $P < 0.05$; **, $P < 0.005$). Blue asterisks, difference among all three groups; red asterisks, difference between shK-1 and shGFP; green asterisks, difference between shK-2 and shGFP.

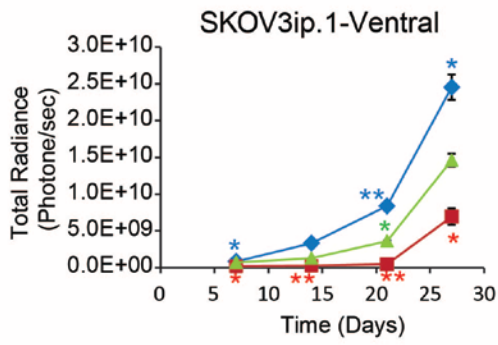
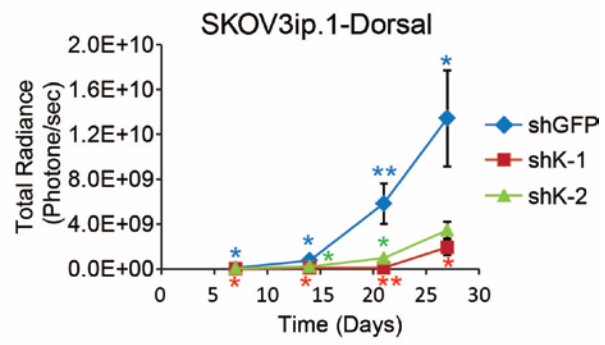
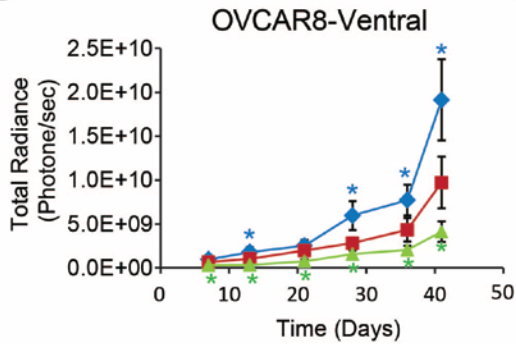
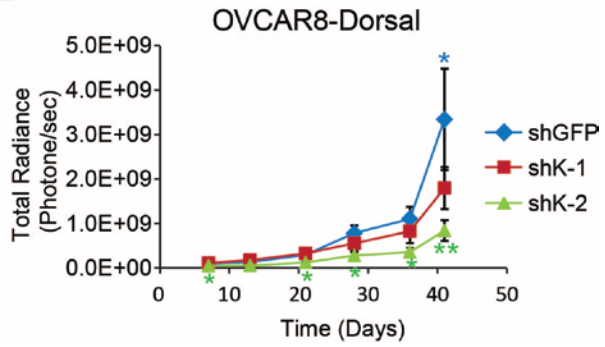
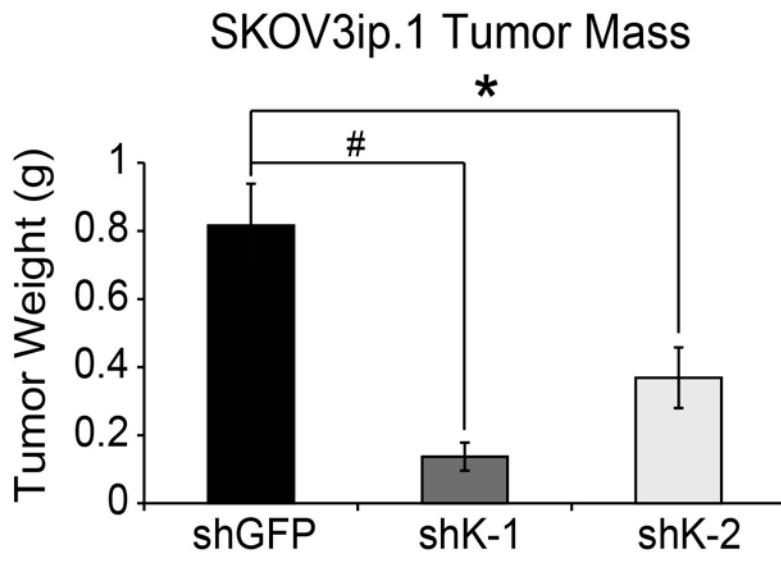
A**B****C****D**

Figure 3.10. KDM4B regulates in vivo peritoneal growth and ascites formation of ovarian cancer cells. **A**, Mean total tumor weight \pm S.E.M. for SKOV3ip.1 xenografts. $n \geq 9$. (*, $P < 0.05$; #, $P < 0.005$, Mann-Whitney U-test). **B**, Mean total tumor weight \pm S.E.M. for OVCAR8 xenografts. $n \geq 9$. (*, $P < 0.05$; #, $P < 0.005$, Mann-Whitney U-test). **C**, Ascites collected from OVCAR8 experiment. Box-Whisker plot of ascites fluid volume. Short bold bar, mean; solid bar, median; $n \geq 9$. (*, $P < 0.05$, determined by Mann-Whitney U-test).

A



B

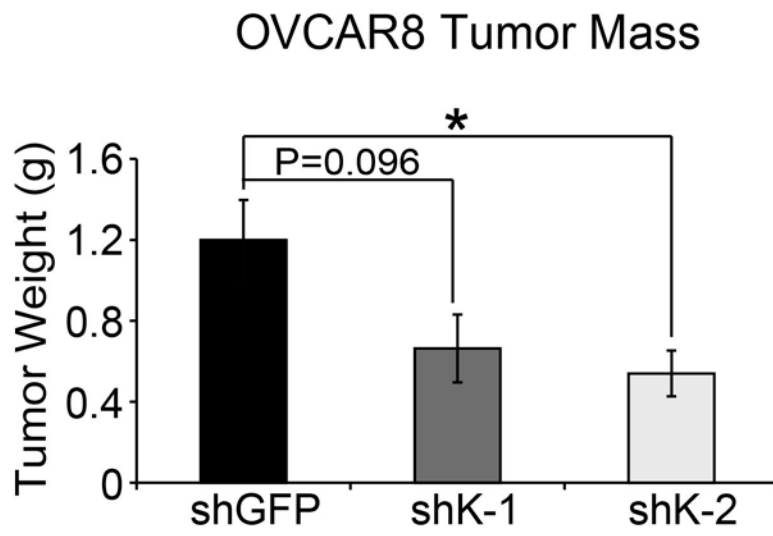


Figure 3.11. KDM4B regulates in vivo peritoneal growth and dissemination of ovarian cancer cells. Representative images of end-point necropsy showing tumor distribution in mice injected with SKOV3ip.1 or OVCAR8 cells carrying shRNA to GFP control or KDM4B, as indicated. Scale bar = 1 cm. Visible tumors are circled in yellow. Note the large cluster of fused omental tumors in the shGFP controls, compared to the knockdown mice.

Figure 3.12. KDM4B is expressed in hypoxic regions of tumor xenografts. A-D, KDM4B. **E-H,** Pimonidazole. **I-L,** PAX8. **M-P,** Ki67. **Q-T,** IgG. **U-X,** H&E. Scale bar, 100 μ m. N, necrosis; H, hypoxia. Panels **A, E, I, M, Q,** and **U** correspond to SKOV3ip.1 shGFP control tumor sections. Panels **B, F, J, N, R,** and **V** correspond to SKOV3ip.1 shK-2 KDM4B knockdown tumor sections. Panels **C, G, K, O, S,** and **W** correspond to OVCAR8 shGFP control tumors. Panels **D, H, L, P, T,** and **X** correspond to OVCAR8 shK-2 tumor sections. All IHC sections were counterstained with hematoxylin to visualize cell nuclei. Images were captured at 100X magnification. Scale bar = 200 μ m.

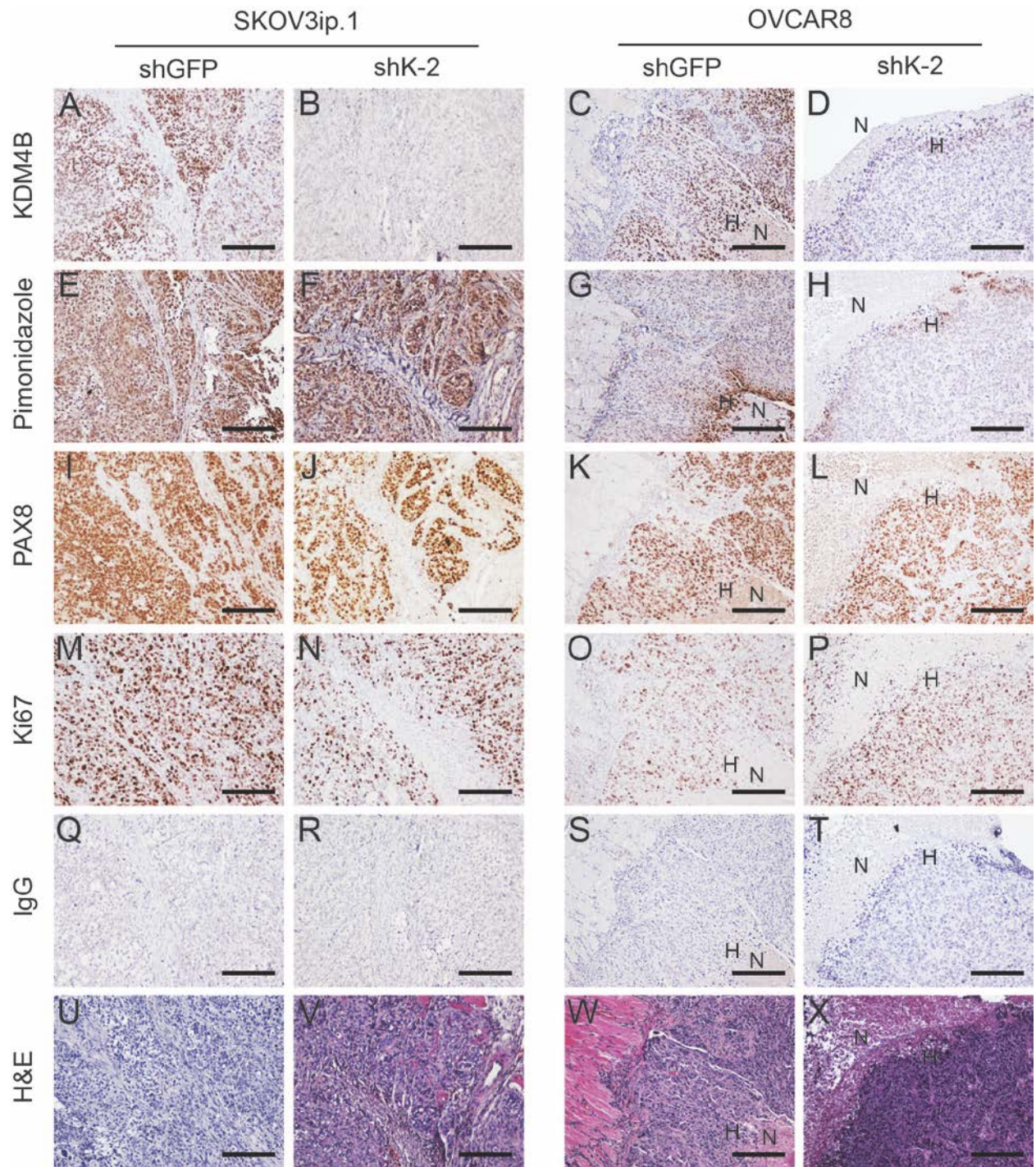
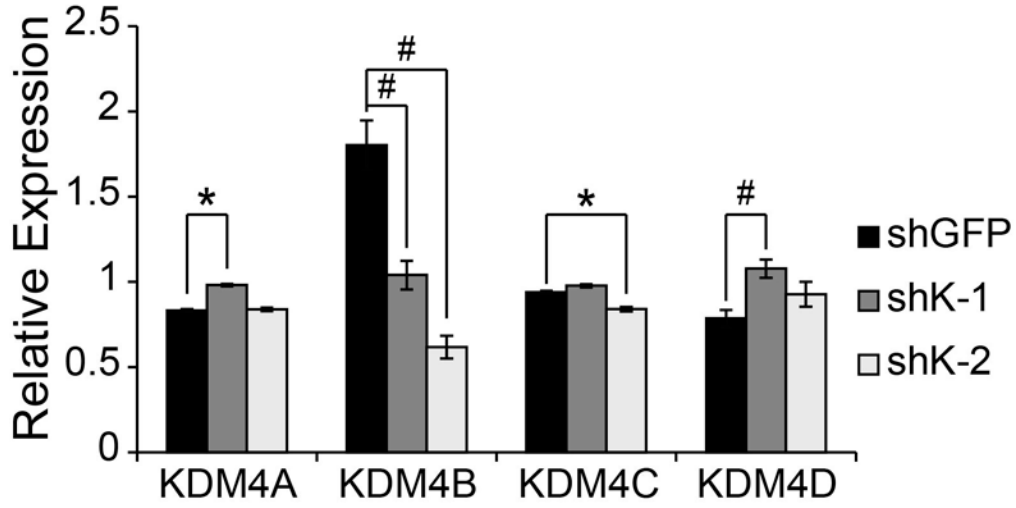


Figure 3.13. Post-mortem KDM4 Family Member Expression. **A**, QRT-PCR measurement of KDM4 subfamily members in SKOV3ip.1 xenograft tumors, as described in Methods. (shGFP, n=9; shK-1, n=9; shK-2, n=8). **B**, QRT-PCR measurement of KDM4 subfamily members in OVCAR8 xenograft tumors. (shGFP, n=10; shK-1, n=9; shK-2, n=8). Data represents average fold change relative to shGFP control, after normalization to homo sapiens *GAPDH*. Significance calculated by Mann Whitney U-test relative to shGFP control (*, $P < 0.05$).

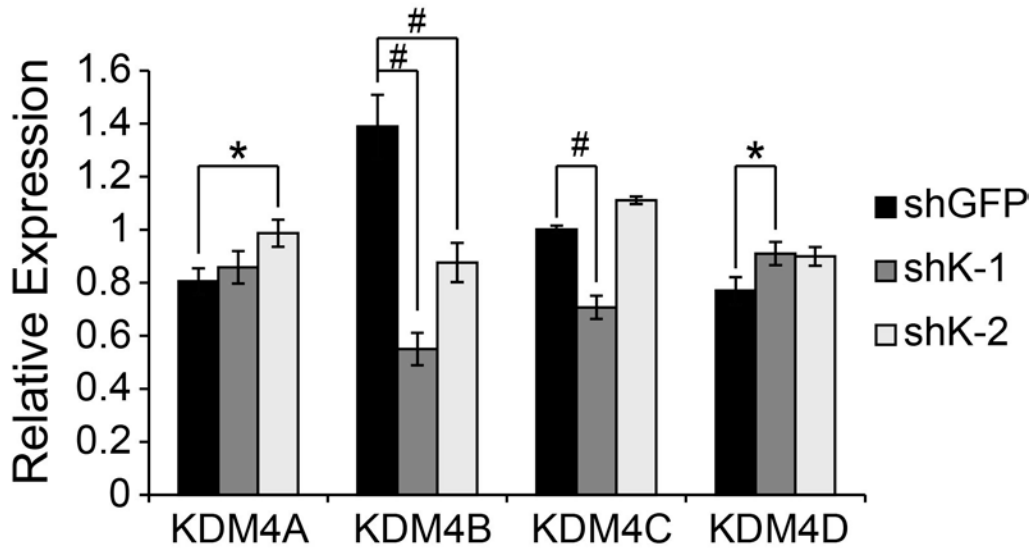
A

SKOV3ip.1 Gene Expression



B

OVCAR8 Gene Expression



tumors (Figure 3.13) provided additional confirmation of stable knockdown of KDM4B, while also identifying slight increases in expression of *KDM4D*.

To further confirm that KDM4B expression in EOC was associated with tumor hypoxia, the expression of Carbonic anhydrase 9 (CA-IX), a potent marker of tumor hypoxia was also scored in the KUCC OVCAR TMAs (Figure 3.14A for representative comparison, and Figure 3.14B for a scatter plot of the IHC scoring, raw score summaries are listed in Table 3.4). Average intensity of CA-IX staining for triplicate tumor sections in the serous tumors (range 0-3) was positively correlated to the percentage of KDM4B-positive tumor nuclei (Pearson's correlation $r = 0.390$, $P = 0.001$, for all tumors combined). When the primary and metastatic tumors were analyzed separately, this correlation extended individually to both groups ($r = 0.357$ and 0.472 , respectively), although significance was achieved only in the metastatic group ($P=0.03$). When samples were divided into "High" and "Low" CA-IX groups (High >2 average score), KDM4B scores were significantly higher in the samples expressing more CA-IX (Figure 3.14C, $p=0.026$, Mann-Whitney U-test for primary and metastatic tumors combined). Similarly, the association between KDM4B and the putative target gene PDGFB was also apparent in the TMA data (Figure 3.14A, D-E). PDGFB was positively correlated with KDM4B expression in all serous tumors ($r=0.245$, $P=0.044$), with similar correlations in the individual primary and metastatic groups ($r= 0.318$ and 0.382 , respectively), although the correlation was only significant in the metastatic tumors ($P=0.043$). When samples were separated by the median KDM4B score for combined primary and metastatic tumors, the segregation of PDGFB scores was also significant ($P=0.01$, Figure 3.14E). Considering the relatively

Figure 3.14. KDM4B is preferentially expressed in hypoxic ovarian cancer tumors to promote progression. **A**, Representative images of high and low KDM4B staining TMA sections with matched CAIX and PDGFB staining. IgG and H&E serve as negative and tissue structure controls, respectively. Scale bar = 50 μ m. **B**, Scatter plot of hypoxia (CA9 staining) vs KDM4B staining in TMA sections. Blue diamonds, primary tumors; red squares, metastatic tumors; green triangles, recurrent tumors. **C**, Box-Whisker Plot of KDM4B staining in High vs Low CA-IX. Data represent combined primary and metastatic tumors. Statistics were calculated by Mann Whitney test. *, $P < 0.05$. **D**, Scatter Plot of PDGFB vs. KDM4B staining in TMA sections. **E**, Box-whisker plot of correlation between KDM4B and PDGFB staining in TMA sections. Samples were segregated by median KDM4B score for primary and metastatic samples combined. Statistics were calculated by Mann Whitney test, relative to shGFP control. *, $P < 0.05$.

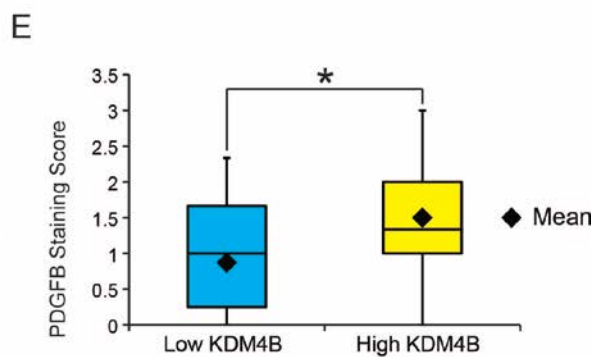
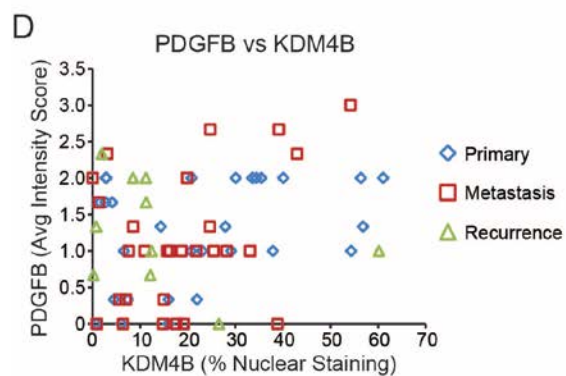
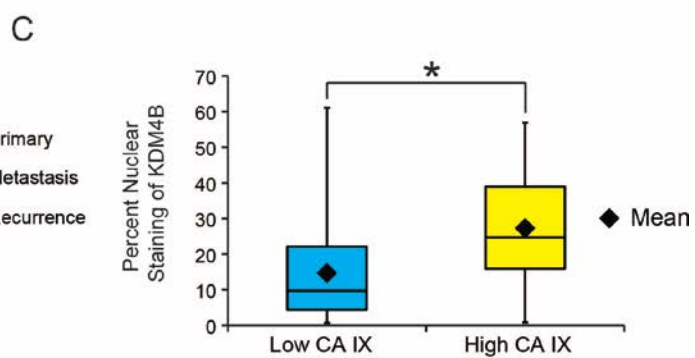
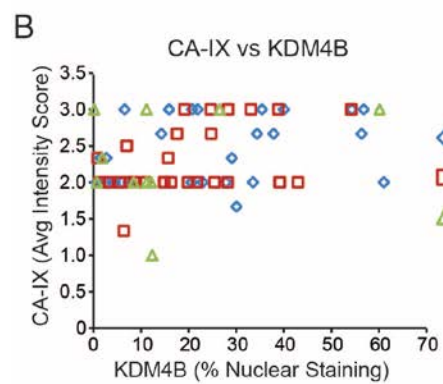
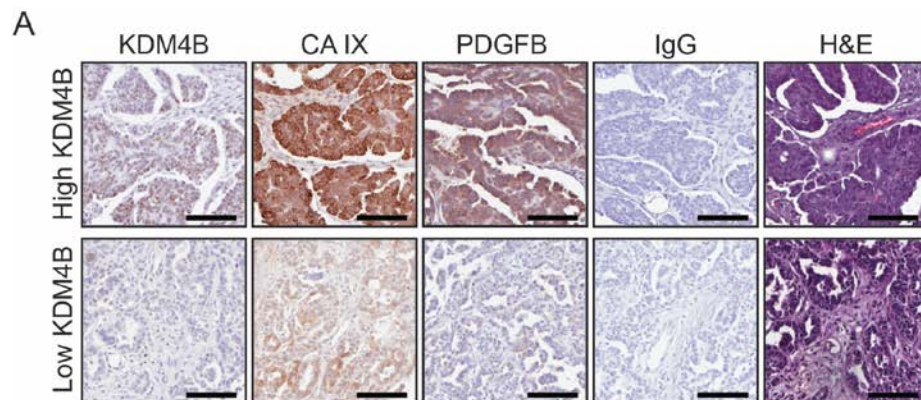


Table 3.4. Immunohistochemical Scoring Data for KUCC OVCA TMA.

Patient	Grade	histosubtype	tumor type	KDM4B (Avg. % nuclear staining)	PDGFB (Avg Intensity score)	CA9 (Avg Intensity Score)
1	III	serous	primary	35.47	2.00	3.00
2	III	serous	primary	2.90	2.00	2.00
3	III	serous	primary	21.93	0.33	3.00
4	III	serous	primary	30.10	2.00	1.67
6	III	serous	primary	1.50	1.67	2.33
7	III	serous	primary	20.70	1.00	2.00
8	II	serous	primary	29.13	1.00	2.33
9		serous	primary	56.40	2.00	2.67
12	III	serous	primary	23.00	1.00	2.00
13		serous	primary	34.43	2.00	2.67
16	III	serous	primary	33.57	2.00	2.00
17	III	serous	primary	6.60	1.00	3.00
20	III	serous	primary	4.13	1.67	2.00
21	III	serous	primary	37.90	1.00	2.67
22	III	serous	primary	27.90	1.33	2.00
23		serous	primary	14.33	1.33	2.67
24	III	serous	primary	54.35	1.00	3.00
25	III	serous	primary	61.07	2.00	2.00
26	III	serous	primary	4.50	0.33	2.00
31	III	serous	primary	40.07	2.00	3.00
38	III	serous	primary	2.73	1.67	2.00
39	III	serous	primary	56.85	1.33	3.00
40	III	serous	primary	0.73	0.00	2.00
41	III	serous	primary	7.37	0.33	2.00
42	III	serous	primary	1.53	1.67	2.00
43	III	serous	primary	15.93	0.00	3.00
45	III	serous	primary	15.97	0.33	3.00
46	III	serous	primary	2.77	2.00	2.33
47	III	serous	primary	6.07	0.00	2.00
49	II	serous	primary	20.83	2.00	3.00
1	III	serous	metastasis	24.73	2.67	2.67
2	III	serous	metastasis	1.33	1.67	2.00

3	III	serous	metastasis	38.87	0.00	3.00
4	III	serous	metastasis	8.53	1.33	2.00
6	III	serous	metastasis	5.60	0.33	2.00
7	III	serous	metastasis	15.70	1.00	2.33
8	II	serous	metastasis	14.97	0.33	2.00
9		serous	metastasis	54.20	3.00	3.00
12	III	serous	metastasis	21.80	1.00	2.00
13		serous	metastasis	24.67	1.33	3.00
16	III	serous	metastasis	25.43	1.00	2.00
17	III	serous	metastasis	28.20	1.00	2.00
20	III	serous	metastasis	6.37	0.00	1.33
21	III	serous	metastasis	18.70	1.00	NA
22	III	serous	metastasis	39.13	2.67	2.00
23		serous	metastasis	16.30	1.00	2.00
24	III	serous	metastasis	42.97	2.33	2.00
25	III	serous	metastasis	19.87	2.00	2.00
26	III	serous	metastasis	7.00	0.33	2.50
38	III	serous	metastasis	10.97	1.00	2.00
39	III	serous	metastasis	33.10	1.00	3.00
40	III	serous	metastasis	14.83	0.00	2.00
41	III	serous	metastasis	17.57	0.00	2.67
42	III	serous	metastasis	0.00	2.00	NA
43	III	serous	metastasis	0.87	0.00	2.33
45	III	serous	metastasis	19.13	0.00	3.00
46	III	serous	metastasis	3.10	2.33	2.00
47	III	serous	metastasis	7.60	1.00	2.00
49	II	serous	metastasis	28.30	NA	3.00
31	III	serous	recurrence	11.20	2.00	3.00
38	III	serous	recurrence	11.23	1.67	2.00
39	III	serous	recurrence	60.17	1.00	3.00
40	III	serous	recurrence	8.50	2.00	2.00
41	III	serous	recurrence	12.13	0.67	2.00
42	III	serous	recurrence	0.77	1.33	2.00
43	III	serous	recurrence	0.20	0.67	3.00
45	III	serous	recurrence	26.57	0.00	3.00
46	III	serous	recurrence	1.93	2.33	2.33
47	III	serous	recurrence	12.40	1.00	1.00

10	II	mixed	primary	1.20	0.67	1.33
18	III	mixed	primary	42.20	1.67	2.00
19	III	mixed	primary	15.43	1.00	2.33
27	III	mixed	primary	44.50	0.67	2.00
28	III	mixed	primary	24.53	0.33	2.00
29	III	mixed	primary	7.97	0.00	3.00
30	III	mixed	primary	13.33	1.33	2.67
32	II	mixed	primary	43.10	2.00	2.00
33	III	mixed	primary	11.60	0.00	2.00
34	III	mixed	primary	1.23	0.33	2.00
35	III	mixed	primary	1.23	1.00	1.00
36	III	mixed	primary	0.47	0.00	2.00
44	III	mixed	primary	21.43	0.67	2.00
48	III	mixed	primary	16.10	1.00	1.00
10	II	mixed	metastasis	30.23	0.33	2.00
18	III	mixed	metastasis	4.50	1.00	2.00
19	III	mixed	metastasis	24.17	1.00	3.00
34	III	mixed	metastasis	4.13	0.33	2.00
35	III	mixed	metastasis	1.30	1.67	1.00
36	III	mixed	metastasis	2.13	0.00	2.00
44	III	mixed	metastasis	11.23	1.00	2.00
48	III	mixed	metastasis	5.70	1.00	2.00
27	III	mixed	recurrence	12.67	0.67	2.00
28	III	mixed	recurrence	12.37	1.00	1.33
29	III	mixed	recurrence	11.10	0.00	3.00
30	III	mixed	recurrence	14.00	1.00	2.67
32	II	mixed	recurrence	3.27	1.33	3.00
33	III	mixed	recurrence	38.47	1.33	3.00
34	III	mixed	recurrence	1.30	0.00	2.00
35	III	mixed	recurrence	3.73	1.00	1.00
36	III	mixed	recurrence	0.30	1.00	2.00
44	III	mixed	recurrence	10.83	0.67	2.00
48	III	mixed	recurrence	4.90	1.00	1.00
5	III	other	primary	27.13	0.00	3.00
11	III	other	primary	19.27	1.33	2.67
14	III	other	primary	10.37	0.00	2.00
15	III	other	primary	17.70	0.67	2.00

5	III	other	metastasis	31.83	1.00	3.00
11	III	other	metastasis	1.83	1.33	2.33
14	III	other	metastasis	5.23	0.00	1.67
15	III	other	metastasis	40.73	1.67	2.33
37	III	not EOC	primary	10.57	0.33	3.00
37	III	not EOC	metastasis	4.53	1.00	2.00
37	III	not EOC	recurrence	30.87	1.00	2.00

Tumors are listed by de-identified patient sample # with corresponding tumor grade (most are FIGO grade III), pathology histological subtype (histosubtype; serous, mixed, other, and not EOC), tumor type (primary, metastasis, recurrence), and average scores for KDM4B nuclear staining (% nuclear staining), PDGFB intensity scores (0-3, in increments of 0.3), and CA9 intensity scores (0-3, in increments of 0.3). Scoring was applied as described in Supplemental Methods, using triplicate spots. Data are ranked by histosubtype, then tumor type, then patient sample #. Sections with damaged spots during IHC are labeled "NA"

small size of the sample set, and the overall heterogeneity of ovarian cancer (Cancer Genome Atlas Research 2011; Tan et al. 2013), these findings provide robust support for our hypothesis that KDM4B expression in hypoxic tumor tissue leads to the expression of genes that facilitate peritoneal dissemination (Apte et al. 2004).

DISCUSSION

Emerging evidence has indicated that dysregulation of histone demethylases play important roles in tumorigenesis (Berry and Janknecht 2013; Hojfeldt et al. 2013). The JmjC domain containing histone demethylase KDM4B is overexpressed in many cancers and plays important roles in cancer proliferation, DNA repair and metastasis (Young et al. 2013; Zhao et al. 2013f; Berry et al. 2014). A few studies have reported KDM4B function in cancer metastasis. In gastric cancer and colon cancer, KDM4B has been shown to interact with β -catenin in regulating gene expression (Zhao et al. 2013f; Berry et al. 2014). In the last chapter, we have demonstrated that KDM4B directly regulated the expression of metastatic genes, such as *PDGFB*, *LCN2*, *LOX* and *LOXL2*, in ovarian cancer cells (Figure 2.9, 2.13 and 2.14). However, whether KDM4B functionally contributed to ovarian cancer metastasis was unknown.

In this chapter, we have determined that KDM4B expression level was elevated in 2/3 of the primary, metastatic, or recurrent ovarian serous adenocarcinoma biopsies tested compared to normal ovarian tissue (Figure 3.1). KDM4B protein expression was induced by hypoxia in a panel of ovarian cancer cell lines (Figure 3.2). Loss of KDM4B by shRNA knockdown severely impaired *in vitro* EOC cell migration, invasion, and attachment-free growth, which are important aspects of the peritoneal dissemination

(Figure 3.4-3.6). When KDM4B was knocked down, *in vivo* EOC tumor growth and peritoneal dissemination in nude mice also decreased significantly (Figure 3.7-3.11).

There has been little improvement in EOC patient mortality over the past 30 years (Lengyel 2010). One main reason for the poor prognosis of EOC patients is that most of the patients are diagnosed at late-stage, where tumors have already spread throughout the peritoneal cavity (Lengyel 2010). The formation of malignant ascites filled with free-floating clusters of cancer cells adds more difficulty for effective removal of residual cancer cells. After the initial surgery and first-line treatment, EOC usually recurs within 2 to 5 years with chemo-resistant tumors. Therefore, it is important to study the underlying mechanism of EOC metastasis.

In contrast to other tumor types, EOC metastasizes in a unique manner. The most common theory is that EOC cells detach from the primary ovarian tumor, grow as single cells or spheroids in peritoneal ascites fluid, and distribute throughout the peritoneum and omentum (Lengyel 2010). Multiple factors may facilitate spheroid formation, maintenance and ultimate establishment to secondary sites, including the epithelial-mesenchymal transition (EMT), binding of the integrins to the extracellular matrix, and activities of the MMPs (Lengyel 2010).

Pradeep et al have recently shown that EOC cells may also use the traditional hematogeneous mechanism to migrate, with a strong predilection to seed on the omentum (Pradeep et al. 2014). They discovered that this tropism relied on the ErbB3/NRG1 signaling axis, whose ligand and target were overexpressed by the omental vascular microenvironment. Nieman et al showed that adipokines such as interleukin-8 (IL-8) can mediate homing, migration and invasion of ovarian cancer cells

to omental adipocytes (Nieman et al. 2011). They also detected fatty acid-binding protein 4 (FABP4) in ovarian cancer cells at the adipocyte-tumor cell interface, suggesting FABP4 may also play an important role in ovarian cancer metastasis to the omentum (Nieman et al. 2011). Hypoxia has been shown to induce the expression of fatty acid binding proteins, including FABP1, FABP3 and FABP4 in placental trophoblasts (Biron-Shental et al. 2007). Since trophoblasts invade stromal tissues in a manner very consistent with cancer cells, there is a clear parallel to ovarian cancer metastasis. Studying the intersection between hypoxia and fat metabolism in ovarian cancer may improve our understanding of the adipose-specific targeting of peritoneal metastases.

The importance of hypoxic signaling as a potential therapeutic target in EOC was highlighted by the relative success of bevacizumab (Avastin) in the treatment of HGSA (Bast 2011), which targets the classical hypoxia-inducible vascular endothelial growth factor receptor (VEGFR). The ability to successfully target a hypoxia-inducible gene indicates that KDM4B and its downstream target genes may be useful for improving the effectiveness of cancer therapies.

Another major challenge to effectively treat advanced stage ovarian cancer is that it is characterized by global genomic instability, suggesting that targeting a single pathway is not sufficient for complete removal of the cancer (Cancer Genome Atlas Research 2011). Therefore, it is important to study alternative mechanisms contributing to attachment-free growth of cancer cells in malignant ascites and invasion of cancer cells into the mesothelium in order to develop more effective methods to attenuate peritoneal dissemination. As a hypoxia-regulated gene that facilitates expression of

multiple tumorigenic pathways in normoxia and hypoxia, KDM4B or its regulated target genes may provide unique opportunities to tailor a combinatorial approach for those patients with elevated KDM4B or hypoxic tumor signatures.

Our results implied that disrupting KDM4B function with an inhibitor of its demethylase activity could serve as a novel chemotherapeutic approach. Recent studies have devoted much effort to designing specific inhibitors of histone demethylases, with the greatest success restricted to inhibition of classes of jumonji domain histone demethylases, as in the case of the KDM6 family (Kruidenier et al. 2012). While these studies show promise for the eventual development of inhibitors specific to families of JMJ-C domain histone demethylases, specificity to each of the more than 20 individual histone demethylases remain a major challenge. Given the important role of KDM4 family members in regulating various aspects of DNA repair, proliferation and embryonic development (Mallette et al. 2012; Young et al. 2013; Das et al. 2014), the inappropriate targeting of these enzymes may lead to severe side effects. Therefore, our ability to design inhibitors that specifically target KDM4B will be crucial in order to use KDM4B for therapeutic improvement. Moreover, the myriad genes regulated by KDM4B in SKOV3ip.1 cells indicate that multiple pathways are involved in supporting EOC metastasis. In order to improve therapy against metastatic EOC cells, our study provides multiple targeting opportunities, such as *PDGFB*, *LCN2*, *LOX* and *LOXL2*, to suppress the establishment of peritoneal tumors from malignant ascites. Blocking PDGFB signaling in SKOV3ip.1 cells with RNA aptamers suppresses growth of peritoneal tumor xenografts (Lu et al. 2010). Combinatorial targeting of other genes regulated by KDM4B in SKOV3ip.1 cells may lead to improved methods to suppress

peritoneal engraftment of EOC tumor cells, ultimately improving the prognosis of patients.

Taken together, our study shows that KDM4B plays an important role in the peritoneal dissemination of EOC cells and may be used as a therapeutic target.

CHAPTER 4:

GENERAL DISCUSSION

I. The Overall Importance of Our Study

In this study, we have demonstrated that the hypoxia-inducible histone demethylase KDM4B regulates 16 common target genes in SKOV3ip.1 ovarian cancer, HCT116 colon cancer and RCC4 renal cell carcinoma cells. In SKOV3ip.1 cells, KDM4B regulates distinct pathways in different oxygen conditions, proliferative pathways in normoxia and metastatic pathways in hypoxia. KDM4B is a potent regulator of cellular processes that contribute to epithelial ovarian cancer (EOC) peritoneal dissemination. KDM4B is overexpressed in the majority of high-grade serous adenocarcinomas and ovarian cancer cell lines tested. Knockdown of KDM4B in two EOC cell lines results in a significant reduction in the peritoneal tumor load *in vivo*, consistent with the observed disruption of key phenotypes associated with peritoneal seeding (attachment-free growth, invasive behavior, and trans-well migration). By demonstrating KDM4B contribution to the metastatic phenotypes of EOC, our study suggests KDM4B or the genes that it specifically regulates in EOC cells may be useful targets to improve the prognosis of EOC patients.

II. Regulation of Cancer Progression by KDM4B is Dependent on Cancer Type and Oxygen Tension

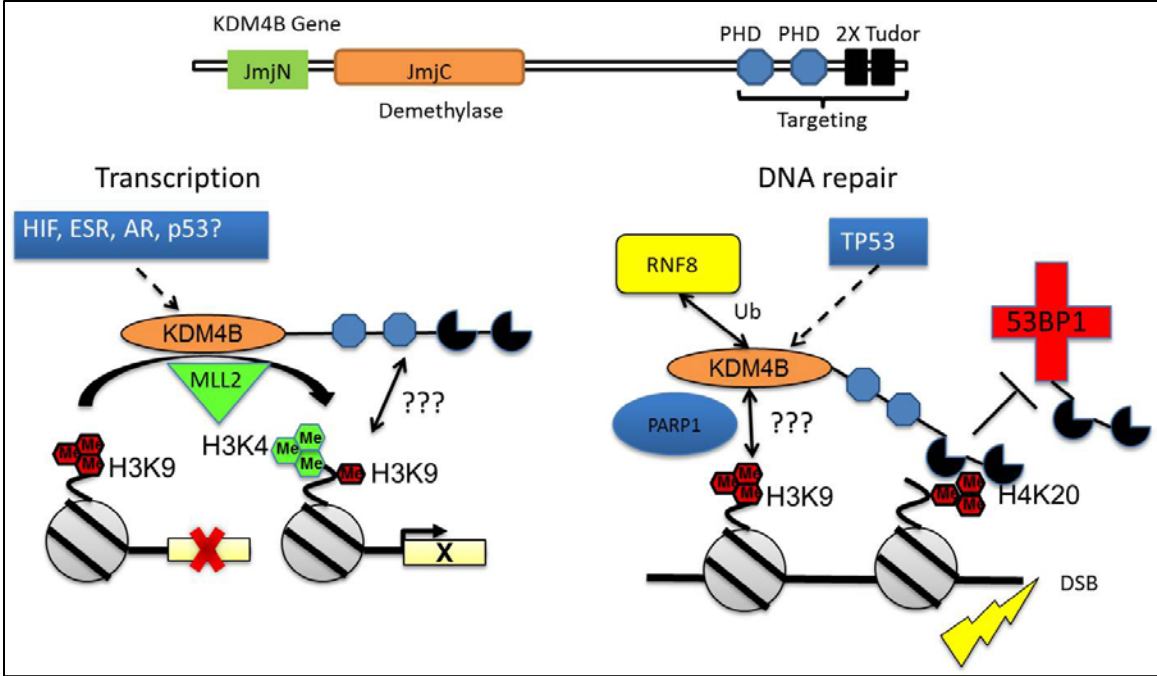
KDM4B overexpression has been shown in multiple cancer types. It may be regulated by HIF, ER, AR and p53 in different tumor microenvironments to promote tumor survival (Beyer et al. 2008; Palomera-Sanchez et al. 2010; Coffey et al. 2013; Gaughan et al. 2013) (Figure 4.1). KDM4B regulates cancer cell proliferation (Kawazu et al. 2011; Kim et al. 2012a), anti-apoptosis (Sun et al. 2014), DNA damage repair (Malette et al. 2012; Zheng et al. 2013; Chen et al. 2014), migration (Zhao et al. 2013f),

and embryonic development (Yoshioka et al. 2009; Ye et al. 2012; Das et al. 2014). Most of these functions are dependent on its histone demethylase activity regulating downstream pathways, including cell-cycle related genes (Yang et al. 2010; Kawazu et al. 2011; Kim et al. 2012a), anti-apoptotic genes like Bcl-2 (Sun et al. 2014), and other transcription factors (Zhao et al. 2013f; Berry et al. 2014; Das et al. 2014). KDM4B has been shown to interact with MLL2, an H3K4 demethylase, to activate gene expression (Figure 4.1). H3K4 methylation is usually found in the promoter region in active transcripts, indicating its role in gene activation (Ruthenburg et al. 2007). However, demethylase-independent function has also been reported of KDM4B, such as recruiting 53BP1 to DNA damage sites through its C-terminal interaction with dimethylated H4K20 (Figure 4.1) (Malette et al. 2012). In our study, KDM4B appeared to contribute to cancer progression by regulating both general and tissue-specific target genes.

Common Regulation by KDM4B in Three Cancer Cell Lines

In this study, we have used microarray analyses to identify potential targets of KDM4B in cancer cell lines derived from three different cancer types, including SKOV3ip.1 ovarian cancer, HCT116 colon cancer, and RCC4 renal cell carcinoma cells. These three cancer cell lines were chosen because they had shown dependence on hypoxic signaling during their development (Birner et al. 2001; Krishnamachary et al. 2003; Gudas et al. 2014). There is also a lack of understanding in how KDM4B function in these cancers. Only four studies have been reported regarding KDM4B function and its target genes in colorectal cancer (CRC), with a few downstream pathways leading to

Figure 4.1. Mechanisms used by KDM4B to promote cancer progression. KDM4B may be regulated by HIF, ER, AR and p53 in different tumor microenvironments to promote tumor survival. KDM4B has been shown to interact with MLL2, an H3K4 demethylase, forming a complex to activate gene expression. KDM4A/B has been shown to inhibit 53BP1 recruitment to DNA damage sites by competitively binding to dimethylated H4K20. During DNA repair response, RNF8 ubiquitylates KDM4A/B, relieving H4K2me2 for 53BP1 recruitment. KDM4D is also recruited to DNA damage sites through a PARP1-dependent manner to promote double-strand break repair. As a closely related subfamily member, KDM4B may also be involved in DNA repair through similar mechanisms.

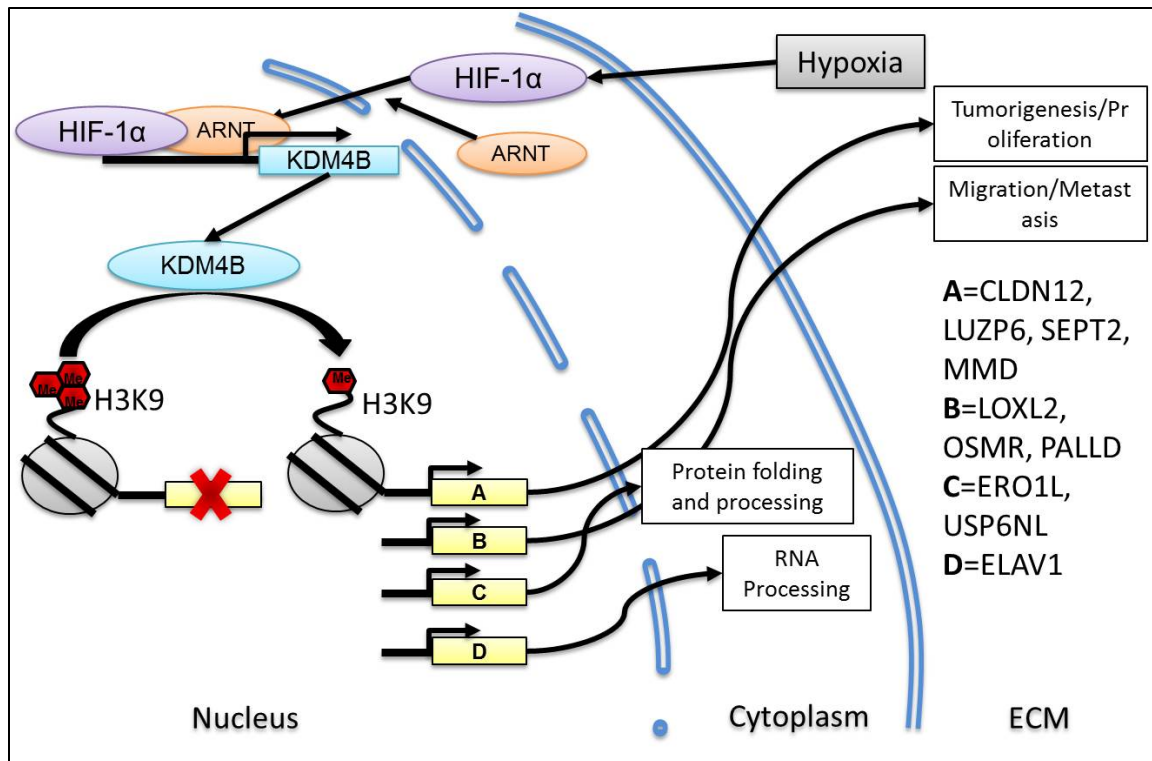


CRC proliferation and progression (Fu et al. 2012; Berry et al. 2014; Chen et al. 2014; Sun et al. 2014). Two studies showed elevated KDM4B expression level in renal cell carcinoma (RCC), yet no group has reported its molecular mechanism in RCC (Beyer et al. 2008; Krieg et al. 2010). To date, no study has been reported regarding KDM4B expression level or its function in epithelial ovarian cancer (EOC).

By comparing KDM4B target genes in these three cell lines, we identified 16 common targets that were regulated by KDM4B in all three cell lines. These genes display a variety of cellular functions, but are mostly related to cancer progression (Table 2.5 and Figures 2.3-2.6). Figure 4.2 illustrates this general regulation by KDM4B as a histone demethylase on target gene expression in hypoxic cancer cells. This finding indicates cancer cells, as heterogeneous as they are, may still share common mechanisms that can be targeted with general cancer therapies.

Transcription factors and epigenetic regulators are known to play important roles in stem-cell differentiation and tumorigenesis through their ability to reprogram gene expression to establish certain cellular functions (Spivakov and Fisher 2007; Black et al. 2012; Yang et al. 2013). Another commonly shared mechanism cancer cells use to promote their own survival and progression is the β -catenin transcription factor (Paul and Dey 2008). KDM4B has been reported to either induce or partner with β -catenin and its co-factor TCF-4 to regulate gene expression. One of the 16 commonly shared KDM4B targets in the three cell lines, DAZAP1, also has been shown to interact with TCF-4 and facilitate its binding to DNA. These findings indicate that multiple layers of regulation are involved in programming cancer cells for their progression to malignancy (Lukas et al. 2009). Understanding the regulation of such transcription factor complexes

Figure 4.2 General model of KDM4B function in cancer cell progression. Hypoxic microenvironment activates the HIF-1 transcription factor, which cooperates with ARNT activating the transcription of the KDM4B gene. KDM4B histone demethylase then catalyzes histone H3K9me3/me2 demethylation and activates transcription of target genes. These target genes may contribute to cancer cell migration, tumor metastasis, angiogenesis and inflammation.



by KDM4B will help us determine the advantages and disadvantages of using KDM4B as a therapeutic target.

Regulation by KDM4B is Dependent on Cancer Type and Oxygen Level

Cancer is a highly heterogeneous disease. Each cancer has its specific genetic mutations and pathological behaviors. Our current knowledge of KDM4B function in cancer points to mechanisms that are specific to each cancer type. For example, in breast cancer, KDM4B is regulated by the estrogen receptor and induces expression of pro-proliferative genes like Cyclin D1 (Yang et al. 2010). Androgens regulate KDM4B in prostate cancer, which in turn promotes PSA expression (Coffey et al. 2013). In colon and gastric cancers, KDM4B regulates β -catenin dependent gene expression and WNT signaling to promote attachment-free growth and metastatic behavior (Berry and Janknecht 2013; Zhao et al. 2013a).

In our study, the three cancer cell lines shared only 16 common KDM4B targets, less than 6% of the total number of genes regulated by KDM4B in each cell line (Figure 2.1). Ingenuity pathway analysis (IPA) also mapped out distinct pathways and disease states influenced by KDM4B in each cell type (Table 2.6-2.7). These pathway analyses showed that although RCC4 had a “pseudo-hypoxic” phenotype due to its lack of functional VHL, regulation by KDM4B in this cell line favored proliferative pathways, similar to its normoxic cohort of downstream pathways in HCT116 and SKOV3ip.1 (Table 2.6), indicating KDM4B sensitivity to oxygen may play a critical role in its activity at target genes.

KDM4B belongs to a family of JmjC-domain demethylases that removes methyl groups from histone lysine residues through hydroxylation, which requires oxygen

(Fodor et al. 2006; Tsukada et al. 2006). Therefore, it is reasonable that KDM4B function may be influenced by oxygen level.

Indeed, we observed that KDM4B regulated distinct pathways in different oxygen conditions, which was most evident in SKOV3ip.1 cells. In normoxic condition, KDM4B regulated pathways more closely related to proliferation (cell cycle, cellular assembly, DNA replication/recombination/repair, and cell death), whereas pathways related to metastasis (cellular movement, cellular development, and cell-to-cell signaling) were preferentially regulated by KDM4B in hypoxia. This finding is significant because of the important role hypoxia plays in angiogenesis and metastasis (Erler et al. 2006; Yang et al. 2013). Induction of KDM4B in hypoxia seemed to further assist HIF regulation while its normoxic function focused on promoting tumor formation and survival.

These findings suggest that KDM4B may play crucial yet distinct roles in each cancer type, even in each tumor microenvironment. Therefore, even though mechanisms of KDM4B functions have been shown in other cancer types, it is still important to further investigate how KDM4B contributes to the progression of ovarian cancer.

III. Mechanism of KDM4B Function in Epithelial Ovarian Cancer

Using microarray analysis, QPCR and ChIP, we have identified several target genes whose expression showed promising dependence on KDM4B expression, including *LOX*, *LOXL2*, *PDGFB*, and *LCN2* (Chapter 2). *LOX* and *LOXL2* are both members of the lysyl oxidase family, which comprises Cu^{2+} - and lysine tyrosylquinone-dependent amine oxidases (Decitre et al. 1998). *LOX* is involved in extracellular matrix (ECM) remodeling by crosslinking collagen for matrix metalloproteinase 2 (MMP2)

cleavage, thus promoting cell invasion and metastasis (Erler et al. 2006). LOXL2 regulates extracellular and intracellular cell signaling pathways as well as function in ECM remodeling (Decitre et al. 1998). Studies have also shown that LOXL2 may play an important role in cell proliferation (Saad et al. 2010; Baker et al. 2011). These oxidases have been linked to poor prognosis in many cancer types (Erler et al. 2009; Le et al. 2009; Baker et al. 2011; Xiao and Ge 2012; Cox et al. 2013; Zaffryar-Eilot et al. 2013).

Our microarray analysis of three different cancer cell lines revealed *LOXL2* as a common KDM4B target expressed in a hypoxia-inducible manner, indicating that it may play important roles in general cancer progression. We observed that transient knockdown of KDM4B robustly decreased the expression of *LOXL2*, however, the regulation was attenuated when KDM4B was stably knocked down with lentiviral shRNA. Our ChIP results confirmed direct interaction between KDM4B and *LOXL2* promoter, indicating KDM4B maybe one of several factors regulating the expression of *LOXL2*. As genes involved in a general cancer progression mechanism in multiple cancer types, having various pathways regulating the induction of these genes appear to give cancer cells a survival advantage.

Among the list of KDM4B target genes, *PDGFB* and *LCN2* expression most robustly followed the expression pattern of KDM4B. *PDGFB* is one of the secreted factors involved in promoting the recruitment of pericytes along the vascular endothelial cells, a process required in tumor angiogenesis (Chantrain et al. 2006). Pericytes function to stabilize the newly formed endothelial tubes, modulate blood flow and vascular permeability (Chantrain et al. 2006). They also regulate endothelial cell

proliferation, survival, migration, differentiation and branching (Chantrain et al. 2006). Growing evidence shows that pericytes are present along the microvasculature in human tumor tissues (Chantrain et al. 2006). Studies have also shown that anti-PDGF drugs significantly inhibited tumor growth and metastasis in tumors that express high levels of PDGFB (Hosaka et al. 2013). These findings suggest that KDM4B may contribute to EOC progression by promoting angiogenesis.

LCN2 has multiple functions depending on its dimerization partner. It exists mainly as a monomer or a homodimer and is released by neutrophils and involved in innate immunity against bacterial infection (Goetz et al. 2002). LCN2 can also dimerize with matrix metalloproteinase 9 (MMP9) to protect it from degradation, thus promoting its gelatinolytic activity on ECM (Yan et al. 2001). LCN2 has been shown to have pro-inflammatory functions and regulates cell growth and adhesion (Chakraborty et al. 2012). Although LCN2 has also been shown to have anticancer activities by inhibiting angiogenesis and inducing apoptosis (Devireddy et al. 2005; Venkatesha et al. 2006; Tong et al. 2008), it serves as a potential oncogene in ovarian cancer (Cho and Kim 2009). LCN2 expression level is significantly higher in multiple cancer types, including ovarian cancer, compared to their normal counter parts (Candido et al. 2014). Therefore, LCN2 demonstrates features of an interesting druggable target worth further investigation.

Considering the large number of genes dependent on KDM4B in SKOV3ip.1 cells, it is unclear at this time which specific genes or mechanistic pathways are primarily responsible for these broad phenotypic effects, although *LCN2*, *LOX*, *LOXL2*, and *PDGFB* make particularly compelling candidates with proven ability to influence

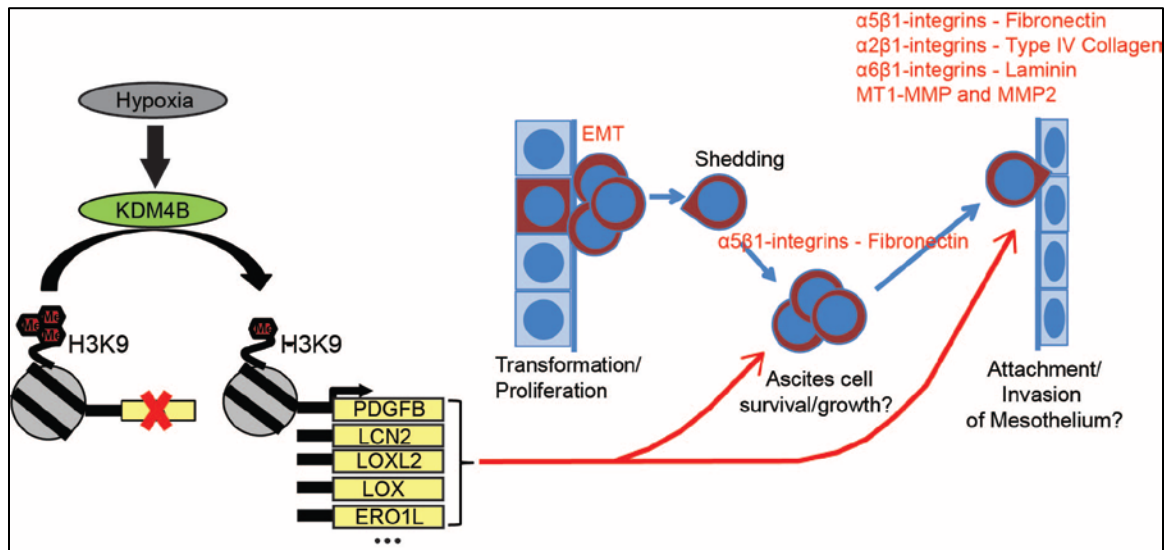
either ovarian cancer growth or general metastasis (Apte et al. 2004; Barker and Erler 2011). Examining the individual contributions of the multiple genes regulated by KDM4B in SKOV3ip.1 and OVCAR8 cells should provide more insight into the specific mechanisms regulating peritoneal dissemination of EOC.

IV. KDM4B Function in Ovarian Cancer

In this study, we have also demonstrated the functional importance of KDM4B expression in EOC. Immunohistochemical (IHC) staining of tissue microarray (TMA) indicated that 2/3 of the primary, metastatic, or recurrent ovarian serous adenocarcinoma biopsies had increased KDM4B expression compared to normal ovarian epithelium (Chapter 3). Knocking down KDM4B significantly decreased the ability of cancer cells to migrate through the Boyden Chamber membrane, to invade through matrigel, and in attachment-free conditions. Our *in vivo* tumor xenograft study also showed that KDM4B knockdown significantly decreased peritoneal seeding and growth of OVCAR cells into tumors. The overall luciferase activity from the tumor cells and total tumor weight were both decreased by KDM4B knockdown.

The metastatic behavior of ovarian cancer is unique in a sense that cells rarely travel through the blood vessels to secondary sites (Lengyel 2010). OVCAR cells detach from the primary ovarian tumor, grow as single cells or spheroids in peritoneal ascites fluid, and are carried by the physiological movement of the ascites to the peritoneum and omentum (Lengyel 2010). Multiple factors may facilitate spheroid formation, maintenance and ultimate establishment to secondary sites (Figure 4.3). Initial detachment of OVCAR cells from their primary tumor site involves the epithelial-mesenchymal transition (EMT), which includes loss of E-cadherin expression and

Figure 4.3. Mechanism of the contribution of KDM4B signaling to ovarian cancer progression. Briefly, hypoxia induces the expression of KDM4B histone demethylase, which catalyzes histone H3K9me3/me2 demethylation at target promoters and enhances expression of genes involved in attachment-free growth in the peritoneal cavity, as well as enhancing invasion and migration of cancer cells to facilitate the formation of metastases in the viscera and peritoneal wall.



increased level of other cadherins (Veatch et al. 1994; Patel et al. 2003; Elloul et al. 2005; Symowicz et al. 2007; Hudson et al. 2008). The E-cadherin ectodomain is cleaved by MMP9, which is induced by clustering of collagen binding integrins ($\alpha 2\beta 1$ - and $\alpha 3\beta 1$ -integrin) on the cancer cells, contributing to their shedding into ascites (Symowicz et al. 2007; Lengyel 2010). Active membrane type 1-MMP (MT1-MMP/MMP14) on cancer cells cleaves $\alpha 3$ -integrin, contributing to the detachment of the spheroid from the primary tumor (Moss et al. 2009). Once shed, OVCAR cells grow as spheroids suspended in ascites fluid accumulated in the peritoneal cavity. These spheroids express high levels of the $\alpha 5\beta 1$ -, $\alpha 6\beta 1$ - and $\alpha 2\beta 1$ -integrins, which bind to fibronectin, laminin and type IV collagen, respectively. These extracellular matrix proteins are abundantly present in ascites and in the mesothelium covering the peritoneum and the omentum (Casey et al. 2001; Lengyel 2010). Therefore, expression of these integrins by spheroids supports their growth in ascites and their eventual adhesion to secondary sites. MMP2 is also preferentially secreted by spheroids than by cells cultured in monolayer, possibly promoting disaggregation of the spheroids upon adhesion to mesothelial cell layers (Lengyel 2010).

Our results indicate that KDM4B is involved in supporting spheroid formation and growth in ascites, as well as cell invasion through the mesothelium (Figure 4.3). These two features are the main factors causing poor prognosis in EOC. Therefore, KDM4B holds interesting therapeutic potential worth further investigation.

V. Relevance of our study: KDM4B as a possible therapeutic target in ovarian cancer

The treatment of EOC, particularly high grade serous adenocarcinoma (HGSA) is

a significant health problem. Because of the difficulty of detecting early stages of the disease, there has been little improvement in patient mortality over the past 30 years (Lengyel 2010). The primary factor in determining the prognosis of epithelial ovarian cancer patients is the degree of peritoneal metastasis at the time of diagnosis (Lengyel 2010). The majority of ovarian serous adenocarcinoma patients are diagnosed with metastatic nodules distributed throughout the abdominal cavity, creating a baseline tumor load that hampers removal of residual microscopic tumors. Malignant ascites filled with free-floating clusters of cancer cells is another barrier to effective removal of residual cancer cell. After surgical debulking and treatment with carboplatin and paclitaxel, recurrent chemo-resistant tumors regain proliferative behavior and reseed the peritoneal cavity within 2 to 5 years, causing mortality through constriction of the visceral tissues and patient cachexia. Developing more effective methods to attenuate peritoneal dissemination and tumor recurrence depends on improved understanding of the underlying processes contributing to attachment-free growth of cancer cells in malignant ascites, invasion of cancer cells into the mesothelium, and establishment of new tumors. In this regard, hypoxia-inducible genes like KDM4B may represent an untapped resource for developing improved diagnostics or therapeutics for EOC patients.

The importance of hypoxic signaling as a potential therapeutic target in EOC is highlighted by the relative success of bevacizumab (Avastin) in the treatment of HGSA (Bast 2011). Bevacizumab targets the receptor of vascular endothelial growth factor (VEGF), which is a classical hypoxia-induced pathway. The ability to successfully target a hypoxia-inducible gene indicate that KDM4B and its downstream target genes may be

useful for improving the effectiveness of cancer therapies. Although only 25% of HGSA patients responded to bevacizumab, with an average increase in disease-free survival of 4 months, this effect was more robust than all other alternate chemotherapies tested to date. Bevacizumab has documented limitations as a general therapeutic stemming from deleterious side effects (e.g. pleural effusions and intestinal perforations), or upregulation of compensatory hypoxic expression stemming from tumor starvation (Conley and Wicha 2012). As a hypoxia-regulated gene that facilitates expression of multiple tumorigenic pathways in normoxia and hypoxia, KDM4B or its regulated target genes may provide unique opportunities to tailor a combinatorial approach for those patients with elevated KDM4B or hypoxic tumor signatures.

A key question rising from our study regards the utility of targeting KDM4B to improve EOC patient outcome. Although a systematic comparison has not been conducted, KDM4B appears to regulate pathways distinct to each cancer type (Yang et al. 2010; Coffey et al. 2013; Zhao et al. 2013f; Berry et al. 2014). In our experiments, although KDM4B regulates distinct pathways in different oxygen tensions, invasive and migratory behaviors appear to be the most robust phenotypes. In all cases, there is the implication that disrupting KDM4B function with an inhibitor of its demethylase activity could serve as a novel chemotherapeutic approach. More generally, there has been a great deal of effort devoted to designing specific inhibitors of histone demethylases, with the greatest success restricted to inhibition of classes of jumonji domain histone demethylases, as in the case of the KDM6 family (Kruidenier et al. 2012). While these studies show promise for the eventual development of inhibitors specific to families of JMJ-C domain histone demethylases, there remain significant barriers to creating a

specific inhibitor against each of the more than 20 individual histone demethylases. Particularly given the important role of KDM4A and KDM4B in regulating various aspects of DNA repair and proliferation (Malette et al. 2012; Young et al. 2013), the inappropriate targeting of these enzymes using non-specific inhibitors would probably not represent a significant improvement over existing anti-proliferatives like carboplatin and paclitaxel. In contrast, the myriad genes regulated by KDM4B in SKOV3ip.1 cells provide multiple opportunities to suppress the establishment of peritoneal tumors from malignant ascites. Genes like *PDGFB*, *LCN2*, *LOX* and *LOXL2* likely represent a small fraction of the types of secreted genes expressed in EOC that could eventually be targeted. As an independent proof of concept, blocking PDGFB signaling in SKOV3ip.1 cells with RNA aptamers suppresses growth of peritoneal tumor xenografts (Lu et al. 2010). Combinatorial targeting of other genes regulated by KDM4B in SKOV3ip.1 cells may lead to improved methods to suppress peritoneal engraftment of EOC tumor cells, ultimately improving the prognosis of patients.

VI. Future directions

Our findings in this study have raised several interesting questions. The first one regards how KDM4B function may differ in cycling versus prolonged hypoxia. In the actual hypoxic tumor microenvironment, tumor cells may experience both prolonged and fluctuating hypoxia caused by ischemia followed by reperfusion (Olbryt et al. 2014; Tellier et al. 2015). Cycling hypoxia has been shown to enhance tumor-promoting inflammation by inducing an amplified inflammatory phenotype in endothelial cells (Tellier et al. 2015). Some of the hypoxia-inducible genes that play important roles in leading to cancer malignancy require oxygen for their enzymatic functions. For example,

LOX protein expression is significantly increased by hypoxia, whereas its catalytic activity is reduced in low oxygen conditions (Postovit et al. 2008). The hypoxia/reoxygenation cycle plays a significant role in LOX function by up-regulating its expression in hypoxia and maximizing its catalytic activity with reoxygenation (Postovit et al. 2008). Normal KDM4B demethylase function also requires oxygen and hypoxia has been shown to reduce KDM4B activity (Beyer et al. 2008). Therefore, it is important to study how KDM4B function may differ in cycling hypoxia compared to prolonged hypoxia. Given the pathways differentially regulated in normal or low oxygen conditions, we hypothesize that the hypoxia/reoxygenation cycling may be a preferred microenvironment for KDM4B to exert its full function in promoting cancer progression.

Another question was raised regarding the potential functional compensation to the loss of KDM4B from the other KDM4 family members, which have shown synergistic functions with KDM4B in regulating embryonic development (Iwamori et al. 2011; Tsurumi et al. 2013; Das et al. 2014). Our results showed that KDM4D mRNA expression was increased when KDM4B was knocked down in OVCAR8 cells. KDM4D protein level increased with shK-1 knockdown in both SKOV3ip.1 and OVCAR8 cell lines. These results indicate that KDM4D may play a role in compensating to loss of KDM4B function. Although KDM4A and KDM4C expression did not change significantly upon loss of KDM4B, it is still possible that they may functionally compensate to regulate target gene expression. In order to test this hypothesis, Chromatin IP with KDM4D, KDM4A and KDM4C antibodies will be a useful method to confirm direct interaction between these histone demethylases and KDM4B target gene promoters. An inhibitor against the KDM4 family, ML324, is available and may be used to test the

potential effect of targeting all members of the KDM4 family. Knocking down KDM4D, KDM4A or KDM4C along with KDM4B knockdown will also determine the potential mechanism of compensation.

Results from our expression and ChIP analyses indicated that KDM4B might not be the only factor influencing the expression of target genes like *PDGFB*, *LCN2* and *LOXL2* (Figure 3.13-14). Stable knockdown with shRNA showed modest decrease in *LOXL2* mRNA expression compared to transient knockdown experiment with siRNA (Figure 2.13), even though KDM4B enrichment at the *LOXL2* promoter still showed significant difference (Figure 2.14). There was also a general decrease of H3K9me3 level on the *PDGFB*, *LCN2* and *LOXL2* promoters in hypoxia compared to normoxia, even though there was still a significant KDM4B-dependent change (Figure 2.14). Despite the potential compensatory mechanism from other KDM4 family members, KDM4B may also interact with other factors to co-activate gene expression. Studies have shown that KDM4B can interact with MLL2, ER, AR and β -catenin in regulating gene expression in breast cancer (Shi et al. 2011; Coffey et al. 2013; Gaughan et al. 2013; Zhao et al. 2013f). To fully understand how KDM4B regulates the expression of these target genes, it would be important to identify KDM4B co-activators in each tumor microenvironment. Moreover, KDM4B demethylase-independent activity has also been demonstrated in the context of DNA repair (Mallette et al. 2012). In order to validate the demethylase-dependence of KDM4B activity, mutagenesis will be used for each domain of the KDM4B gene and cells expressing each construct will be tested for disruption in target gene expression and cellular functions.

VII. Significance

Taken collectively, we have determined that the hypoxia-inducible histone demethylase KDM4B regulates general, tissue-specific, and oxygen dependent pathways in cancer progression. It is robustly expressed in the majority of EOC tumors assayed and regulates pathways to support cellular functions associated with peritoneal dissemination of cancer cells, the primary cause of EOC patient morbidity and mortality. KDM4B or the genes that it specifically regulates in EOC cells may be useful targets to improve the prognosis of EOC patients.

REFERENCES

- ACS. 2015. American Cancer Society: Cancer Facts and Figures 2015 American Cancer Society, Atlanta, Ga.
- Agger K, Cloos PA, Rudkjaer L, Williams K, Andersen G, Christensen J, Helin K. 2009. The H3K27me3 demethylase JMJD3 contributes to the activation of the INK4A-ARF locus in response to oncogene- and stress-induced senescence. *Genes Dev* **23**: 1171-1176.
- Ameln AK, Muschter A, Mamlouk S, Kalucka J, Prade I, Franke K, Rezaei M, Poitz DM, Breier G, Wielockx B. 2011. Inhibition of HIF prolyl hydroxylase-2 blocks tumor growth in mice through the antiproliferative activity of TGFbeta. *Cancer research* **71**: 3306-3316.
- Anderton JA, Bose S, Vockerodt M, Vrzalikova K, Wei W, Kuo M, Helin K, Christensen J, Rowe M, Murray PG et al. 2011. The H3K27me3 demethylase, KDM6B, is induced by Epstein-Barr virus and over-expressed in Hodgkin's Lymphoma. *Oncogene* **30**: 2037-2043.
- Apte SM, Bucana CD, Killion JJ, Gershenson DM, Fidler IJ. 2004. Expression of platelet-derived growth factor and activated receptor in clinical specimens of epithelial ovarian cancer and ovarian carcinoma cell lines. *Gynecologic oncology* **93**: 78-86.
- Baker AM, Cox TR, Bird D, Lang G, Murray GI, Sun XF, Southall SM, Wilson JR, Erler JT. 2011. The role of lysyl oxidase in SRC-dependent proliferation and metastasis of colorectal cancer. *J Natl Cancer Inst* **103**: 407-424.

- Barker HE, Chang J, Cox TR, Lang G, Bird D, Nicolau M, Evans HR, Gartland A, Erler JT. 2011. LOXL2-mediated matrix remodeling in metastasis and mammary gland involution. *Cancer Res* **71**: 1561-1572.
- Barker HE, Erler JT. 2011. The potential for LOXL2 as a target for future cancer treatment. *Future Oncol* **7**: 707-710.
- Barradas M, Anderton E, Acosta JC, Li S, Banito A, Rodriguez-Niedenfuhr M, Maertens G, Banck M, Zhou MM, Walsh MJ et al. 2009. Histone demethylase JMJD3 contributes to epigenetic control of INK4a/ARF by oncogenic RAS. *Genes Dev* **23**: 1177-1182.
- Bast RC, Jr. 2011. Molecular approaches to personalizing management of ovarian cancer. *Annals of oncology : official journal of the European Society for Medical Oncology / ESMO* **22 Suppl 8**: viii5-viii15.
- Benjamini Y, Hochberg Y. 1995. Controlling the False Discovery Rate - a Practical and Powerful Approach to Multiple Testing. *J Roy Stat Soc B Met* **57**: 289-300.
- Berry WL, Janknecht R. 2013. KDM4/JMJD2 histone demethylases: epigenetic regulators in cancer cells. *Cancer Res* **73**: 2936-2942.
- Berry WL, Kim TD, Janknecht R. 2014. Stimulation of beta-catenin and colon cancer cell growth by the KDM4B histone demethylase. *International journal of oncology* **44**: 1341-1348.
- Beyer S, Kristensen MM, Jensen KS, Johansen JV, Staller P. 2008. The histone demethylases JMJD1A and JMJD2B are transcriptional targets of hypoxia-inducible factor HIF. *J Biol Chem* **283**: 36542-36552.

- Birner P, Schindl M, Obermair A, Breitenecker G, Oberhuber G. 2001. Expression of hypoxia-inducible factor 1alpha in epithelial ovarian tumors: its impact on prognosis and on response to chemotherapy. *Clin Cancer Res* **7**: 1661-1668.
- Birol G, Wang S, Budzynski E, Wangsa-Wirawan ND, Linsenmeier RA. 2007. Oxygen distribution and consumption in the macaque retina. *American journal of physiology Heart and circulatory physiology* **293**: H1696-1704.
- Biron-Shental T, Schaiff WT, Ratajczak CK, Bildirici I, Nelson DM, Sadovsky Y. 2007. Hypoxia regulates the expression of fatty acid-binding proteins in primary term human trophoblasts. *American journal of obstetrics and gynecology* **197**: 516 e511-516.
- Black JC, Van Rechem C, Whetstine JR. 2012. Histone lysine methylation dynamics: establishment, regulation, and biological impact. *Mol Cell* **48**: 491-507.
- Blancher C, Moore JW, Talks KL, Houlbrook S, Harris AL. 2000. Relationship of hypoxia-inducible factor (HIF)-1alpha and HIF-2alpha expression to vascular endothelial growth factor induction and hypoxia survival in human breast cancer cell lines. *Cancer research* **60**: 7106-7113.
- Brigati C, Banelli B, di Vinci A, Casciano I, Allemanni G, Forlani A, Borzi L, Romani M. 2010. Inflammation, HIF-1, and the epigenetics that follows. *Mediators of inflammation* **2010**: 263914.
- Cabibbo A, Pagani M, Fabbri M, Rocchi M, Farmery MR, Bulleid NJ, Sitia R. 2000. ERO1-L, a human protein that favors disulfide bond formation in the endoplasmic reticulum. *J Biol Chem* **275**: 4827-4833.

- Campeau E, Ruhl VE, Rodier F, Smith CL, Rahmberg BL, Fuss JO, Campisi J, Yaswen P, Cooper PK, Kaufman PD. 2009. A versatile viral system for expression and depletion of proteins in mammalian cells. *PLoS One* **4**: e6529.
- Cancer Genome Atlas N. 2012. Comprehensive molecular characterization of human colon and rectal cancer. *Nature* **487**: 330-337.
- Cancer Genome Atlas Research N. 2011. Integrated genomic analyses of ovarian carcinoma. *Nature* **474**: 609-615.
- Candido S, Maestro R, Polesel J, Catania A, Maira F, Signorelli SS, McCubrey JA, Libra M. 2014. Roles of neutrophil gelatinase-associated lipocalin (NGAL) in human cancer. *Oncotarget* **5**: 1576-1594.
- Casey RC, Burleson KM, Skubitz KM, Pambuccian SE, Oegema TR, Jr., Ruff LE, Skubitz AP. 2001. Beta 1-integrins regulate the formation and adhesion of ovarian carcinoma multicellular spheroids. *The American journal of pathology* **159**: 2071-2080.
- Cedar H. 1988. DNA methylation and gene activity. *Cell* **53**: 3-4.
- Chakraborty S, Kaur S, Guha S, Batra SK. 2012. The multifaceted roles of neutrophil gelatinase associated lipocalin (NGAL) in inflammation and cancer. *Biochimica et biophysica acta* **1826**: 129-169.
- Chan DA, Giaccia AJ. 2007. Hypoxia, gene expression, and metastasis. *Cancer Metastasis Rev* **26**: 333-339.
- Chan DA, Sutphin PD, Denko NC, Giaccia AJ. 2002. Role of prolyl hydroxylation in oncogenically stabilized hypoxia-inducible factor-1alpha. *J Biol Chem* **277**: 40112-40117.

- Chan DA, Sutphin PD, Yen SE, Giaccia AJ. 2005. Coordinate regulation of the oxygen-dependent degradation domains of hypoxia-inducible factor 1 alpha. *Molecular and cellular biology* **25**: 6415-6426.
- Chantrain CF, Henriot P, Jodele S, Emonard H, Feron O, Courtoy PJ, DeClerck YA, Marbaix E. 2006. Mechanisms of pericyte recruitment in tumour angiogenesis: a new role for metalloproteinases. *Eur J Cancer* **42**: 310-318.
- Chawla RK, Watson WH, Jones DP. 1996. Effect of hypoxia on hepatic DNA methylation and tRNA methyltransferase in rat: similarities to effects of methyl-deficient diets. *Journal of cellular biochemistry* **61**: 72-80.
- Chen L, Fu L, Kong X, Xu J, Wang Z, Ma X, Akiyama Y, Chen Y, Fang J. 2014. Jumonji domain-containing protein 2B silencing induces DNA damage response via STAT3 pathway in colorectal cancer. *British journal of cancer* **110**: 1014-1026.
- Cheng H, Liu P, Wang ZC, Zou L, Santiago S, Garbitt V, Gjoerup OV, Iglehart JD, Miron A, Richardson AL et al. 2009. SIK1 couples LKB1 to p53-dependent anoikis and suppresses metastasis. *Sci Signal* **2**: ra35.
- Cheng X. 2014. Structural and functional coordination of DNA and histone methylation. *Cold Spring Harb Perspect Biol* **6**.
- Chi JT, Wang Z, Nuyten DS, Rodriguez EH, Schaner ME, Salim A, Wang Y, Kristensen GB, Helland A, Borresen-Dale AL et al. 2006. Gene expression programs in response to hypoxia: cell type specificity and prognostic significance in human cancers. *PLoS medicine* **3**: e47.

- Cho H, Kim JH. 2009. Lipocalin2 expressions correlate significantly with tumor differentiation in epithelial ovarian cancer. *The journal of histochemistry and cytochemistry : official journal of the Histochemistry Society* **57**: 513-521.
- Chu CH, Wang LY, Hsu KC, Chen CC, Cheng HH, Wang SM, Wu CM, Chen TJ, Li LT, Liu R et al. 2014. KDM4B as a target for prostate cancer: structural analysis and selective inhibition by a novel inhibitor. *J Med Chem* **57**: 5975-5985.
- Cloos PA, Christensen J, Agger K, Helin K. 2008. Erasing the methyl mark: histone demethylases at the center of cellular differentiation and disease. *Genes Dev* **22**: 1115-1140.
- Cloos PA, Christensen J, Agger K, Maiolica A, Rappsilber J, Antal T, Hansen KH, Helin K. 2006. The putative oncogene GASC1 demethylates tri- and dimethylated lysine 9 on histone H3. *Nature* **442**: 307-311.
- Coffey K, Rogerson L, Ryan-Munden C, Alkharaif D, Stockley J, Heer R, Sahadevan K, O'Neill D, Jones D, Darby S et al. 2013. The lysine demethylase, KDM4B, is a key molecule in androgen receptor signalling and turnover. *Nucleic acids research* **41**: 4433-4446.
- Conley SJ, Wicha MS. 2012. Antiangiogenic agents: Fueling cancer's hypoxic roots. *Cell Cycle* **11**.
- Cox TR, Bird D, Baker AM, Barker HE, Ho MW, Lang G, Erler JT. 2013. LOX-mediated collagen crosslinking is responsible for fibrosis-enhanced metastasis. *Cancer Res* **73**: 1721-1732.

- Dalgliesh GL, Furge K, Greenman C, Chen L, Bignell G, Butler A, Davies H, Edkins S, Hardy C, Latimer C et al. 2010. Systematic sequencing of renal carcinoma reveals inactivation of histone modifying genes. *Nature* **463**: 360-363.
- Das PP, Shao Z, Beyaz S, Apostolou E, Pinello L, De Los Angeles A, O'Brien K, Atsma JM, Fujiwara Y, Nguyen M et al. 2014. Distinct and combinatorial functions of Jmjd2b/Kdm4b and Jmjd2c/Kdm4c in mouse embryonic stem cell identity. *Mol Cell* **53**: 32-48.
- de Gramont A, Figer A, Seymour M, Homerin M, Hmissi A, Cassidy J, Boni C, Cortes-Funes H, Cervantes A, Freyer G et al. 2000. Leucovorin and fluorouracil with or without oxaliplatin as first-line treatment in advanced colorectal cancer. *Journal of clinical oncology : official journal of the American Society of Clinical Oncology* **18**: 2938-2947.
- Decitre M, Gleyzal C, Raccurt M, Peyrol S, Aubert-Foucher E, Csiszar K, Sommer P. 1998. Lysyl oxidase-like protein localizes to sites of de novo fibrinogenesis in fibrosis and in the early stromal reaction of ductal breast carcinomas. *Lab Invest* **78**: 143-151.
- Devireddy LR, Gazin C, Zhu X, Green MR. 2005. A cell-surface receptor for lipocalin 24p3 selectively mediates apoptosis and iron uptake. *Cell* **123**: 1293-1305.
- Douillard JY, Cunningham D, Roth AD, Navarro M, James RD, Karasek P, Jandik P, Iveson T, Carmichael J, Alakl M et al. 2000. Irinotecan combined with fluorouracil compared with fluorouracil alone as first-line treatment for metastatic colorectal cancer: a multicentre randomised trial. *Lancet* **355**: 1041-1047.

- Edgar R, Domrachev M, Lash AE. 2002. Gene Expression Omnibus: NCBI gene expression and hybridization array data repository. *Nucleic acids research* **30**: 207-210.
- el-Deiry WS, Harper JW, O'Connor PM, Velculescu VE, Canman CE, Jackman J, Pietenpol JA, Burrell M, Hill DE, Wang Y et al. 1994. WAF1/CIP1 is induced in p53-mediated G1 arrest and apoptosis. *Cancer Res* **54**: 1169-1174.
- Elloul S, Elstrand MB, Nesland JM, Trope CG, Kvalheim G, Goldberg I, Reich R, Davidson B. 2005. Snail, Slug, and Smad-interacting protein 1 as novel parameters of disease aggressiveness in metastatic ovarian and breast carcinoma. *Cancer* **103**: 1631-1643.
- Elmore JM, Kadesky KT, Koeneman KS, Sagalowsky AI. 2003. Reassessment of the 1997 TNM classification system for renal cell carcinoma. *Cancer* **98**: 2329-2334.
- Erler JT, Bennewith KL, Cox TR, Lang G, Bird D, Koong A, Le QT, Giaccia AJ. 2009. Hypoxia-induced lysyl oxidase is a critical mediator of bone marrow cell recruitment to form the premetastatic niche. *Cancer Cell* **15**: 35-44.
- Erler JT, Bennewith KL, Nicolau M, Dornhofer N, Kong C, Le QT, Chi JT, Jeffrey SS, Giaccia AJ. 2006. Lysyl oxidase is essential for hypoxia-induced metastasis. *Nature* **440**: 1222-1226.
- Erler JT, Giaccia AJ. 2006. Lysyl oxidase mediates hypoxic control of metastasis. *Cancer research* **66**: 10238-10241.
- Farzan M, Schnitzler CE, Vasilieva N, Leung D, Choe H. 2000. BACE2, a beta - secretase homolog, cleaves at the beta site and within the amyloid-beta region of the amyloid-beta precursor protein. *Proc Natl Acad Sci U S A* **97**: 9712-9717.

- Fodor BD, Kubicek S, Yonezawa M, O'Sullivan RJ, Sengupta R, Perez-Burgos L, Opravil S, Mechtler K, Schotta G, Jenuwein T. 2006. Jmjd2b antagonizes H3K9 trimethylation at pericentric heterochromatin in mammalian cells. *Genes Dev* **20**: 1557-1562.
- Forsythe JA, Jiang BH, Iyer NV, Agani F, Leung SW, Koos RD, Semenza GL. 1996. Activation of vascular endothelial growth factor gene transcription by hypoxia-inducible factor 1. *Mol Cell Biol* **16**: 4604-4613.
- Fossey SL, Bear MD, Kisseberth WC, Pennell M, London CA. 2011. Oncostatin M promotes STAT3 activation, VEGF production, and invasion in osteosarcoma cell lines. *BMC cancer* **11**: 125.
- Fu L, Chen L, Yang J, Ye T, Chen Y, Fang J. 2012. HIF-1alpha-induced histone demethylase JMJD2B contributes to the malignant phenotype of colorectal cancer cells via an epigenetic mechanism. *Carcinogenesis* **33**: 1664-1673.
- Gaughan L, Stockley J, Coffey K, O'Neill D, Jones DL, Wade M, Wright J, Moore M, Tse S, Rogerson L et al. 2013. KDM4B is a master regulator of the estrogen receptor signalling cascade. *Nucleic acids research* **41**: 6892-6904.
- Goetz DH, Holmes MA, Borregaard N, Bluhm ME, Raymond KN, Strong RK. 2002. The neutrophil lipocalin NGAL is a bacteriostatic agent that interferes with siderophore-mediated iron acquisition. *Molecular cell* **10**: 1033-1043.
- Goicoechea SM, Bednarski B, Garcia-Mata R, Prentice-Dunn H, Kim HJ, Otey CA. 2009. Palladin contributes to invasive motility in human breast cancer cells. *Oncogene* **28**: 587-598.

- Gore ME, Larkin JM. 2011. Challenges and opportunities for converting renal cell carcinoma into a chronic disease with targeted therapies. *British journal of cancer* **104**: 399-406.
- Grimsby JL, Lucero HA, Trackman PC, Ravid K, Kagan HM. 2010. Role of lysyl oxidase propeptide in secretion and enzyme activity. *Journal of cellular biochemistry* **111**: 1231-1243.
- Grone J, Weber B, Staub E, Heinze M, Klamann I, Pilarsky C, Hermann K, Castanos-Velez E, Ropcke S, Mann B et al. 2007. Differential expression of genes encoding tight junction proteins in colorectal cancer: frequent dysregulation of claudin-1, -8 and -12. *International journal of colorectal disease* **22**: 651-659.
- Gudas LJ, Fu L, Minton DR, Mongan NP, Nanus DM. 2014. The role of HIF1alpha in renal cell carcinoma tumorigenesis. *J Mol Med (Berl)* **92**: 825-836.
- Guo X, Shi M, Sun L, Wang Y, Gui Y, Cai Z, Duan X. 2011. The expression of histone demethylase JMJD1A in renal cell carcinoma. *Neoplasma* **58**: 153-157.
- Halamkova J, Kiss I, Pavlovsky Z, Tomasek J, Jarkovsky J, Cech Z, Tucek S, Hanakova L, Moulis M, Zavrelouva J et al. 2011. Clinical significance of the plasminogen activator system in relation to grade of tumor and treatment response in colorectal carcinoma patients. *Neoplasma* **58**: 377-385.
- Hamilton TC, Young RC, Ozols RF. 1984. Experimental model systems of ovarian cancer: applications to the design and evaluation of new treatment approaches. *Semin Oncol* **11**: 285-298.
- Hanahan D, Weinberg RA. 2000. The hallmarks of cancer. *Cell* **100**: 57-70.

He TC, Sparks AB, Rago C, Hermeking H, Zawel L, da Costa LT, Morin PJ, Vogelstein B, Kinzler KW. 1998. Identification of c-MYC as a target of the APC pathway.

Science **281**: 1509-1512.

Hojfeldt JW, Agger K, Helin K. 2013. Histone lysine demethylases as targets for anticancer therapy. *Nat Rev Drug Discov* **12**: 917-930.

Horiuchi A, Hayashi T, Kikuchi N, Hayashi A, Fuseya C, Shiozawa T, Konishi I. 2012. Hypoxia upregulates ovarian cancer invasiveness via the binding of HIF-1alpha to a hypoxia-induced, methylation-free hypoxia response element of S100A4 gene. *International journal of cancer Journal international du cancer* **131**: 1755-1767.

Hosaka K, Yang Y, Seki T, Nakamura M, Andersson P, Rouhi P, Yang X, Jensen L, Lim S, Feng N et al. 2013. Tumour PDGF-BB expression levels determine dual effects of anti-PDGF drugs on vascular remodelling and metastasis. *Nature communications* **4**: 2129.

Hu Z, Gomes I, Horrigan SK, Kravarusic J, Mar B, Arbieva Z, Chyna B, Fulton N, Edassery S, Raza A et al. 2001. A novel nuclear protein, 5qNCA (LOC51780) is a candidate for the myeloid leukemia tumor suppressor gene on chromosome 5 band q31. *Oncogene* **20**: 6946-6954.

Hudson LG, Zeineldin R, Stack MS. 2008. Phenotypic plasticity of neoplastic ovarian epithelium: unique cadherin profiles in tumor progression. *Clinical & experimental metastasis* **25**: 643-655.

Irizarry RA, Hobbs B, Collin F, Beazer-Barclay YD, Antonellis KJ, Scherf U, Speed TP.

2003. Exploration, normalization, and summaries of high density oligonucleotide array probe level data. *Biostatistics* **4**: 249-264.

Ivan M, Kondo K, Yang H, Kim W, Valiando J, Ohh M, Salic A, Asara JM, Lane WS,

Kaelin WG, Jr. 2001. HIF α targeted for VHL-mediated destruction by proline hydroxylation: implications for O₂ sensing. *Science* **292**: 464-468.

Iwamori N, Zhao M, Meistrich ML, Matzuk MM. 2011. The testis-enriched histone

demethylase, KDM4D, regulates methylation of histone H3 lysine 9 during spermatogenesis in the mouse but is dispensable for fertility. *Biology of reproduction* **84**: 1225-1234.

Jaakkola P, Mole DR, Tian YM, Wilson MI, Gielbert J, Gaskell SJ, Kriegsheim A,

Hebestreit HF, Mukherji M, Schofield CJ et al. 2001. Targeting of HIF- α to the von Hippel-Lindau ubiquitylation complex by O₂-regulated prolyl hydroxylation. *Science* **292**: 468-472.

Jamal-Hanjani M, Quezada SA, Larkin J, Swanton C. 2015. Translational Implications of

Tumor Heterogeneity. *Clin Cancer Res* **21**: 1258-1266.

Ji F, Wang Y, Qiu L, Li S, Zhu J, Liang Z, Wan Y, Di W. 2013. Hypoxia inducible factor

1 α -mediated LOX expression correlates with migration and invasion in epithelial ovarian cancer. *International journal of oncology* **42**: 1578-1588.

Johansson C, Tumber A, Che K, Cain P, Nowak R, Gileadi C, Oppermann U. 2014. The

roles of Jumonji-type oxygenases in human disease. *Epigenomics* **6**: 89-120.

- Jonasch E, Futreal PA, Davis IJ, Bailey ST, Kim WY, Brugarolas J, Giaccia AJ, Kurban G, Pause A, Frydman J et al. 2012. State of the science: an update on renal cell carcinoma. *Molecular cancer research : MCR* **10**: 859-880.
- Jonasch E, Gao J, Rathmell WK. 2014. Renal cell carcinoma. *Bmj* **349**: g4797.
- Jones A, Fujiyama C, Blanche C, Moore JW, Fuggle S, Cranston D, Bicknell R, Harris AL. 2001. Relation of vascular endothelial growth factor production to expression and regulation of hypoxia-inducible factor-1 alpha and hypoxia-inducible factor-2 alpha in human bladder tumors and cell lines. *Clinical cancer research : an official journal of the American Association for Cancer Research* **7**: 1263-1272.
- Katoh Y, Katoh M. 2007. Comparative integromics on JMJD2A, JMJD2B and JMJD2C: preferential expression of JMJD2C in undifferentiated ES cells. *International journal of molecular medicine* **20**: 269-273.
- Kawazu M, Saso K, Tong KI, McQuire T, Goto K, Son DO, Wakeham A, Miyagishi M, Mak TW, Okada H. 2011. Histone demethylase JMJD2B functions as a co-factor of estrogen receptor in breast cancer proliferation and mammary gland development. *PLoS One* **6**: e17830.
- Khoury-Haddad H, Guttmann-Raviv N, Ipenberg I, Huggins D, Jeyasekharan AD, Ayoub N. 2014. PARP1-dependent recruitment of KDM4D histone demethylase to DNA damage sites promotes double-strand break repair. *Proc Natl Acad Sci U S A* **111**: E728-737.
- Kim JG, Yi JM, Park SJ, Kim JS, Son TG, Yang K, Yoo MA, Heo K. 2012a. Histone demethylase JMJD2B-mediated cell proliferation regulated by hypoxia and radiation in gastric cancer cell. *Biochimica et biophysica acta* **1819**: 1200-1207.

- Kim JY, Kim KB, Eom GH, Choe N, Kee HJ, Son HJ, Oh ST, Kim DW, Pak JH, Baek HJ et al. 2012i. KDM3B is the H3K9 demethylase involved in transcriptional activation of *lmo2* in leukemia. *Mol Cell Biol* **32**: 2917-2933.
- Klose RJ, Gardner KE, Liang G, Erdjument-Bromage H, Tempst P, Zhang Y. 2007. Demethylation of histone H3K36 and H3K9 by Rph1: a vestige of an H3K9 methylation system in *Saccharomyces cerevisiae*? *Mol Cell Biol* **27**: 3951-3961.
- Klose RJ, Yamane K, Bae Y, Zhang D, Erdjument-Bromage H, Tempst P, Wong J, Zhang Y. 2006. The transcriptional repressor JHDM3A demethylates trimethyl histone H3 lysine 9 and lysine 36. *Nature* **442**: 312-316.
- Koi M, Boland CR. 2011. Tumor hypoxia and genetic alterations in sporadic cancers. *The journal of obstetrics and gynaecology research* **37**: 85-98.
- Kopetz S, Chang GJ, Overman MJ, Eng C, Sargent DJ, Larson DW, Grothey A, Vauthey JN, Nagorney DM, McWilliams RR. 2009. Improved survival in metastatic colorectal cancer is associated with adoption of hepatic resection and improved chemotherapy. *Journal of clinical oncology : official journal of the American Society of Clinical Oncology* **27**: 3677-3683.
- Kops GJ, Weaver BA, Cleveland DW. 2005. On the road to cancer: aneuploidy and the mitotic checkpoint. *Nature reviews Cancer* **5**: 773-785.
- Kouzarides T. 2002. Histone methylation in transcriptional control. *Current opinion in genetics & development* **12**: 198-209.
- Krieg AJ, Rankin EB, Chan D, Razorenova O, Fernandez S, Giaccia AJ. 2010. Regulation of the histone demethylase JMJD1A by hypoxia-inducible factor 1

- alpha enhances hypoxic gene expression and tumor growth. *Mol Cell Biol* **30**: 344-353.
- Krishnamachary B, Berg-Dixon S, Kelly B, Agani F, Feldser D, Ferreira G, Iyer N, LaRusch J, Pak B, Taghavi P et al. 2003. Regulation of colon carcinoma cell invasion by hypoxia-inducible factor 1. *Cancer Res* **63**: 1138-1143.
- Kruidenier L, Chung CW, Cheng Z, Liddle J, Che K, Joberty G, Bantscheff M, Bountra C, Bridges A, Diallo H et al. 2012. A selective jumonji H3K27 demethylase inhibitor modulates the proinflammatory macrophage response. *Nature* **488**: 404-408.
- Kutomi G, Tamura Y, Tanaka T, Kajiwara T, Kukita K, Ohmura T, Shima H, Takamaru T, Satomi F, Suzuki Y et al. 2013. Human endoplasmic reticulum oxidoreductin 1-alpha is a novel predictor for poor prognosis of breast cancer. *Cancer science* **104**: 1091-1096.
- Kuzbicki L, Lange D, Straczynska-Niemiec A, Chwirot BW. 2013. JARID1B expression in human melanoma and benign melanocytic skin lesions. *Melanoma research* **23**: 8-12.
- Lachner M, Jenuwein T. 2002. The many faces of histone lysine methylation. *Current opinion in cell biology* **14**: 286-298.
- Lal S, Burkhart RA, Beeharry N, Bhattacharjee V, Londin ER, Cozzitorto JA, Romeo C, Jimbo M, Norris ZA, Yeo CJ et al. 2014. HuR posttranscriptionally regulates WEE1: implications for the DNA damage response in pancreatic cancer cells. *Cancer Res* **74**: 1128-1140.

- Lando D, Peet DJ, Gorman JJ, Whelan DA, Whitelaw ML, Bruick RK. 2002. FIH-1 is an asparaginyl hydroxylase enzyme that regulates the transcriptional activity of hypoxia-inducible factor. *Genes Dev* **16**: 1466-1471.
- Le QT, Harris J, Magliocco AM, Kong CS, Diaz R, Shin B, Cao H, Trotti A, Erler JT, Chung CH et al. 2009. Validation of lysyl oxidase as a prognostic marker for metastasis and survival in head and neck squamous cell carcinoma: Radiation Therapy Oncology Group trial 90-03. *Journal of clinical oncology : official journal of the American Society of Clinical Oncology* **27**: 4281-4286.
- Lee S, Garner EI, Welch WR, Berkowitz RS, Mok SC. 2007. Over-expression of hypoxia-inducible factor 1 alpha in ovarian clear cell carcinoma. *Gynecologic oncology* **106**: 311-317.
- Lengyel E. 2010. Ovarian cancer development and metastasis. *The American journal of pathology* **177**: 1053-1064.
- Li Q, Shi L, Gui B, Yu W, Wang J, Zhang D, Han X, Yao Z, Shang Y. 2011a. Binding of the JmjC demethylase JARID1B to LSD1/NuRD suppresses angiogenesis and metastasis in breast cancer cells by repressing chemokine CCL14. *Cancer Res* **71**: 6899-6908.
- Li W, He F. 2014. Monocyte to macrophage differentiation-associated (MMD) targeted by miR-140-5p regulates tumor growth in non-small cell lung cancer. *Biochem Biophys Res Commun* **450**: 844-850.
- Li W, Zhao L, Zang W, Liu Z, Chen L, Liu T, Xu D, Jia J. 2011b. Histone demethylase JMJD2B is required for tumor cell proliferation and survival and is overexpressed in gastric cancer. *Biochem Biophys Res Commun*.

- Li X, Dong S. 2015. Histone demethylase JMJD2B and JMJD2C induce fibroblast growth factor 2: mediated tumorigenesis of osteosarcoma. *Medical oncology* **32**: 53.
- Li Y, Xu J, Xiong H, Ma Z, Wang Z, Kipreos ET, Dalton S, Zhao S. 2014. Cancer driver candidate genes AVL9, DENND5A and NUPL1 contribute to MDCK cystogenesis. *Oncoscience* **1**: 854-865.
- Liang D, Ma Y, Liu J, Trope CG, Holm R, Nesland JM, Suo Z. 2012. The hypoxic microenvironment upgrades stem-like properties of ovarian cancer cells. *BMC cancer* **12**: 201.
- Licata LA, Hostetter CL, Crismale J, Sheth A, Keen JC. 2010. The RNA-binding protein HuR regulates GATA3 mRNA stability in human breast cancer cell lines. *Breast cancer research and treatment* **122**: 55-63.
- Liu M, Shen S, Chen F, Yu W, Yu L. 2010. Linking the septin expression with carcinogenesis. *Molecular biology reports* **37**: 3601-3608.
- Liu Q, Zheng J, Yin DD, Xiang J, He F, Wang YC, Liang L, Qin HY, Liu L, Liang YM et al. 2012. Monocyte to macrophage differentiation-associated (MMD) positively regulates ERK and Akt activation and TNF-alpha and NO production in macrophages. *Molecular biology reports* **39**: 5643-5650.
- Loboda A, Jozkowicz A, Dulak J. 2010. HIF-1 and HIF-2 transcription factors--similar but not identical. *Molecules and cells* **29**: 435-442.
- Lu C, Shahzad MM, Moreno-Smith M, Lin YG, Jennings NB, Allen JK, Landen CN, Mangala LS, Armaiz-Pena GN, Schmandt R et al. 2010. Targeting pericytes with

- a PDGF-B aptamer in human ovarian carcinoma models. *Cancer biology & therapy* **9**: 176-182.
- Lu PJ, Sundquist K, Baeckstrom D, Poulsom R, Hanby A, Meier-Ewert S, Jones T, Mitchell M, Pitha-Rowe P, Freemont P et al. 1999. A novel gene (PLU-1) containing highly conserved putative DNA/chromatin binding motifs is specifically up-regulated in breast cancer. *J Biol Chem* **274**: 15633-15645.
- Lu Y, Chu A, Turker MS, Glazer PM. 2011. Hypoxia-induced epigenetic regulation and silencing of the BRCA1 promoter. *Molecular and cellular biology* **31**: 3339-3350.
- Luger K, Mader AW, Richmond RK, Sargent DF, Richmond TJ. 1997. Crystal structure of the nucleosome core particle at 2.8 Å resolution. *Nature* **389**: 251-260.
- Lukas J, Mazna P, Valenta T, Doubravska L, Pospichalova V, Vojtechova M, Fafilek B, Ivanek R, Plachy J, Novak J et al. 2009. Dazap2 modulates transcription driven by the Wnt effector TCF-4. *Nucleic acids research* **37**: 3007-3020.
- Luo SQ, Hu JP, Qu Q, Li J, Ren W, Zhang JM, Zhong Y, Hu WX. 2012. The effects of promoter methylation on downregulation of DAZAP2 in multiple myeloma cell lines. *PLoS One* **7**: e40475.
- Ma MK, Heath C, Hair A, West AG. 2011. Histone crosstalk directed by H2B ubiquitination is required for chromatin boundary integrity. *PLoS genetics* **7**: e1002175.
- Mahon PC, Hirota K, Semenza GL. 2001. FIH-1: a novel protein that interacts with HIF-1α and VHL to mediate repression of HIF-1 transcriptional activity. *Genes Dev* **15**: 2675-2686.

- Majmundar AJ, Wong WJ, Simon MC. 2010. Hypoxia-inducible factors and the response to hypoxic stress. *Molecular cell* **40**: 294-309.
- Makino Y, Cao R, Svensson K, Bertilsson G, Asman M, Tanaka H, Cao Y, Berkenstam A, Poellinger L. 2001. Inhibitory PAS domain protein is a negative regulator of hypoxia-inducible gene expression. *Nature* **414**: 550-554.
- Mallette FA, Mattioli F, Cui G, Young LC, Hendzel MJ, Mer G, Sixma TK, Richard S. 2012. RNF8- and RNF168-dependent degradation of KDM4A/JMJD2A triggers 53BP1 recruitment to DNA damage sites. *The EMBO journal* **31**: 1865-1878.
- Margueron R, Trojer P, Reinberg D. 2005. The key to development: interpreting the histone code? *Curr Opin Genet Dev* **15**: 163-176.
- Maxwell PH, Wiesener MS, Chang GW, Clifford SC, Vaux EC, Cockman ME, Wykoff CC, Pugh CW, Maher ER, Ratcliffe PJ. 1999. The tumour suppressor protein VHL targets hypoxia-inducible factors for oxygen-dependent proteolysis. *Nature* **399**: 271-275.
- May D, Itin A, Gal O, Kalinski H, Feinstein E, Keshet E. 2005. Ero1-L alpha plays a key role in a HIF-1-mediated pathway to improve disulfide bond formation and VEGF secretion under hypoxia: implication for cancer. *Oncogene* **24**: 1011-1020.
- McCleary NJ, Meyerhardt JA, Green E, Yothers G, de Gramont A, Van Cutsem E, O'Connell M, Twelves CJ, Saltz LB, Haller DG et al. 2013. Impact of age on the efficacy of newer adjuvant therapies in patients with stage II/III colon cancer: findings from the ACCENT database. *Journal of clinical oncology : official journal of the American Society of Clinical Oncology* **31**: 2600-2606.

- McNeill LA, Hewitson KS, Claridge TD, Seibel JF, Horsfall LE, Schofield CJ. 2002. Hypoxia-inducible factor asparaginyl hydroxylase (FIH-1) catalyses hydroxylation at the beta-carbon of asparagine-803. *Biochem J* **367**: 571-575.
- Metzen E, Stiehl DP, Doege K, Marxsen JH, Hellwig-Burgel T, Jelkmann W. 2005. Regulation of the prolyl hydroxylase domain protein 2 (phd2/egln-1) gene: identification of a functional hypoxia-responsive element. *The Biochemical journal* **387**: 711-717.
- Metzger E, Wissmann M, Yin N, Muller JM, Schneider R, Peters AH, Gunther T, Buettner R, Schule R. 2005. LSD1 demethylates repressive histone marks to promote androgen-receptor-dependent transcription. *Nature* **437**: 436-439.
- Mimura I, Tanaka T, Wada Y, Kodama T, Nangaku M. 2011. Pathophysiological response to hypoxia - from the molecular mechanisms of malady to drug discovery: epigenetic regulation of the hypoxic response via hypoxia-inducible factor and histone modifying enzymes. *Journal of pharmacological sciences* **115**: 453-458.
- Morita K, Morita NI, Nemoto K, Nakamura Y, Miyachi Y, Muto M. 2008. Expression of claudin in melanoma cells. *The Journal of dermatology* **35**: 36-38.
- Mosammamarast N, Shi Y. 2010. Reversal of histone methylation: biochemical and molecular mechanisms of histone demethylases. *Annual review of biochemistry* **79**: 155-179.
- Moss NM, Barbolina MV, Liu Y, Sun L, Munshi HG, Stack MS. 2009. Ovarian cancer cell detachment and multicellular aggregate formation are regulated by

- membrane type 1 matrix metalloproteinase: a potential role in l.p. metastatic dissemination. *Cancer Res* **69**: 7121-7129.
- Motzer RJ, Mazumdar M, Bacik J, Berg W, Amsterdam A, Ferrara J. 1999. Survival and prognostic stratification of 670 patients with advanced renal cell carcinoma. *Journal of clinical oncology : official journal of the American Society of Clinical Oncology* **17**: 2530-2540.
- Naora H, Montell DJ. 2005. Ovarian cancer metastasis: integrating insights from disparate model organisms. *Nature reviews Cancer* **5**: 355-366.
- Nieman KM, Kenny HA, Penicka CV, Ladanyi A, Buell-Gutbrod R, Zillhardt MR, Romero IL, Carey MS, Mills GB, Hotamisligil GS et al. 2011. Adipocytes promote ovarian cancer metastasis and provide energy for rapid tumor growth. *Nature medicine* **17**: 1498-1503.
- Noffsinger AE. 2009. Serrated polyps and colorectal cancer: new pathway to malignancy. *Annual review of pathology* **4**: 343-364.
- Nozawa-Suzuki N, Nagasawa H, Ohnishi K, Morishige K. 2015. The inhibitory effect of hypoxic cytotoxin on the expansion of cancer stem cells in ovarian cancer. *Biochem Biophys Res Commun* **457**: 706-711.
- O'Connor PM, Jackman J, Bae I, Myers TG, Fan S, Mutoh M, Scudiero DA, Monks A, Sausville EA, Weinstein JN et al. 1997. Characterization of the p53 tumor suppressor pathway in cell lines of the National Cancer Institute anticancer drug screen and correlations with the growth-inhibitory potency of 123 anticancer agents. *Cancer Res* **57**: 4285-4300.

- Oelgeschlager M, Larrain J, Geissert D, De Robertis EM. 2000. The evolutionarily conserved BMP-binding protein Twisted gastrulation promotes BMP signalling. *Nature* **405**: 757-763.
- Ohh M, Park CW, Ivan M, Hoffman MA, Kim TY, Huang LE, Pavletich N, Chau V, Kaelin WG. 2000. Ubiquitination of hypoxia-inducible factor requires direct binding to the beta-domain of the von Hippel-Lindau protein. *Nature cell biology* **2**: 423-427.
- Okada Y, Tateishi K, Zhang Y. 2010. Histone demethylase JHDM2A is involved in male infertility and obesity. *Journal of andrology* **31**: 75-78.
- Olbryt M, Habryka A, Student S, Jarzab M, Tyszkiewicz T, Lisowska KM. 2014. Global gene expression profiling in three tumor cell lines subjected to experimental cycling and chronic hypoxia. *PLoS One* **9**: e105104.
- Osada R, Horiuchi A, Kikuchi N, Yoshida J, Hayashi A, Ota M, Katsuyama Y, Melillo G, Konishi I. 2007. Expression of hypoxia-inducible factor 1alpha, hypoxia-inducible factor 2alpha, and von Hippel-Lindau protein in epithelial ovarian neoplasms and allelic loss of von Hippel-Lindau gene: nuclear expression of hypoxia-inducible factor 1alpha is an independent prognostic factor in ovarian carcinoma. *Human pathology* **38**: 1310-1320.
- Osawa T, Tsuchida R, Muramatsu M, Shimamura T, Wang F, Suehiro J, Kanki Y, Wada Y, Yuasa Y, Aburatani H et al. 2013. Inhibition of histone demethylase JMJD1A improves anti-angiogenic therapy and reduces tumor-associated macrophages. *Cancer Res* **73**: 3019-3028.
- Oszajca K, Bieniasz M, Brown G, Swiatkowska M, Bartkowiak J, Szemraj J. 2008. Effect of oxidative stress on the expression of t-PA, u-PA, u-PAR, and PAI-1 in

- endothelial cells. *Biochemistry and cell biology = Biochimie et biologie cellulaire* **86**: 477-486.
- Palamidessi A, Frittoli E, Ducano N, Offenhauser N, Sigismund S, Kajiho H, Parazzoli D, Oldani A, Gobbi M, Serini G et al. 2013. The GTPase-activating protein RN-tre controls focal adhesion turnover and cell migration. *Current biology : CB* **23**: 2355-2364.
- Palomera-Sanchez Z, Bucio-Mendez A, Valadez-Graham V, Reynaud E, Zurita M. 2010. Drosophila p53 is required to increase the levels of the dKDM4B demethylase after UV-induced DNA damage to demethylate histone H3 lysine 9. *J Biol Chem* **285**: 31370-31379.
- Patel IS, Madan P, Getsios S, Bertrand MA, MacCalman CD. 2003. Cadherin switching in ovarian cancer progression. *International journal of cancer Journal international du cancer* **106**: 172-177.
- Paul S, Dey A. 2008. Wnt signaling and cancer development: therapeutic implication. *Neoplasia* **55**: 165-176.
- Pedersen MT, Helin K. 2010. Histone demethylases in development and disease. *Trends Cell Biol* **20**: 662-671.
- Pena-Llopis S, Vega-Rubin-de-Celis S, Liao A, Leng N, Pavia-Jimenez A, Wang S, Yamasaki T, Zhrebker L, Sivanand S, Spence P et al. 2012. BAP1 loss defines a new class of renal cell carcinoma. *Nat Genet* **44**: 751-759.
- Pereira F, Barbachano A, Silva J, Bonilla F, Campbell MJ, Munoz A, Larriba MJ. 2011. KDM6B/JMJD3 histone demethylase is induced by vitamin D and modulates its effects in colon cancer cells. *Human molecular genetics* **20**: 4655-4665.

- Perets R, Wyant GA, Muto KW, Bijron JG, Poole BB, Chin KT, Chen JY, Ohman AW, Stepule CD, Kwak S et al. 2013. Transformation of the fallopian tube secretory epithelium leads to high-grade serous ovarian cancer in Brca;Tp53;Pten models. *Cancer Cell* **24**: 751-765.
- Pollard PJ, Loenarz C, Mole DR, McDonough MA, Gleadle JM, Schofield CJ, Ratcliffe PJ. 2008. Regulation of Jumonji-domain-containing histone demethylases by hypoxia-inducible factor (HIF)-1alpha. *Biochem J* **416**: 387-394.
- Postovit LM, Abbott DE, Payne SL, Wheaton WW, Margaryan NV, Sullivan R, Jansen MK, Csiszar K, Hendrix MJ, Kirschmann DA. 2008. Hypoxia/reoxygenation: a dynamic regulator of lysyl oxidase-facilitated breast cancer migration. *Journal of cellular biochemistry* **103**: 1369-1378.
- Pradeep S, Kim SW, Wu SY, Nishimura M, Chaluvally-Raghavan P, Miyake T, Pecot CV, Kim SJ, Choi HJ, Bischoff FZ et al. 2014. Hematogenous metastasis of ovarian cancer: rethinking mode of spread. *Cancer Cell* **26**: 77-91.
- Pryor JG, Brown-Kipphut BA, Iqbal A, Scott GA. 2011. Microarray comparative genomic hybridization detection of copy number changes in desmoplastic melanoma and malignant peripheral nerve sheath tumor. *The American Journal of dermatopathology* **33**: 780-785.
- Qi J, Nakayama K, Cardiff RD, Borowsky AD, Kaul K, Williams R, Krajewski S, Mercola D, Carpenter PM, Bowtell D et al. 2010. Siah2-dependent concerted activity of HIF and FoxA2 regulates formation of neuroendocrine phenotype and neuroendocrine prostate tumors. *Cancer Cell* **18**: 23-38.

- Qu B, Liu O, Fang X, Zhang H, Wang Y, Quan H, Zhang J, Zhou J, Zuo J, Tang J et al. 2014. Distal-less homeobox 2 promotes the osteogenic differentiation potential of stem cells from apical papilla. *Cell and tissue research* **357**: 133-143.
- Ramadoss S, Chen X, Wang CY. 2012. Histone demethylase KDM6B promotes epithelial-mesenchymal transition. *J Biol Chem* **287**: 44508-44517.
- Rankin EB, Fuh KC, Taylor TE, Krieg AJ, Musser M, Yuan J, Wei K, Kuo CJ, Longacre TA, Giaccia AJ. 2010. AXL is an essential factor and therapeutic target for metastatic ovarian cancer. *Cancer Res* **70**: 7570-7579.
- Ratcliffe PJ. 2007. HIF-1 and HIF-2: working alone or together in hypoxia? *The Journal of clinical investigation* **117**: 862-865.
- Roesch A, Fukunaga-Kalabis M, Schmidt EC, Zabierowski SE, Brafford PA, Vultur A, Basu D, Gimotty P, Vogt T, Herlyn M. 2010. A temporarily distinct subpopulation of slow-cycling melanoma cells is required for continuous tumor growth. *Cell* **141**: 583-594.
- Rohwer N, Cramer T. 2011. Hypoxia-mediated drug resistance: novel insights on the functional interaction of HIFs and cell death pathways. *Drug resistance updates : reviews and commentaries in antimicrobial and anticancer chemotherapy* **14**: 191-201.
- Ruthenburg AJ, Allis CD, Wysocka J. 2007. Methylation of lysine 4 on histone H3: intricacy of writing and reading a single epigenetic mark. *Mol Cell* **25**: 15-30.
- Saad FA, Torres M, Wang H, Graham L. 2010. Intracellular lysyl oxidase: effect of a specific inhibitor on nuclear mass in proliferating cells. *Biochem Biophys Res Commun* **396**: 944-949.

- Saltz LB, Cox JV, Blanke C, Rosen LS, Fehrenbacher L, Moore MJ, Maroun JA, Ackland SP, Locker PK, Pirodda N et al. 2000. Irinotecan plus fluorouracil and leucovorin for metastatic colorectal cancer. Irinotecan Study Group. *The New England journal of medicine* **343**: 905-914.
- Schito L, Rey S, Tafani M, Zhang H, Wong CC, Russo A, Russo MA, Semenza GL. 2012. Hypoxia-inducible factor 1-dependent expression of platelet-derived growth factor B promotes lymphatic metastasis of hypoxic breast cancer cells. *Proc Natl Acad Sci U S A* **109**: E2707-2716.
- Semenza GL. 1998. Hypoxia-inducible factor 1: master regulator of O₂ homeostasis. *Current opinion in genetics & development* **8**: 588-594.
- . 2012. Hypoxia-inducible factors: mediators of cancer progression and targets for cancer therapy. *Trends in pharmacological sciences* **33**: 207-214.
- Semenza GL, Agani F, Booth G, Forsythe J, Iyer N, Jiang BH, Leung S, Roe R, Wiener C, Yu A. 1997. Structural and functional analysis of hypoxia-inducible factor 1. *Kidney international* **51**: 553-555.
- Semenza GL, Jiang BH, Leung SW, Passantino R, Concordet JP, Maire P, Giallongo A. 1996. Hypoxia response elements in the aldolase A, enolase 1, and lactate dehydrogenase A gene promoters contain essential binding sites for hypoxia-inducible factor 1. *The Journal of biological chemistry* **271**: 32529-32537.
- Semenza GL, Roth PH, Fang HM, Wang GL. 1994. Transcriptional regulation of genes encoding glycolytic enzymes by hypoxia-inducible factor 1. *The Journal of biological chemistry* **269**: 23757-23763.

- Semenza GL, Wang GL. 1992. A nuclear factor induced by hypoxia via de novo protein synthesis binds to the human erythropoietin gene enhancer at a site required for transcriptional activation. *Molecular and cellular biology* **12**: 5447-5454.
- Shi L, Sun L, Li Q, Liang J, Yu W, Yi X, Yang X, Li Y, Han X, Zhang Y et al. 2011. Histone demethylase JMJD2B coordinates H3K4/H3K9 methylation and promotes hormonally responsive breast carcinogenesis. *Proc Natl Acad Sci U S A* **108**: 7541-7546.
- Shi Y, Lan F, Matson C, Mulligan P, Whetstine JR, Cole PA, Casero RA, Shi Y. 2004. Histone demethylation mediated by the nuclear amine oxidase homolog LSD1. *Cell* **119**: 941-953.
- Shi Y, Whetstine JR. 2007. Dynamic regulation of histone lysine methylation by demethylases. *Mol Cell* **25**: 1-14.
- Shi YW, Shen R, Ren W, Tang LJ, Tan DR, Hu WX. 2007. Molecular features and expression of DAZAP2 in human multiple myeloma. *Chin Med J (Engl)* **120**: 1659-1665.
- Siegel R, Desantis C, Jemal A. 2014a. Colorectal cancer statistics, 2014. *CA: a cancer journal for clinicians* **64**: 104-117.
- Siegel R, Ma J, Zou Z, Jemal A. 2014d. Cancer statistics, 2014. *CA: a cancer journal for clinicians* **64**: 9-29.
- Simon MC, Keith B. 2008. The role of oxygen availability in embryonic development and stem cell function. *Nature reviews Molecular cell biology* **9**: 285-296.
- Slee RB, Steiner CM, Herbert BS, Vance GH, Hickey RJ, Schwarz T, Christan S, Radovich M, Schneider BP, Schindelbauer D et al. 2011. Cancer-associated

- alteration of pericentromeric heterochromatin may contribute to chromosome instability. *Oncogene*.
- . 2012. Cancer-associated alteration of pericentromeric heterochromatin may contribute to chromosome instability. *Oncogene* **31**: 3244-3253.
- Spivakov M, Fisher AG. 2007. Epigenetic signatures of stem-cell identity. *Nat Rev Genet* **8**: 263-271.
- Stintzing S. 2014. Management of colorectal cancer. *F1000prime reports* **6**: 108.
- Su Y, Loos M, Giese N, Metzen E, Buchler MW, Friess H, Kornberg A, Buchler P. 2011. Prolyl hydroxylase-2 (PHD2) exerts tumor-suppressive activity in pancreatic cancer. *Cancer*.
- Sun BB, Fu LN, Wang YQ, Gao QY, Xu J, Cao ZJ, Chen YX, Fang JY. 2014. Silencing of JMJD2B induces cell apoptosis via mitochondria-mediated and death receptor-mediated pathway activation in colorectal cancer. *Journal of digestive diseases* **15**: 491-500.
- Swenson-Fields KI, Vivian CJ, Salah SM, Peda JD, Davis BM, van Rooijen N, Wallace DP, Fields TA. 2013. Macrophages promote polycystic kidney disease progression. *Kidney international* **83**: 855-864.
- Symowicz J, Adley BP, Gleason KJ, Johnson JJ, Ghosh S, Fishman DA, Hudson LG, Stack MS. 2007. Engagement of collagen-binding integrins promotes matrix metalloproteinase-9-dependent E-cadherin ectodomain shedding in ovarian carcinoma cells. *Cancer Res* **67**: 2030-2039.
- Tan TZ, Miow QH, Huang RY, Wong MK, Ye J, Lau JA, Wu MC, Bin Abdul Hadi LH, Soong R, Choolani M et al. 2013. Functional genomics identifies five distinct

- molecular subtypes with clinical relevance and pathways for growth control in epithelial ovarian cancer. *EMBO molecular medicine* **5**: 983-998.
- Tang MH, Varadan V, Kamalakaran S, Zhang MQ, Dimitrova N, Hicks J. 2012. Major chromosomal breakpoint intervals in breast cancer co-localize with differentially methylated regions. *Frontiers in oncology* **2**: 197.
- Teicher BA. 1994. Hypoxia and drug resistance. *Cancer metastasis reviews* **13**: 139-168.
- Tellier C, Desmet D, Petit L, Finet L, Graux C, Raes M, Feron O, Michiels C. 2015. Cycling hypoxia induces a specific amplified inflammatory phenotype in endothelial cells and enhances tumor-promoting inflammation in vivo. *Neoplasia* **17**: 66-78.
- Thomlinson RH, Gray LH. 1955. The histological structure of some human lung cancers and the possible implications for radiotherapy. *British journal of cancer* **9**: 539-549.
- Tian X, Fang J. 2007. Current perspectives on histone demethylases. *Acta Biochim Biophys Sin (Shanghai)* **39**: 81-88.
- Tong Z, Kunnumakkara AB, Wang H, Matsuo Y, Diagaradjane P, Harikumar KB, Ramachandran V, Sung B, Chakraborty A, Bresalier RS et al. 2008. Neutrophil gelatinase-associated lipocalin: a novel suppressor of invasion and angiogenesis in pancreatic cancer. *Cancer research* **68**: 6100-6108.
- Toyokawa G, Cho HS, Iwai Y, Yoshimatsu M, Takawa M, Hayami S, Maejima K, Shimizu N, Tanaka H, Tsunoda T et al. 2011. The histone demethylase JMJD2B

- plays an essential role in human carcinogenesis through positive regulation of cyclin-dependent kinase 6. *Cancer prevention research* **4**: 2051-2061.
- Tsukada Y, Fang J, Erdjument-Bromage H, Warren ME, Borchers CH, Tempst P, Zhang Y. 2006. Histone demethylation by a family of JmjC domain-containing proteins. *Nature* **439**: 811-816.
- Tsurumi A, Dutta P, Shang R, Yan SJ, Li WX. 2013. Drosophila Kdm4 demethylases in histone H3 lysine 9 demethylation and ecdysteroid signaling. *Sci Rep* **3**: 2894.
- Uemura M, Yamamoto H, Takemasa I, Mimori K, Hemmi H, Mizushima T, Ikeda M, Sekimoto M, Matsuura N, Doki Y et al. 2010. Jumonji domain containing 1A is a novel prognostic marker for colorectal cancer: in vivo identification from hypoxic tumor cells. *Clin Cancer Res* **16**: 4636-4646.
- Vang R, Shih le M, Kurman RJ. 2009. Ovarian low-grade and high-grade serous carcinoma: pathogenesis, clinicopathologic and molecular biologic features, and diagnostic problems. *Advances in anatomic pathology* **16**: 267-282.
- Varela I, Tarpey P, Raine K, Huang D, Ong CK, Stephens P, Davies H, Jones D, Lin ML, Teague J et al. 2011. Exome sequencing identifies frequent mutation of the SWI/SNF complex gene PBRM1 in renal carcinoma. *Nature* **469**: 539-542.
- Vaupel P. 2004. The role of hypoxia-induced factors in tumor progression. *The oncologist* **9 Suppl 5**: 10-17.
- Veatch AL, Carson LF, Ramakrishnan S. 1994. Differential expression of the cell-cell adhesion molecule E-cadherin in ascites and solid human ovarian tumor cells. *International journal of cancer Journal international du cancer* **58**: 393-399.

- Venkatesha S, Hanai J, Seth P, Karumanchi SA, Sukhatme VP. 2006. Lipocalin 2 antagonizes the proangiogenic action of ras in transformed cells. *Molecular cancer research : MCR* **4**: 821-829.
- Verhoest G, Avakian R, Bensalah K, Thuret R, Ficarra V, Artibani W, Tostain J, Guille F, Cindolo L, De La Taille A et al. 2009. Urinary collecting system invasion is an independent prognostic factor of organ confined renal cell carcinoma. *The Journal of urology* **182**: 854-859.
- Vinci M, Gowan S, Boxall F, Patterson L, Zimmermann M, Court W, Lomas C, Mendiola M, Hardisson D, Eccles SA. 2012. Advances in establishment and analysis of three-dimensional tumor spheroid-based functional assays for target validation and drug evaluation. *BMC biology* **10**: 29.
- Vogelstein B, Fearon ER, Hamilton SR, Kern SE, Preisinger AC, Leppert M, Nakamura Y, White R, Smits AM, Bos JL. 1988. Genetic alterations during colorectal-tumor development. *The New England journal of medicine* **319**: 525-532.
- Wang GL, Semenza GL. 1993a. Characterization of hypoxia-inducible factor 1 and regulation of DNA binding activity by hypoxia. *The Journal of biological chemistry* **268**: 21513-21518.
- . 1993b. General involvement of hypoxia-inducible factor 1 in transcriptional response to hypoxia. *Proceedings of the National Academy of Sciences of the United States of America* **90**: 4304-4308.
- Wang YC, Juric D, Francisco B, Yu RX, Duran GE, Chen GK, Chen X, Sikic BI. 2006. Regional activation of chromosomal arm 7q with and without gene amplification

- in taxane-selected human ovarian cancer cell lines. *Genes, chromosomes & cancer* **45**: 365-374.
- Welford SM, Bedogni B, Gradin K, Poellinger L, Broome Powell M, Giaccia AJ. 2006. HIF1alpha delays premature senescence through the activation of MIF. *Genes Dev* **20**: 3366-3371.
- Wellmann S, Bettkober M, Zelmer A, Seeger K, Faigle M, Eltzhig HK, Buhner C. 2008. Hypoxia upregulates the histone demethylase JMJD1A via HIF-1. *Biochem Biophys Res Commun* **372**: 892-897.
- Whetstine JR, Nottke A, Lan F, Huarte M, Smolikov S, Chen Z, Spooner E, Li E, Zhang G, Colaiacovo M et al. 2006. Reversal of histone lysine trimethylation by the JMJD2 family of histone demethylases. *Cell* **125**: 467-481.
- Widmer N, Bardin C, Chatelut E, Paci A, Beijnen J, Leveque D, Veal G, Astier A. 2014. Review of therapeutic drug monitoring of anticancer drugs part two--targeted therapies. *Eur J Cancer* **50**: 2020-2036.
- Wiesener MS, Jurgensen JS, Rosenberger C, Scholze CK, Horstrup JH, Warnecke C, Mandriota S, Bechmann I, Frei UA, Pugh CW et al. 2003. Widespread hypoxia-inducible expression of HIF-2alpha in distinct cell populations of different organs. *The FASEB journal : official publication of the Federation of American Societies for Experimental Biology* **17**: 271-273.
- Winkler C, Doller A, Imre G, Badawi A, Schmid T, Schulz S, Steinmeyer N, Pfeilschifter J, Rajalingam K, Eberhardt W. 2014. Attenuation of the ELAV1-like protein HuR sensitizes adenocarcinoma cells to the intrinsic apoptotic pathway by increasing the translation of caspase-2L. *Cell death & disease* **5**: e1321.

- Wolf SS, Patchev VK, Obendorf M. 2007. A novel variant of the putative demethylase gene, s-JMJD1C, is a coactivator of the AR. *Archives of biochemistry and biophysics* **460**: 56-66.
- Wong C, Wellman TL, Lounsbury KM. 2003. VEGF and HIF-1alpha expression are increased in advanced stages of epithelial ovarian cancer. *Gynecologic oncology* **91**: 513-517.
- Wouters J, Stas M, Gremeaux L, Govaere O, Van den Broeck A, Maes H, Agostinis P, Roskams T, van den Oord JJ, Vankelecom H. 2013. The human melanoma side population displays molecular and functional characteristics of enriched chemoresistance and tumorigenesis. *PLoS One* **8**: e76550.
- Xia X, Lemieux ME, Li W, Carroll JS, Brown M, Liu XS, Kung AL. 2009. Integrative analysis of HIF binding and transactivation reveals its role in maintaining histone methylation homeostasis. *Proc Natl Acad Sci U S A* **106**: 4260-4265.
- Xiao Q, Ge G. 2012. Lysyl oxidase, extracellular matrix remodeling and cancer metastasis. *Cancer microenvironment : official journal of the International Cancer Microenvironment Society* **5**: 261-273.
- Xie Z, Dong Y, Maeda U, Moir RD, Xia W, Culley DJ, Crosby G, Tanzi RE. 2007. The inhalation anesthetic isoflurane induces a vicious cycle of apoptosis and amyloid beta-protein accumulation. *The Journal of neuroscience : the official journal of the Society for Neuroscience* **27**: 1247-1254.
- Xiong Z, Liu E, Yan Y, Silver RT, Yang F, Chen IH, Chen Y, Verstovsek S, Wang H, Prchal J et al. 2006. An unconventional antigen translated by a novel internal

- ribosome entry site elicits antitumor humoral immune reactions. *Journal of immunology* **177**: 4907-4916.
- Yamada D, Kobayashi S, Yamamoto H, Tomimaru Y, Noda T, Uemura M, Wada H, Marubashi S, Eguchi H, Tanemura M et al. 2012. Role of the hypoxia-related gene, JMJD1A, in hepatocellular carcinoma: clinical impact on recurrence after hepatic resection. *Annals of surgical oncology* **19 Suppl 3**: S355-364.
- Yamane K, Toumazou C, Tsukada Y, Erdjument-Bromage H, Tempst P, Wong J, Zhang Y. 2006. JHDM2A, a JmjC-containing H3K9 demethylase, facilitates transcription activation by androgen receptor. *Cell* **125**: 483-495.
- Yan L, Borregaard N, Kjeldsen L, Moses MA. 2001. The high molecular weight urinary matrix metalloproteinase (MMP) activity is a complex of gelatinase B/MMP-9 and neutrophil gelatinase-associated lipocalin (NGAL). Modulation of MMP-9 activity by NGAL. *The Journal of biological chemistry* **276**: 37258-37265.
- Yan SM, Tang JJ, Huang CY, Xi SY, Huang MY, Liang JZ, Jiang YX, Li YH, Zhou ZW, Ernberg I et al. 2013. Reduced expression of ZDHHC2 is associated with lymph node metastasis and poor prognosis in gastric adenocarcinoma. *PLoS One* **8**: e56366.
- Yang J, Jubb AM, Pike L, Buffa FM, Turley H, Baban D, Leek R, Gatter KC, Ragoussis J, Harris AL. 2010. The histone demethylase JMJD2B is regulated by estrogen receptor alpha and hypoxia, and is a key mediator of estrogen induced growth. *Cancer Res* **70**: 6456-6466.

- Yang J, Ledaki I, Turley H, Gatter KC, Montero JC, Li JL, Harris AL. 2009. Role of hypoxia-inducible factors in epigenetic regulation via histone demethylases. *Ann N Y Acad Sci* **1177**: 185-197.
- Yang JJ. 2002. Mixed lineage kinase ZAK utilizing MKK7 and not MKK4 to activate the c-Jun N-terminal kinase and playing a role in the cell arrest. *Biochem Biophys Res Commun* **297**: 105-110.
- Yang Y, Sun M, Wang L, Jiao B. 2013. HIFs, angiogenesis, and cancer. *Journal of cellular biochemistry* **114**: 967-974.
- Ye L, Fan Z, Yu B, Chang J, Al Hezaimi K, Zhou X, Park NH, Wang CY. 2012. Histone demethylases KDM4B and KDM6B promotes osteogenic differentiation of human MSCs. *Cell stem cell* **11**: 50-61.
- Yoneda J, Kuniyasu H, Crispens MA, Price JE, Bucana CD, Fidler IJ. 1998. Expression of angiogenesis-related genes and progression of human ovarian carcinomas in nude mice. *J Natl Cancer Inst* **90**: 447-454.
- Yoshioka H, McCarrey JR, Yamazaki Y. 2009. Dynamic nuclear organization of constitutive heterochromatin during fetal male germ cell development in mice. *Biology of reproduction* **80**: 804-812.
- Young LC, McDonald DW, Hendzel MJ. 2013. Kdm4b histone demethylase is a DNA damage response protein and confers a survival advantage following gamma-irradiation. *J Biol Chem* **288**: 21376-21388.
- Yu D, Wolf JK, Scanlon M, Price JE, Hung MC. 1993. Enhanced c-erbB-2/neu expression in human ovarian cancer cells correlates with more severe malignancy that can be suppressed by E1A. *Cancer Res* **53**: 891-898.

- Yu W, Ding X, Chen F, Liu M, Shen S, Gu X, Yu L. 2009. The phosphorylation of SEPT2 on Ser218 by casein kinase 2 is important to hepatoma carcinoma cell proliferation. *Molecular and cellular biochemistry* **325**: 61-67.
- Zaffryar-Eilot S, Marshall D, Voloshin T, Bar-Zion A, Spangler R, Kessler O, Ghermazien H, Brekhman V, Suss-Toby E, Adam D et al. 2013. Lysyl oxidase-like-2 promotes tumour angiogenesis and is a potential therapeutic target in angiogenic tumours. *Carcinogenesis* **34**: 2370-2379.
- Zawacka-Pankau J, Grinkevich VV, Hunten S, Nikulenkov F, Gluch A, Li H, Enge M, Kel A, Selivanova G. 2011. Inhibition of Glycolytic Enzymes Mediated by Pharmacologically Activated p53: TARGETING WARBURG EFFECT TO FIGHT CANCER. *The Journal of biological chemistry* **286**: 41600-41615.
- Zhang J, Planey SL, Ceballos C, Stevens SM, Jr., Keay SK, Zacharias DA. 2008. Identification of CKAP4/p63 as a major substrate of the palmitoyl acyltransferase DHHC2, a putative tumor suppressor, using a novel proteomics method. *Molecular & cellular proteomics : MCP* **7**: 1378-1388.
- Zhao JJ, Gjoerup OV, Subramanian RR, Cheng Y, Chen W, Roberts TM, Hahn WC. 2003. Human mammary epithelial cell transformation through the activation of phosphatidylinositol 3-kinase. *Cancer Cell* **3**: 483-495.
- Zhao L, Li W, Zang W, Liu Z, Xu X, Yu H, Yang Q, Jia J. 2013a. JMJD2B Promotes Epithelial-Mesenchymal Transition by Cooperating with beta-Catenin and Enhances Gastric Cancer Metastasis. *Clin Cancer Res*.
- . 2013f. JMJD2B promotes epithelial-mesenchymal transition by cooperating with beta-catenin and enhances gastric cancer metastasis. *Clin Cancer Res* **19**: 6419-6429.

Zheng H, Chen L, Pledger WJ, Fang J, Chen J. 2013. p53 promotes repair of heterochromatin DNA by regulating JMJD2b and SUV39H1 expression.

Oncogene.

Zhu S, Li Y, Zhao L, Hou P, Shangguan C, Yao R, Zhang W, Zhang Y, Tan J, Huang B et al. 2012. TSA-induced JMJD2B downregulation is associated with cyclin B1-dependent survivin degradation and apoptosis in LNCap cells. *Journal of cellular biochemistry* **113**: 2375-2382.